Stony Brook University

Harvesting Mechanical Energy from the Diurnal Cycle using Shape Memory Alloy

A Thesis Presented

by

Joseph Lawrence Kellogg

to

The Graduate School

in Partial Fulfillment of the

Requirements

for the Degree of

Master of Science

in

Mechanical Engineering

Stony Brook University

May 2013

Stony Brook University

The Graduate School

Joseph Lawrence Kellogg

We, the thesis committee for the above candidate for the

Master of Science degree, hereby recommend

acceptance of this thesis.

Dr. Qiaode Ge – Thesis Advisor
Department of Mechanical Engineering

Dr. Maen Alkhader – Second Reader
Department of Mechanical Engineering

Dr. Qing Chang—Committee Member
Department of Mechanical Engineering

This thesis is accepted by the Graduate School

Charles Taber
Interim Dean of the Graduate School

Abstract of the Thesis

Harvesting Mechanical Energy from the Diurnal Cycle using Shape Memory Alloy

by

Joseph Lawrence Kellogg

in

Master of Science

Mechanical Engineering

Stony Brook University

2013

An investigative study into the feasibility of using nitinol to harvest atmospheric thermal energy is presented. A determination of the thermal characteristic behavior of the atmosphere is made. An investigation into the use of evaporative coolants is conducted. A brief investigation into the heat treatments of 0.5mm nitinol wires is conducted. A mechanism capable of harvesting low grade thermal energy from the normal atmospheric cycling and a method of storing the energy in mechanical form to avoid losses from converting the energy from one form to another and to avoid losses during storage of said energy is built to demonstrate the feasibility of this technology.

Table of Contents

Chapter 1 Introduction to Nitinol and Shape Memory Alloys.....7
Chapter 2 Thermodynamic Behavior of the Atmosphere.....15
Chapter 3 An Investigation Into Evaporative Cooling.....25
Chapter 4 Materials Characterization.....34
Chapter 5 Proof of Concept Prototype.....39
Chapter 6 Future Work.....42
Appendix A.....49
Appendix B.....71
Appendix C.....76
Appendix D.....88

List of Figures

Figure 1.1……7
Figure 1.2……8
Figure 1.3……8
Figure 1.4……9
Figure 1.5……10
Figure 1.6……11
Figure 1.7……12
Figure 1.8……12
Figure 1.9……13
Figure 2.1……16
Figure 2.2……17
Figure 2.3……18
Figure 2.4……19
Figure 2.5……20
Figure 2.6……21
Figure 2.7……22
Figure 2.8……23
Figure 2.9……24
Figure 3.1……25
Figure 3.2……28
Figure 3.3……29
Figure 3.4……30
Figure 3.5……30
Figure 3.6……31
Figure 3.7……32
Figure 4.1……34
Figure 4.2……35
Figure 4.3……36
Figure 4.4……36
Figure 4.5……37
Figure 5.1……39
Figure 5.2……40
Figure 6.1……42

List of Tables

Table 4.1……………………………………………………………………………………………38

Chapter 1: Introduction

1.1 Background:

These days, energy is a precious commodity. We can no longer consider our fossil fuel resources to be infinite or even a long term solution for energy.[1] Therefore, we need to look to renewable resources to generate sustainable energy to propel our nation into the future. Large amounts of research has been spent on developing biofuels as a replacement for crude oil.[2-5] Substituting wood chips for coal is another sustainable energy that has received substantial research.[2,3,5] Frequently, the wood chips are residue from the logging industry and were previously considered waste. These new technologies have reduced our carbon footprint, improved air quality, and extended the length of time that our society can run on the fossil fuels available.

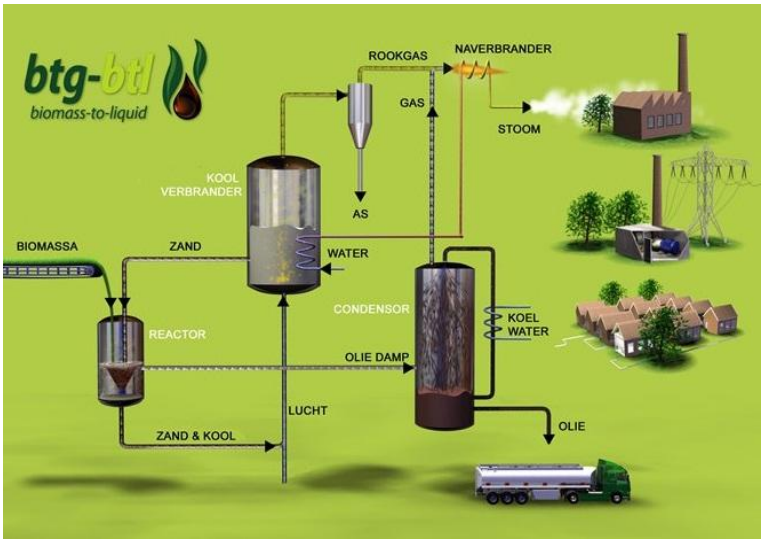

Figure 1.1: A diagram illustrating a cutting edge biofuel technology from the IMPACT Instute at University of Twente.

However, the problem with biofuels is that they are terribly inefficient to produce. Typically, less than 1% of the sunlight absorbed by a plant is turned into plant matter.[6] In the case of liquid biofuels is that the plant matter must then be fermented, which has substantial waste and then it must be burned at a low efficiency to be turned into usable power. Wood chips, while they don't have the production waste found in liquid biofuels, must be dried--consuming a large portion of the chemical energy contained in the wood chip--and then burned at a low efficiency to create usable power.[7] So biofuels have a net efficiency of far less than 1% from solar radiation to usable energy.

What we need is a way to transform the incredible amount of energy that is transmitted to the Earth from the Sun into a form of energy that we can use. Nitinol is one of several alloys known as shape memory alloys (SMAs).[8] SMAs are different from other metals in that, when heated, they undergo a solid state phase transformation that results in mechanical motion.[9] The efficiency is very low, but it has the possibility to transform the very low grade energy found in air and transform it into high grade mechanical energy. If this is possible, then the applications are endless.

The term low grade energy generally refers to heat at temperatures less than 180°F (80°C).[10] Depending on the industry, this number can vary substantially. For example, process steam is often considered 'waste' well above 120°C while, waste heat from heating buildings is

usually at a temperature of 20°C. However, for the purpose of this paper, the term 'low grade energy' refers to temperatures lower than 80°C.

1.2 Introduction to Nitinol:

Nitinol is an alloy of nickel and titanium with 50-60% nickel content and the remainder being titanium.[8,9,11-15] The shape memory properties were serendipitously discovered by researchers at the Naval Ordinance Laboratories (now Naval Surface Weapons Center) who were looking for a new material to be used in the nose cones of rockets.[16,17] During a test that involved hitting a sample with a hammer, it was observed that, at a high temperature, the metal gave a ringing sound. But, at a low temperature, the sample returned a dull thud. This was the first indication that nitinol had different properties at different temperatures.

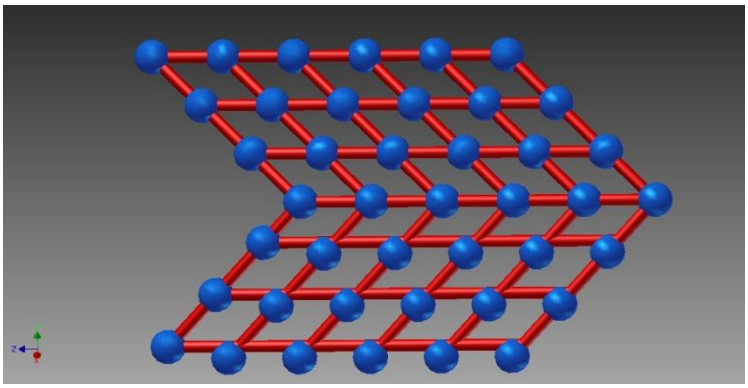

Figure 1.2: An illustration of a twinned crystal lattice.

After considerable research, it was determined that the shape memory effect (SME) stems from the martensite-austenite transformation.[8,9,14,15] The terms martensite and austenite were first assigned to crystal structures observed in steel but have since been observed in numerous alloys.[18,19] While the M A transformation always results in a change in physical properties, most do not result in an SME. The SME arises when the martensite crystal structure has a very high degree of twinning.[19] Twinning is defined as when the atoms of normally regular crystal lattice are rotated by a partial lattice spacing. This is different from slip in two ways: 1. Slip typically occurs on a single or a series of planes and 2. Slip is always measurable in distances of whole lattice spacing. This is because, in slip, the chemical bonds between the atoms are broken and then re-connected after the slip has stopped.[18]

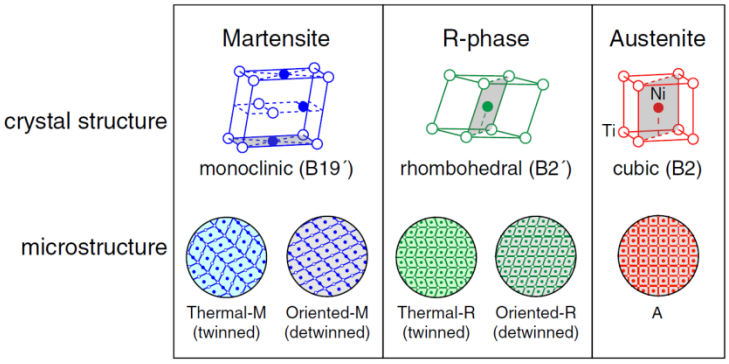

Figure 1.3: Schematics of crystal structures and microstructures in nitinol[13]

Twinning differs from diffusion in that it is not dependent on single atoms moving around inside a crystal lattice. Twinning involves the rotation of an entire section of the lattice by a fractional lattice spacing. There are two types of twinning found in crystals: impact induced twinning and thermally induced twinning. Impact induced twinning occurs when a large impact deforms the lattice within a single grain. Most crystalline structures will exhibit some degree of impact induced twinning. Thermally induced twinning results from a specific heat treatment profile. This heat

treatment profile will differ from alloy to alloy.[8,18] This is why nitinol does not have a shape memory effect after manufacture until it has been properly annealed.[19,20] Very highly twinned samples of nitinol may have as many as five layers of thermally induced twinning.[19]

In nitinol, there is a third thermally induced crystal structure. The austenitic phase has a cubic (B2) structure and the martensitic phase has a monoclinic (B19') structure.[15,17,20-24] This third phase is a rhombohedral structure known as the R-phase. This phase can occur before the martensitic transformation or in conjunction with it.[9,13] Typically, the R-phase can sustain less than 1% shape recovery. However, R-phase does not have a hysteresis and generally occurs over a very narrow band—sometimes as small as 1°C. After 10^6 cycles, the R-phase transition maintains most of its original properties. This is why it is usually used in sensors.

Now, the shape memory effect is not exclusive to metals. There are certain polymers which exhibit a shape memory effect. Typically, a shape memory polymer (SMP) will exhibit a thermo-elastic deformation greater than 400%. However, since SMP's have a recovery stress roughly equal to 1% of nitinol alloys, this makes it impractical to use them in many situations.[25-30]

It is important to note that when a sample of nitinol is fully austenitic and is placed under stress, a portion of the austenite converts back into martensite. This martensite is termed stress induced martensite or SIM. Since martensite is highly deformable with full recovery, an austenitic sample of nitinol can undergo extreme deformation with no plastic deformation. This phenomenon is known as superelasticity. It is generally agreed that a superelastic sample of nitinol can undergo a 50% strain with no plastic deformation.[29,31-37]

1.3 Basic Thermomechanical Properties of Nitinol:

Nitinol is considered valuable because its mechanical properties change with temperature—giving rise to the shape memory effect. From an engineering standpoint, it is impossible to work with nitinol without a basic understanding of the thermomechanical properties of nitinol. As was briefly mentioned in chapter 1.2, there are three crystal structures of consequence in nitinol: austenite (B2), martensite (B19'), and rhombohedral (B2') with austenite occurring at high temperatures, martensite at low temperatures, and R occurring in between. Frequently in literature, austenite is referred to as the parent state.

1.3.1 Hysteresis: When you go to the store to buy nitinol, everyone asks you what A_f you want.[31] A_f is the austenite finish temperature, commonly referred to as the transition temperature. However, there is so much more to nitinol than the A_f temperature. In the realm of

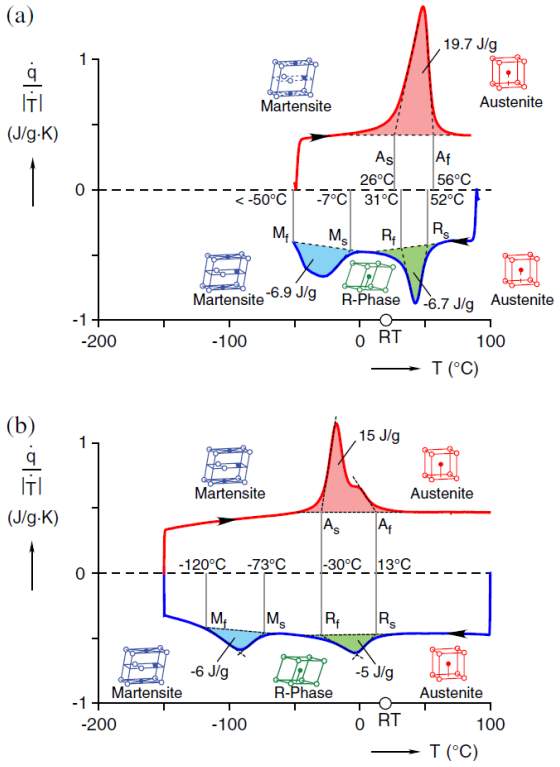

Figure 1.4: Differential scanning calorimetry thermograms of two nitinol alloys: a. Shape memory wire and b. Superelastic wire.[13]

shape memory nitinol, there are a total of seven temperatures to pay attention to. In order of lowest to highest, they are: M_f, M_s[1], R_s[2], R_f, M_0, A_s, and A_f. Here, M, R, and A refer to the three phases of nitinol and the subscripts S and F are the start and finish temperatures of each phase. The thermal hysteresis of an alloy is generally measured from M_f to A_f, the temperature difference required to make a full transformation.[13,31] An example of this can be seen in Figure 1.4.

The thermal hysteresis of a nitinol sample causes the material to remember its recent thermal history. Take, for example, sample B from Figure 1.4. It would be impossible to know what the crystallographic structure was at -45°C unless it was known what the most recent phase transition was. If the sample was being cooled from 15°C, it would remain fully austenite until it was cooled below the M_s temperature, -73°C.[13]

The seventh temperature, M_0 is the equilibrium temperature. This temperature is only of concern in alloys where $M_s > A_s$. In situations such as this, the Gibbs free energy of the existing phase overpowers the desire for the alloy to change phases. The equilibrium temperature is the temperature at which the Gibbs free energies of both phases are equal and a slight temperature change will cause the phase transformation to begin. M_0 is not a measured temperature—like the other temperatures involved with nitinol—rather it is calculated by: $M_0 = \frac{M_S + A_S}{2}$.[17] In the realm of superelasticity, we add the M_d—or martensite difficult temperature. Above M_d, it is too difficult to form stress induced martensite, so a nitinol sample is always 100% Austenite. Above M_d, nitinol behaves as a normal linear-elastic solid.[32]

With so many temperatures that may or may not affect a design with nitinol, it is very important to determine as many of the temperatures as deemed necessary for the project at hand. While many methods exist for determining the transition temperature of a nitinol alloy, ASTM International only recognizes two: Bend and Free Recovery and Thermal Analysis.[39-42] The downside to Bend and Free Recovery is that it can only determine A_s and A_f. If the project requires knowledge beyond these two temperatures, then Thermal Analysis using a differential scanning calorimeter is absolutely necessary.[13] One shortcoming of BFR and DSC are that they only measure free recovery. Because SIM is created when austenite is strained, A_f increases when a nitinol sample is under load.[39-40] However, as of the publishing date of this paper, ASTM has not established a standardized test for strained/constrained recovery.

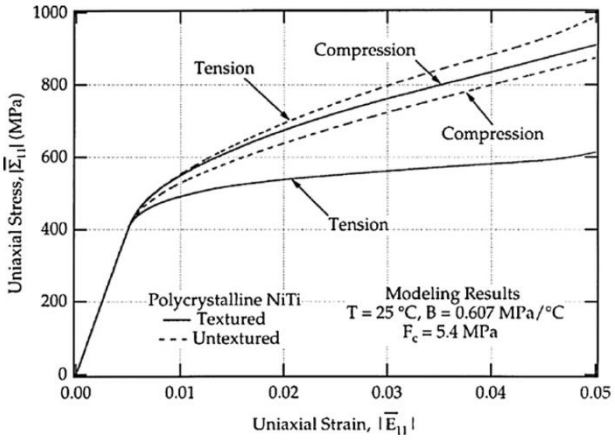

Figure 1.5: Polycrystalline nitinol demonstrating the predicted stress/strain curves.[45]

1.3.2 Fatigue: As is always the case with fracture mechanics, we must take a look at the continuum mechanics surrounding nitinol and the shape memory effect before we can discuss the fatigue properties. Most materials

[11] In certain low hysteresis alloys, M_s may be equal to or higher than A_s.

[2] As seen in Figure 1.4, the R-phase transition may be indistinguishable from the martensite-austenite phase transition.

are considered to be linear-elastic, isotropic solids—to make the math required for modeling them simple. However, nitinol is considered to be a non-linear, anisotropic, pseudoplastic (or thermoelastic) solid.[9,14,19,43-48] Additionally, the crystal size substantially affects the properties of nitinol. The smaller the crystal size, the greater the strength and shape recovery capabilities.[14,44-46]

It is generally agreed that, while nitinol is considered thermoelastic, the SME process is not quite 100% recoverable.[32,43-45,47] So, while nitinol can thermoelasticly recover a 12% strain, it really can only do it once. Reducing the strain to 10% improves the fatigue life to 100 cycles. Reducing strain to 5% extends the fatigue life to 10^5 cycles. Reducing strain even further to 2.5% results in a fatigue life of 10^6-10^8 cycles.[44,45,47] Additionally, Fonte tells us that the crystallographic orientation "greatly influences" the ability of nitinol to resist fatigue.[45] Smaller grain sizes also result in a greater fatigue resistance.[14,44,45] Some sample data from several researchers is shown in Figure 1.6. Fonte, et al. has determined that both the strength and the fatigue resistance of nitinol are better in tension in compression.[44-45] Therefore, when a nitinol machine is built, considerable time must be relegated to designing for fatigue resistance.

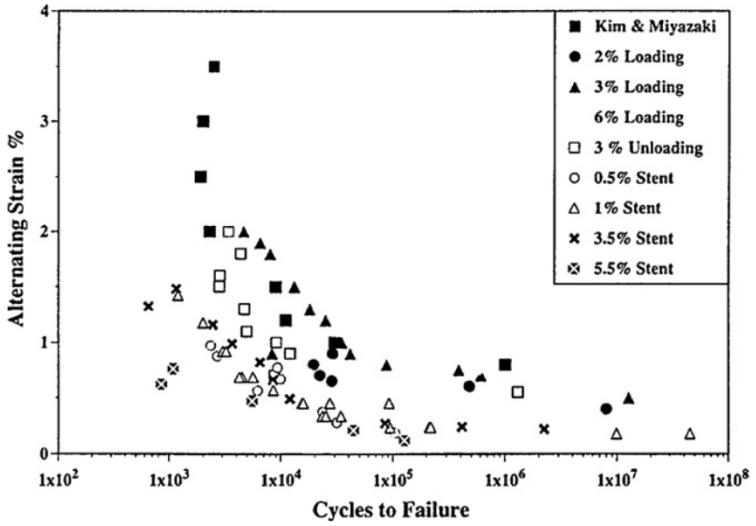

Figure 1.6: Various experiments on fatigue response of nitinol[45]

1.3.3 Applications: The applications for nitinol are so endless, that only the limit of the usefulness of nitinol is the limit of the creativity of the researcher using it. So, while an exhaustive search into the various uses for nitinol and the shape memory effect is outside the realm of this paper, a brief excursion into the field is certainly warranted.

The largest consumer of nitinol worldwide is the medical industry. Within the medical world, nitinol is used to create staples for use inside the body, make replacement joints, build stents to open arteries, make baskets for stone recovery, the list goes on. Some of these designs take advantage of the high fracture toughness of superelastic nitinol. Others take advantage of the shape memory effect to allow for minimally invasive surgeries—making once major surgeries something that can be done by cutting just a few small holes in the patient. Still others take advantage of the damping qualities of nitinol. However, the biggest advantage of nitinol is the very, very high biocompatibility.[47,49-53]

Industry and consumer applications, while they don't consume as large a quantity of nitinol, have a much broader range of uses. The first such application happened in 1970 when a Cryofit™ fitting was used on a F-14 fighter to secure hydraulic fittings at very high pressure by using the constrained recovery properties of nitinol. Since then, superelastic nitinol has been used in eyeglasses, brassieres, and cell phone antennas very extensively. As actuators, nitinol has been used in fuel injectors, antiscald safety valves, sprinkler valves, current interrupters, coffee makers, rice cookers, fishing line, robots, the list goes on.[8,9,51,54-58]

In civil engineering, the damping properties of nitinol are frequently used to adapt structures to deal with the rigors of earthquakes. Bridges are also damped with nitinol to extend the fatigue life of the beams. More recently, 'green' buildings, which use minimal energy use nitinol to switch between heating and cooling modes.[59-60]

1.3.4 Previous Work in Heat Engines: Since the discovery of nitinol researchers and tinkerers alike have been attempting to assemble heat engines to generate power from low grade heat. These engines typically run in the area of 1-4% efficiency, which sounds absolutely terrible. However, since low grade heat is usually discarded as waste, any kind of generation is creating useful power from waste and, therefore, creating value. Sources of low grade heat used range from solar-thermal water to boiler wastewater to the temperature differential found in the ocean. All that is needed is the ability to overcome the thermal hysteresis of nitinol and you can generate useful, high grade mechanical energy from low grade heat.

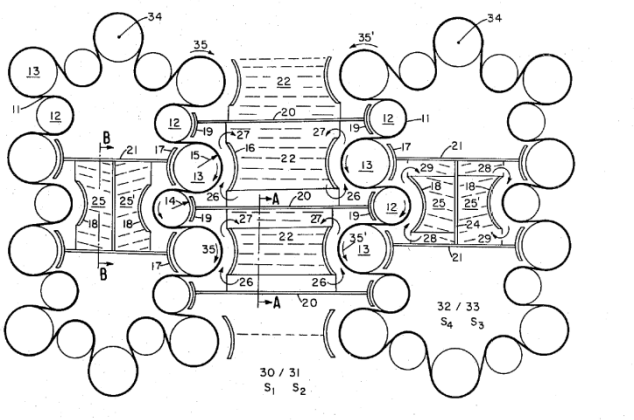

Figure 1.7: An example of a continuous band nitinol heat engine.[61]

Many designs utilize a continuous nitinol band which can be continually moved from hot to cold in one ongoing cycle. The advantage to these heat engines is that with a continuous cycle, it makes maximum use of the nitinol as it typically has a cycle frequency on the order of 1000 RPM. Power generated by these engines—at least as originally documented—ranged as high as one kilowatt. Of course, most of these engines had the capacity to be scaled up, almost indefinitely. Other heat engines used numerous short wires to generate power. Generally, each wire was individually dipped into hot and cold reservoirs to provide the necessary heat flow.[61-65]

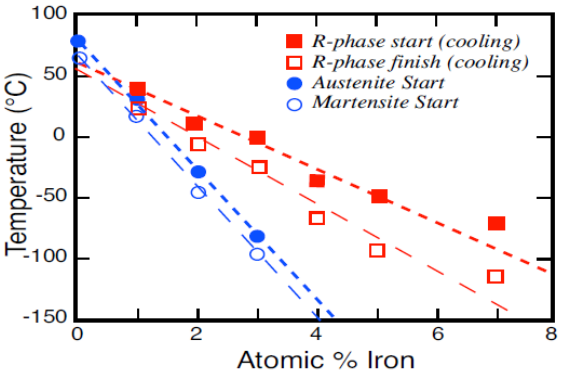

Figure 1.8: The effects of adding iron as a ternary element in a nitinol alloy

- Increase transformation temperatures
- Decreasing transformation temperatures

1.4 Ternary Alloys[43]

1.4.1 Background: Traditionally, nitinol is defined as the binary alloy of nickel and titanium—specifically with a nickel content between 49 and 51 percent. However, there is a growing amount of research documenting the benefits of ternary alloys where a portion of the nickel is replaced by a third element. Some of the benefits achieved by ternary alloys include:

- Increasing austenitic strength
- Increasing creep resistance
- Increasing hysteresis
- Decreasing hysteresis

- Increasing corrosion resistance
- Increasing radiopacity

While a full discussion of ternary (and quaternary) alloys is outside the scope of this paper, we will take a brief look at some of the more important ternary alloys. While there are some applications where they are desirable, we will consider oxygen and carbon interstitial alloys to be impurities which are undesirable.

1.4.2 Martensitic Suppression: In some applications, it is desirable to have very low transition temperatures. This allows the alloy to maintain the ductility of having a low nickel content but having the transition temperature of a high nickel content. Frequently, ternary alloys are more controllable than the binary nitinol. For example, in binary nitinol, a 1 at.% change in nickel content is responsible for changing the transition temperature from -100°C to 100°C, whereas, a substitution of 3 at.% Fe also drops the transition temperature to -100°C. Figure 1.8 shows the effects of adding iron to a binary alloy. Ternary elements that result in martensitic suppression include iron, cobalt, vanadium, chromium, aluminum and tantalum.

1.4.3 Martensitic Stabilization: Sometimes, it is beneficial to have very high transition temperatures. One of these is in the field of robotics where low transition temperatures can cause accidental actuation. Another is power generation where higher temperatures result in greater efficiencies. The most extreme of the martensitic stabilizers are platinum and palladium. Some researchers have documented transition temperatures as high as 1100°C for platinum and 600°C for palladium. While this has some obvious benefits, the cost of using 30 at.% platinum is tremendous. This, combined with the fact that it is more difficult to work with than binary nitinol makes platinum and palladium alloys impractical for industrial use.

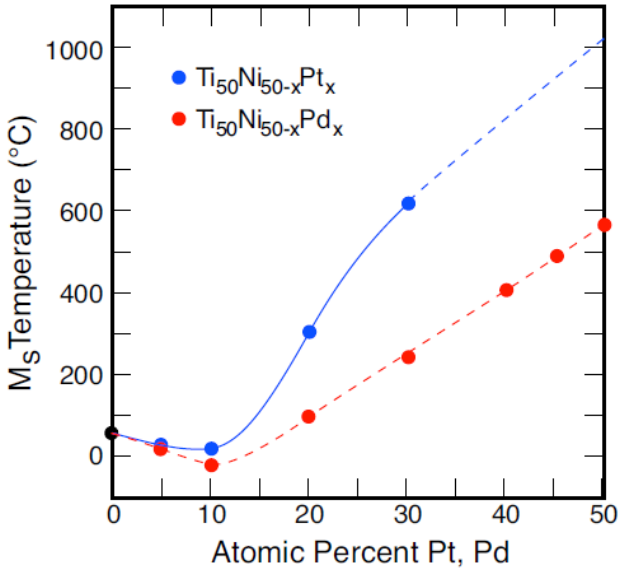

Figure 1.9: Martensitic suppression due to ternary alloying with platinum and palladium.

Other ternary elements include hafnium and zirconium with hafnium being more popular in industry. Hafnium alloys can typically be acquired commercially with transition temperatures up to 130°C while some researchers have created alloys with transition temperatures over 150°C. The cost and workability of NiTiHf are similar to nitinol, so it is a good substitution for nitinol.

1.4.4 Hysteresis Expansion: One of the first commercial applications of nitinol was the Cryofit® hose fittings to secure hydraulic hoses on fighter airplanes. These are loops of nitinol which are cooled to cryogenic temperatures and then stretched in the martensitic state. These fittings must be stored at and installed below A_s or else they will shrink prematurely and be worthless. Also, they must not drop below M_s or else they will loosen and the hydraulic line will rupture—a devastating occasion on an aircraft. The need for a very wide hysteresis alloy led to

the discovery of the ternary alloy with niobium. By adding niobium, a hysteresis as large as 120°C is achievable.

1.4.5 Hysteresis Reduction: In some areas, it is important to have a narrow hysteresis so that it is easier to cause the martensitic transformation. Copper is the one element that can be alloyed with nitinol to reduce the hysteresis. Substituting 20 at.% copper for nickel closes the hysteresis down to just 5°C. However, several factors make it impractical to use NiTiCu alloys with more than 10 at.% Cu. Even at 10 at.% Cu, NiTiCu has a hysteresis of just 11°C, a huge improvement over the 40°C hysteresis of binary nitinol.

There are also several other benefits that come with alloying copper into nitinol. Not the least of these is reducing cyclic deterioration of all sorts. While binary nitinol has lost a substantial portion of its original shape memory characteristics after 10,000 cycles, NiTiCu loses less than 1% of its shape memory characteristics after 1,000,000 cycles. Another beneficial effect is that with copper concentrations in the range of 5-7 at.%, the two-way shape memory effect is amplified.

Chapter 2: Thermodynamic Behavior of the Atmosphere

2.1 Experimental location

2.1.1 It is common knowledge that on most days, the atmosphere experiences thermal cycling due to solar heating by day and radiant cooling by night. There are, of course, other factors involved such as moving air masses that occasionally alter this daily thermal cycling, but, by and large, the atmosphere warms up during the daytime and cools off at night--at least on a local basis.

2.1.2 The National Weather Service reports that in areas of Arizona and Nevada, the daily temperature change can be more than 50°C. On the other hand, areas that are near large bodies of water have a much more moderated daily temperature change, especially on days with heavy cloud cover. Nonetheless, if we assume that the average daily temperature change is only 15°C, the amount of energy sourced daily by the air in the 1000m closest to the surface of the earth is approximately 9.3×10^{18} kJ, making the atmosphere the largest available solar collector. Because the air contains such a tremendous amount of energy, this makes the 1% efficiency reported for nitinol engines quite lucrative.

2.1.3 One common engineering practice is to design for the worst possible scenario. So, to follow this principle, we should choose a test location which is located near a large body of water and frequently cloudy skies. Rochester, NY is a choice location due to its location on Lake Ontario and frequently overcast skies. The National Weather Service (NWS) has a data collection point at the Greater Rochester International Airport and publishes atmospheric data online on an hourly basis. Due to this convenient reference point, we set up a data collection point approximately 300m from the NWS data collection point.

2.1.4 Because of the possibility of using this daily temperature change as a power source for vehicle applications, an area on the edge of a parking lot was chosen for data collection. This ensures that the data collected would be very similar to what the vehicle would observe.

2.2 Data Collection in an Automotive Situation

2.2.1 Instrumentation: We utilized an Omega OM-EL-USB-TC data logger to collect temperature data. We set the time interval to 10s to optimize the accuracy of data collection and the frequency of downloading and re-setting the logger. This allowed us to collect data for 3 ½ days between data dumps. We briefly studied whether or not we were missing critical data by not collecting data at 1s intervals. We found that it was rare to catch a substantially higher high or lower low. So, this—factored in with the fact that the logger was unable to capture a full 24-hour cycle at 1s time intervals—made the 10s time interval preferred.

2.2.2 Experimental Set-up: We placed two data loggers under the hood of a silver 2009 Chevrolet Uplander to determine the daily thermal cycles. It is commonly known that the presence of asphalt substantially affects the localized air temperature. Clearly, an ideal situation would be to park the test vehicle on an infinite sheet of asphalt on a sunny day. However, roads and driveways are generally narrow and have a limited effect on the local air temperature. So, to continue our desire to design for the worst case scenario, we parked the Uplander in the corner of

the parking lot. We measured the temperature at the top of the engine compartment as well as at the bottom to determine if there was any difference.

2.2.3 Data Collection & Analysis: As expected, we found that most days had a sinusoidal temperature pattern with the highest temperature occurring in the afternoon and the coolest temperature occurring shortly before sunrise as seen in Figure 2.1.

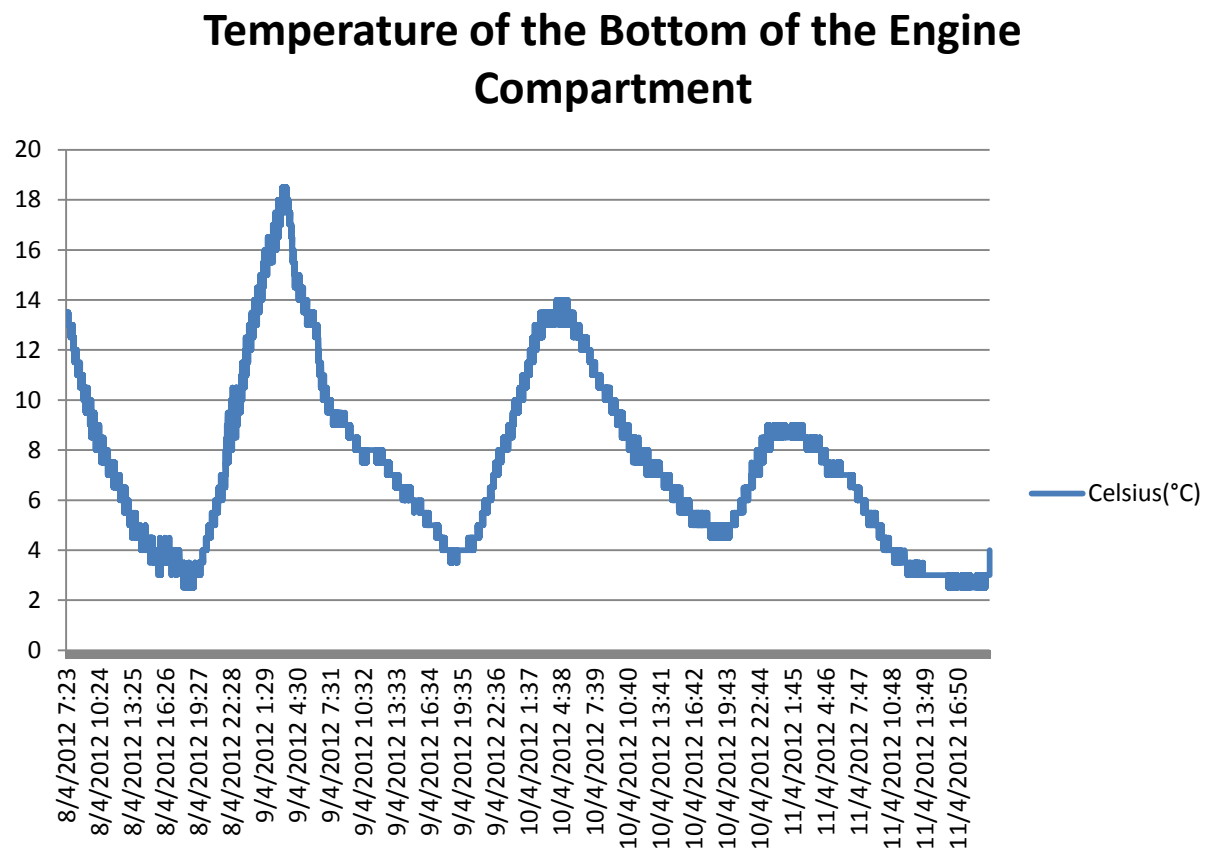

Figure 2.1 An example of the sinusoidal heating-cooling cycles typically experienced in the atmosphere near the surface of the earth. Note that increased cloud cover results in decreased variation in temperature.

However, on days that the sky was overcast, the temperature changed by only a few degrees while on some days, moving air masses overpowered the solar warming so that the air temperature continued to fall during the day or rise at night. An example of this can be seen in Figure 2.2.

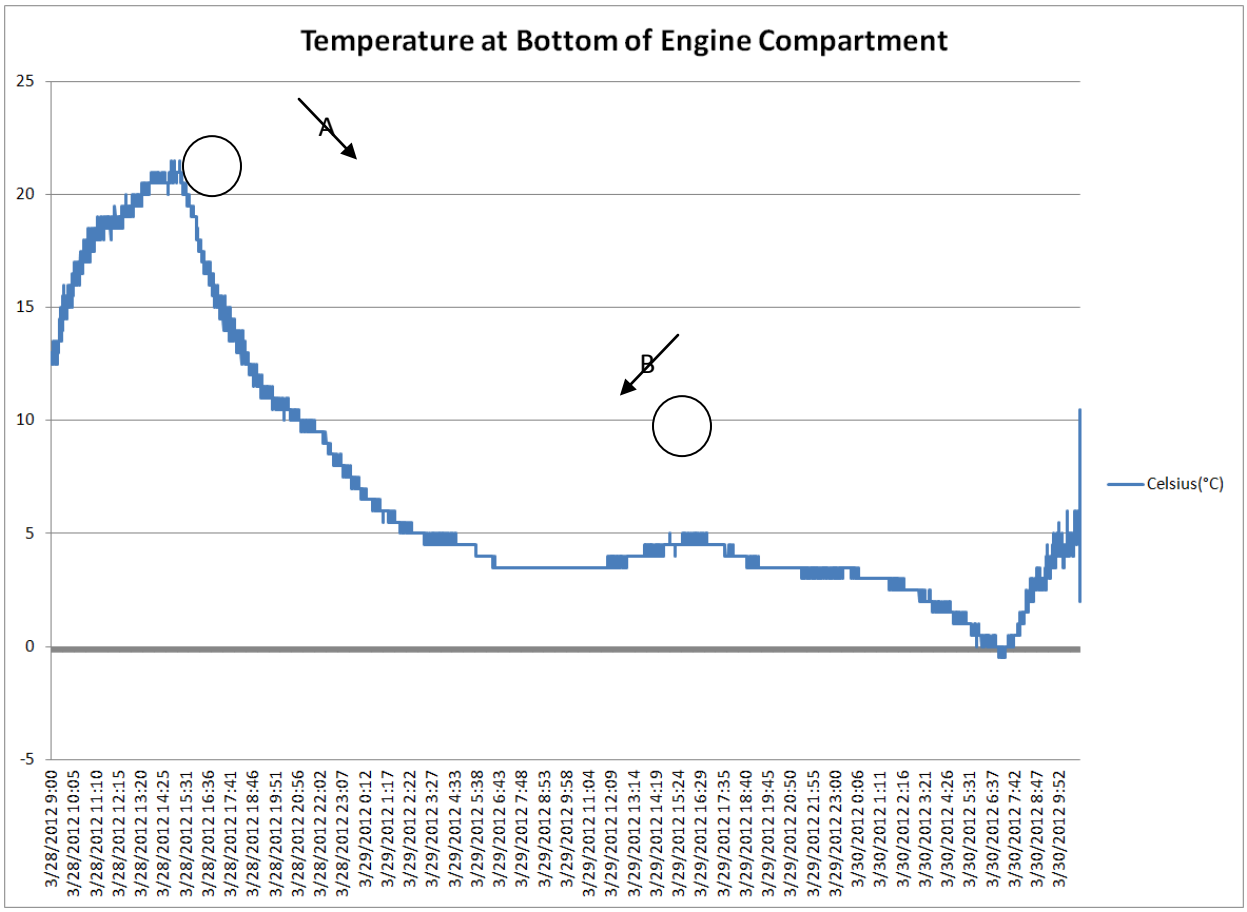

Figure 2.2 A) An example of a typical sunny day resulting in ΔT on the order of 20°C and at B) we have an example of a very overcast day resulting in ΔT of only 1.5°C

As we discussed in Chapter 1, binary nitinol has a thermal hysteresis of approximately 40°C. Since, even on the best of days, the air only changed by approximately 20°C, this makes generating mechanical energy from the daily thermal flux of the atmosphere extremely difficult--if possible at all in areas that are not classified as deserts. However, these temperature measurements are taken at the bottom of the engine compartment which has minimal solar exposure and maximum convective cooling.

For the top of the engine compartment, we are not so concerned about the actual temperature. What is far more useful is the difference between the top and the bottom of the engine compartment. Figure 2.3 demonstrates a typical sample of this temperature difference.

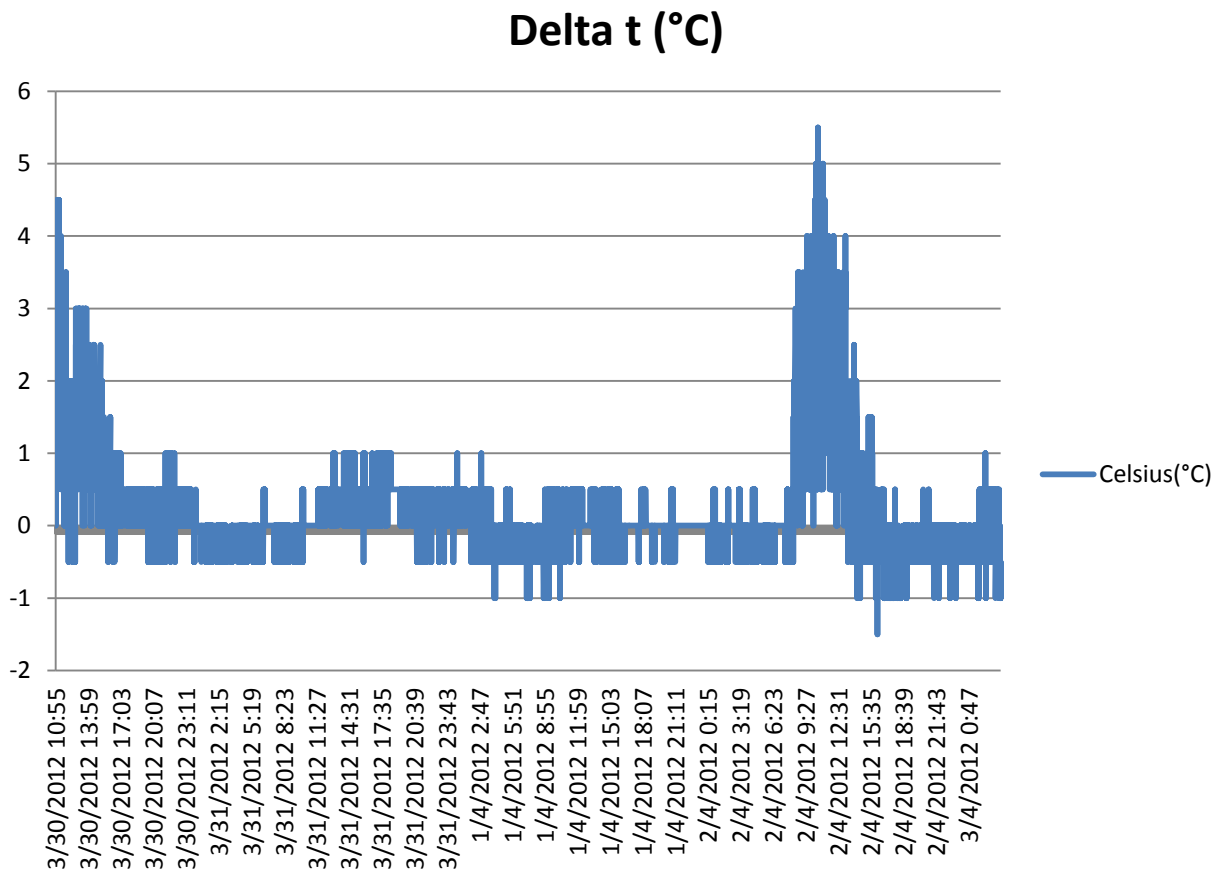

Figure 2.3: The difference in temperature between the top and bottom of the engine compartment $\Delta \boldsymbol{T} = \boldsymbol{T_{Top}} - \boldsymbol{T_{Bottom}}$

Here, we notice that the temperature can easily be five degrees warmer on a sunny day (and even just a little bit warmer on an overcast day). But what is surprising is that, while there are higher highs, as expected, the lows are roughly 1°C cooler at the top of the engine compartment than at the bottom. This brings our daily ΔT to 26°C, or even slightly higher. While this doesn't completely solve the problem, it is enough to allow for a partial phase transformation which would generate at least some energy--a step in the right direction.

Now, what happens when we take temperature measurements inside the vehicle? So, we left one data logger at the top of the engine compartment and placed the other one on the floor of the van. As before, it doesn't matter very much what the actual temperature was since this is a parameter that can be accommodated by design. We are far more interested in the difference in temperature between the engine compartment and the passenger compartment. This can be seen in Figure 2.4.

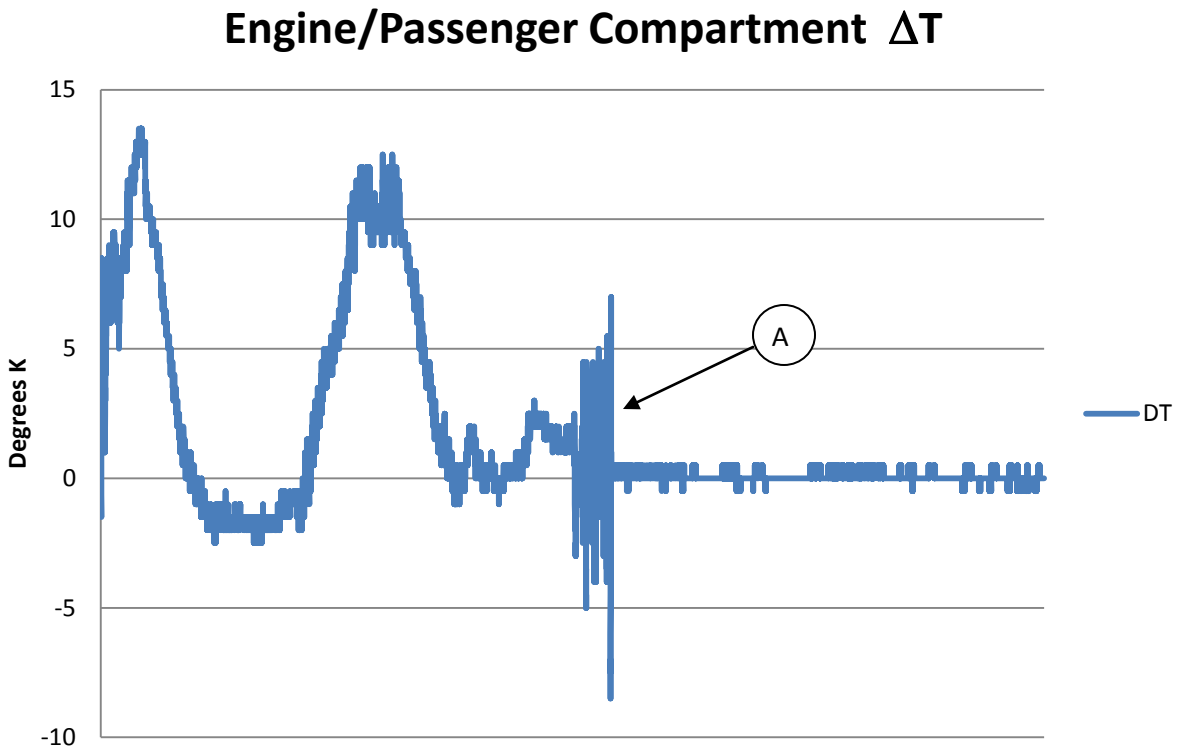

Figure 2.4 Difference in temperature between engine compartment and passenger compartment. Point A was a windy day of mixed sun and clouds. $\Delta \boldsymbol{T} = \boldsymbol{T_{Pass}} - \boldsymbol{T_{Engine}}$

As expected, the highs are some 13°C higher inside the passenger compartment than they are inside the engine compartment. However, what is surprising is that, at night, the low drops down 2°C cooler than the engine compartment. A simple explanation for this is the existence of the thermal inertia of the engine block in the engine compartment to keep it warm through the night. This also explains the temperature swings as large as 10°C found at point A. So, by removing the thermal inertia of a 500# steel engine block and by tightly sealing the compartment, the daily temperature change was exaggerated by an additional 15°C, bringing the possible change to 41°--the full value of the thermal hysteresis for binary nitinol. Unfortunately, this is not perfectly cumulative.

For one more test, let's see how much placing the thermocouple in direct sunlight inside the passenger compartment adds to the temperature change. To test this, we kept one data logger on the floor of the van while placing the other one on the dashboard. The dashboard of the test vehicle was grey in color, so it did not act as a perfect black body but it certainly helped. A side by side comparison of the temperature of the floor and the dashboard can be found in Figure 2.5

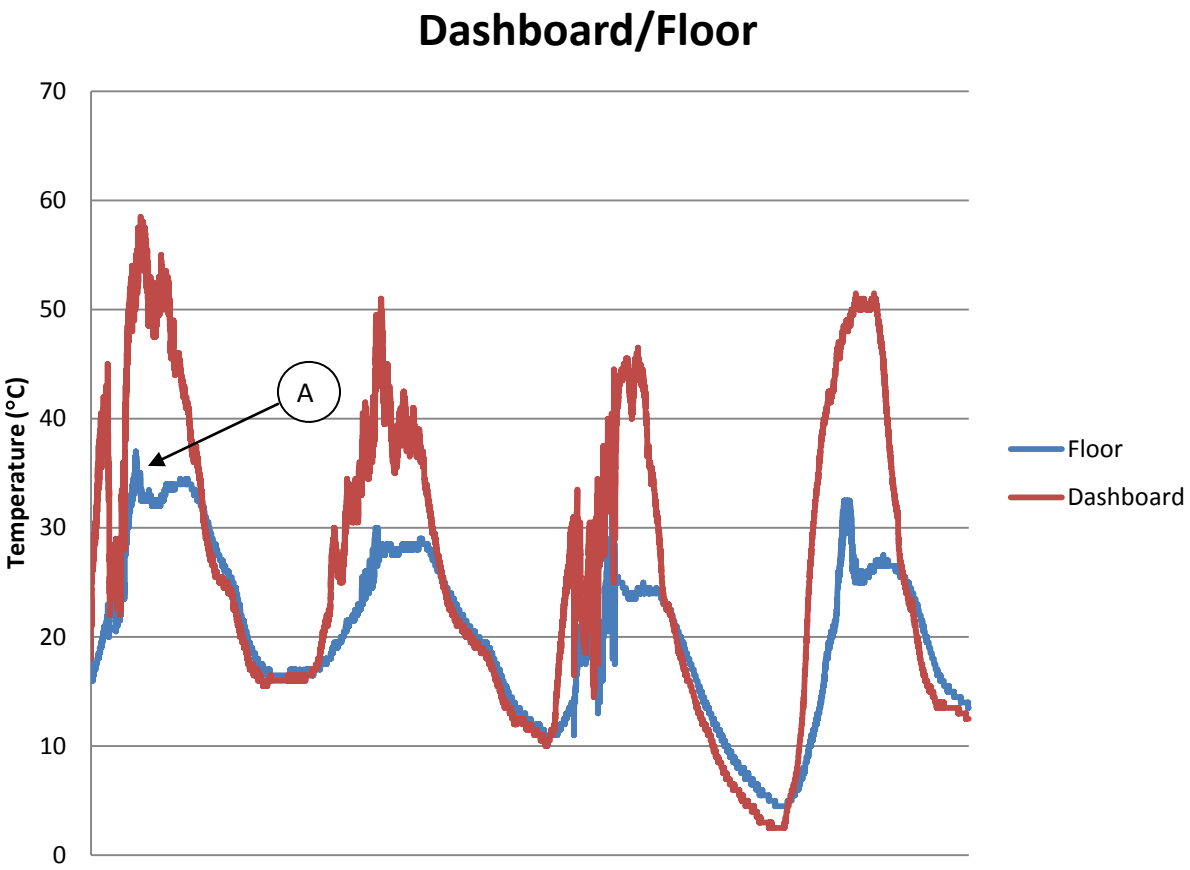

Figure 2.5 A side by side comparison of the temperatures recorded on the dashboard of the vehicle as well as on the floor of the vehicle. Point A is pointing out a spike that occurred nearly every day, but only on the measurements collected from the floor of the vehicle.

As you we can see, on a sunny day, the temperature swing easily surpasses the 40°C required to fully overcome the thermal hysteresis of binary nitinol. It is interesting to note that, even though we are strictly talking about an air system, being near the edge of the car resulted in enough lower thermal inertia that the temperature typically dropped 1-3°C lower than the readings taken in the center of the car.

The spikes like the one seen at point A on Figure 2.5 are quite concerning. Especially since the spikes are so large and they tend to happen near the top of an otherwise smooth warming/cooling curve and they only occur on the floor. After some discussion, we decided that these spikes are caused by the sun shining directly on the data logger through the window of the van.

Therefore, we determined that, while the under hood temperatures aren't enough to overcome the thermal hysteresis in nitinol, the temperature range on the dashboard of a car is plenty enough to overcome the thermal hysteresis. Another important lesson learned here is that everything—even air—has thermal inertia and will affect the magnitude of the temperature change. This is something that must be taken into account when developing working models.

2.3 Data Collection Using Greenhouse Effects

2.3.1 Experimental Set-up: After collecting some basic data from what an automobile experiences, it is important to attempt to replicate and optimize this in other situations. We built a total of four boxes to test various possible means of constructing a fully working prototype. Two boxes were built out of 0.063" thick aluminum and measured approximately 4" x 4" x 8". One end was affixed using caulk to ensure an airtight seal while the other end was sealed off using 2" wide polypropylene tape to allow access to the data logger that was contained inside. One box was painted black while the other box maintained a brushed aluminum finish.

The other two boxes were constructed of ¼" Lexan® and measured 5" x 5.5" x 9". Five sides were secured to each other using caulk while the sixth side was attached by polypropylene tape as with the aluminum boxes to allow access to the data logger contained within. For this test, we used the same data loggers as were used in Chapter 2.2. One of the Lexan® boxes had the bottom of the inside painted black. The paint used was a polyurethane spray paint 'Dull Black', acquired from Pacific West Chemical Corp; Corte Madera, CA 94976 (NSN: 8010-01-441-0162).

Before we began the experiment, we ran a congruency test to make sure that all four data loggers record measurements that are comparable to each other. To test this, we connected all four thermocouples together and placed them in the cold lab oven with the temperature set to 100°C. The data loggers were set to record measurements every second and all four data loggers were synchronized to take measurements at the same time. The thermal profile that was measured can be seen in Figure 2.6. The door of the oven was opened at 2666 seconds to retrieve the thermocouples. This is seen by a sudden drop in temperature.

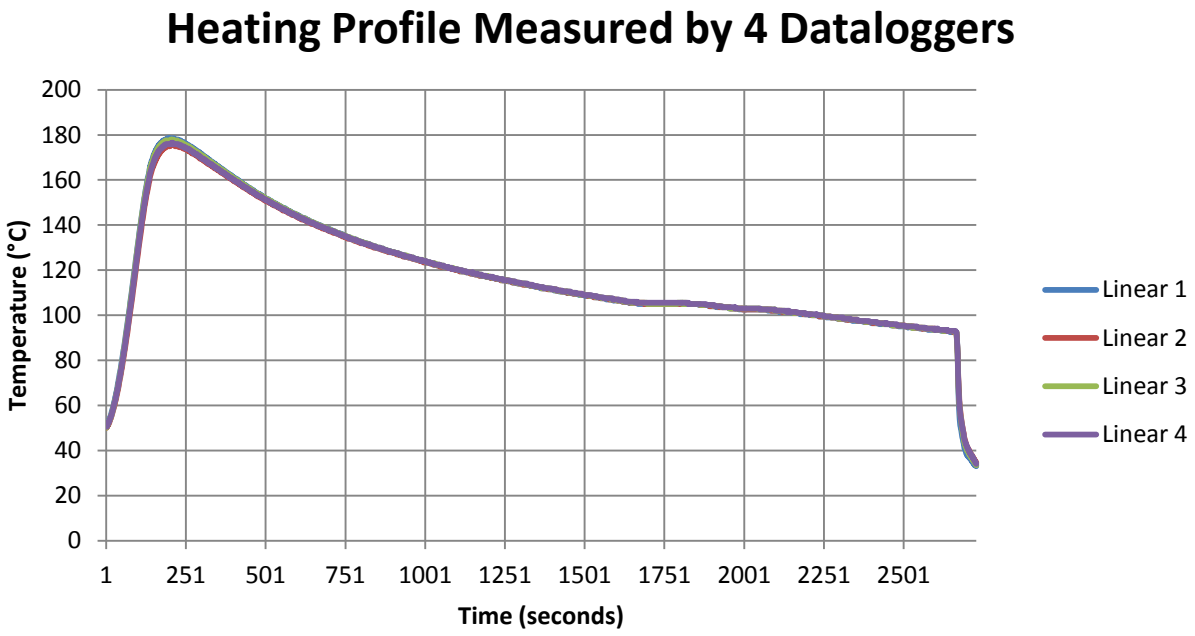

Figure 2.6 Heating profile of our lab oven set to 100°C as measured by the four data loggers,

Next, we tested the congruency of the four data loggers by measuring the difference between them. For this test, we standardized our data to logger #1. The results of this can be seen in Figure 2.7.

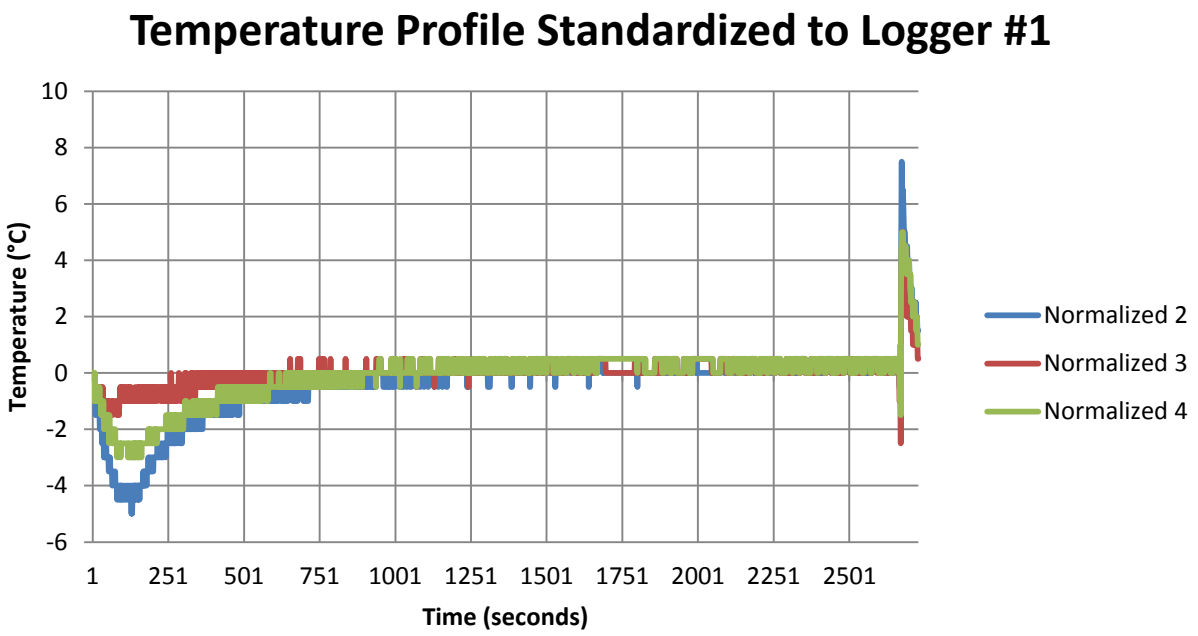

Figure 2.7: Variation of data logger measurements taken to determine congruency.

For most of the duration of the experiment, all four data loggers were within 0.5°C of logger #1—the resolution of the data logger. However, during times of rapid temperature change, there was substantial deviation. Upon closer examination, the loggers are congruent within 0.5°C as long as $\frac{\partial T}{\partial t} \leq 3\ ^{\circ}\mathrm{C}/_{S}$. As it turns out, our loggers experience $\frac{\partial T}{\partial t} \leq 1\ ^{\circ}\mathrm{C}/_{S}$ for this experiment. This gives us a high degree of confidence that all four loggers are interchangeable in the four boxes.

Now, it was time to determine how much the sun can warm things up in our own system, to see how it compares to an automobile. To test this, we attached our four boxes to a large concrete block placed on the edge of the parking lot. With the data loggers set to capture temperature data on a ten second interval, we began capturing data. We took data for two months and compared the data with information gathered from the National Weather Service. An early set of data can be seen in Figure 2.8.

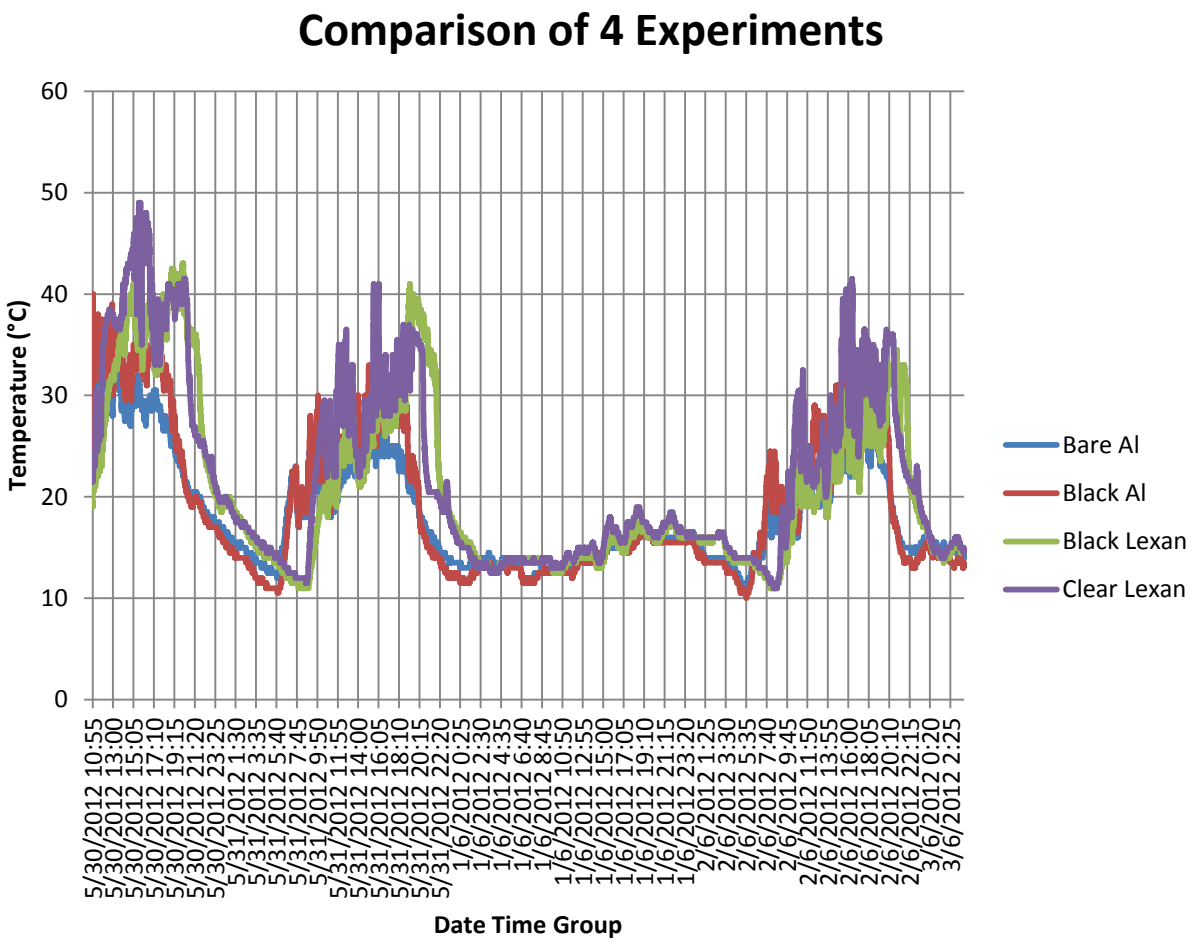

Figure 2.8: A side by side comparison of all four boxes.

At first glance, there is nothing surprising about the data—the magnitude of the solar warming depends on the intensity of the solar radiation. On days with partial clouds or overcast skies, the thermal cycle is substantially reduced. Digging into the data analysis a little more, we see that the temperature of the aluminum boxes spikes up faster than the Lexan boxes. However, the surprising factor is that the black Lexan box typically is cooler than the clear box—except for in the late afternoon. With a little bit of experimental analysis, it turned out that the black Lexan box wasn't receiving quite as much sunshine as the other boxes were. So, a more realistic data sample from the Lexan boxes can be found in Figure 2.9

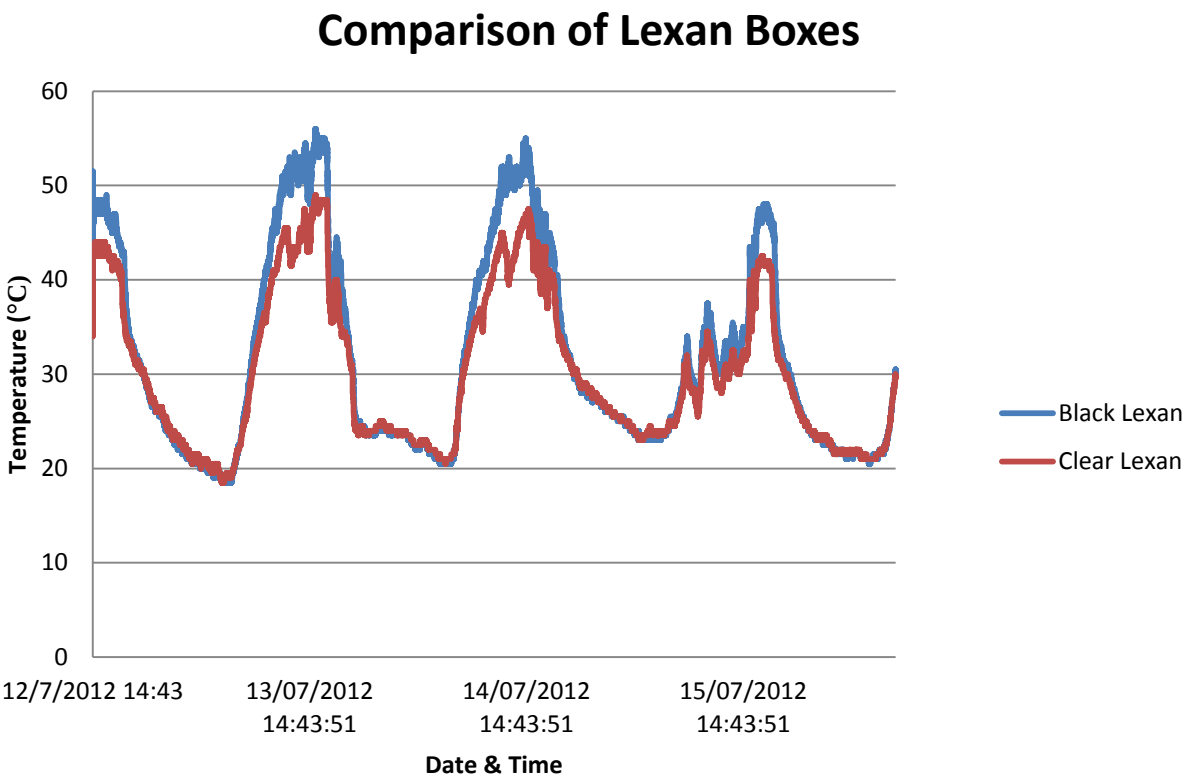

Figure 2.9: A comparison of the Lexan boxes after correcting the problem of not receiving the same amount of sunlight.

Here, we see that painting the bottom of the Lexan box black allows for up to an additional 8 degrees of heating as opposed to regular Lexan. Upon comparing our data from the Lexan boxes to our data from the Uplander, we see that, while the Lexan boxes were able to achieve 35°C of warming, this is a far cry from the 47°C that we witnessed on the dashboard of the Uplander. Now, it is possible that this is due in part to the thermal inertia of the concrete block. However, it certainly tells us that if we want to enclose our nitinol element to create a solar-thermal heat engine, the optical properties of our enclosure are very important.

Binary nitinol has a thermal hysteresis of approximately 40°C. With a daily temperature change of an impressive 35°C, this is not enough to overcome the thermal hysteresis on a daily basis. Of course, to make matters worse, this assumes that the temperature in the morning starts at M_f, warms up by 35°C, and then returns to M_f. This idea situation will rarely occur in nature, so we must design accordingly. This is where ternary alloys come in to play. In Chapter 1.4, we discussed the various benefits that could be found from using ternary elements in nitinol alloys. One of these benefits was hysteresis reduction. By adding up to 10% copper to a nitinol alloy, the thermal hysteresis can be cut down to a mere 11°C—acheivable even on an overcast day. If sunny days are assumed, then the acceptable range of air temperature that will cause the nitinol to cycle expands to 60°C—making it such that one alloy is applicable for nearly all four seasons.

Chapter 3: Evaporative Cooling

3.1 Background: In the power generation industry, it is common to use evaporation to provide a heat sink for the heat engines used.[1] At nuclear power plants as well as other power generation facilities, it is not uncommon to see large cooling towers with large plumes of water vapor rising out of them. These towers take advantage of water's high heat of vaporization and good vapor pressure to extract large amounts of waste heat from the heat engine system that is being used to generate power. To the best knowledge of the author, only one researcher has mentioned using evaporation as part of a nitinol heat engine and it was only generally alluded to rather than directly pursued.[2] In this chapter, we investigated three different liquids which are readily available to be used as bulk coolants.

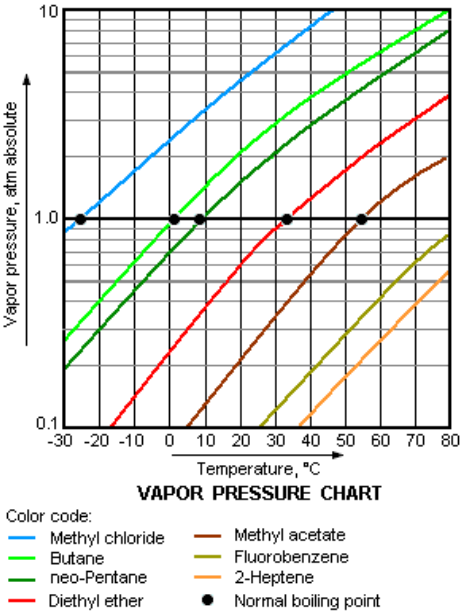

Figure 3.1: Vapor pressures of various liquids[3]

Vapor pressure is the pressure exerted by a vapor in thermodynamic equilibrium with its condensed phases (solid or liquid) at a given temperature in a closed system.[3] Vapor pressure can be estimated mathematically using the Antoine Equation:

$$\log P = A - \frac{B}{T} \tag{3.1}$$

Where A and B are material specific constants, T is the absolute temperature and P is the absolute pressure. It is the mechanism which governs sublimation, evaporation and boiling. Boiling occurs when the vapor pressure of a given liquid rises above atmospheric pressure. Sublimation occurs when the vapor pressure of a solid is greater than the local atmospheric pressure and evaporation is the governing mechanism when the vapor pressure of a given solid or liquid is below the atmospheric pressure. A good example of this is shown in Figure 3.1.

For solutions where multiple liquids are dissolved together, each liquid has its own vapor pressure based on the physical properties of the given liquid. The total vapor pressure of the solution can be found using Raoult's Law:

$$P_{Total} = \sum_i p_i \tau_i \tag{3.2}$$

Where p_i is the vapor pressure of the i-th component of the solution and τ_i is the mole fraction of the i-th component of the solution. Raoult's law is not a perfect mathematical model. Some solutions deviate either positively or negatively from Raoult's law, giving higher or lower vapor pressures and boiling points respectively. One good example of a positively deviated solution is a 95% ethanol-water solution. An example of a negative deviation is a chloroform-acetone solution.

The evaporative mass flow across a liquid-gas interface can be modeled by

$$E = m(n_L \boldsymbol{v}_L - n_G \boldsymbol{v}_G) \quad (3.3)$$

where E is the evaporative mass flow, m is the molecular mass of the liquid, n_i is the density of the molecules (in molecules per square cm of interface) and v_i is the molecular velocity. Since we are dealing with a liquid/air boundary at temperatures far above the boiling point of air, we can model air as an ideal gas. This tells us that

$$n_G = \frac{p}{RT_G} \quad (3.4)$$

where T_G is the temperature of the air and R is the ideal gas constant. Since the velocity of a molecule is known to be $^1/_2 mv^2 = kT_G$ where k is Boltzmann's constant and the mean perpendicular velocity **v** is proportional to the mean velocity v as **v** = rv, we can rewrite the gas portion of Equation 3.3 as

$$n_G \boldsymbol{v}_G = \frac{\frac{r}{R}\left(\frac{2k}{m}\right)^{1/2}}{T_G{}^{1/2}} \quad (3.5)$$

For the liquid phase, since the molecular density is largely independent of temperature, we will denote it as the constant μ. The average molecular kinetic energy is given by kT_L, so

$$\boldsymbol{v_L} = r\left(\frac{2kT_L}{m}\right)^{1/2} \quad (3.6)$$

Inserting Equations 3.5 and 3.6 back into Equation 3.3 tells us that the mass flow rate of evaporation is given by

$$E = r(2km)^{1/2}\left[T_L{}^{1/2} - \frac{p/R}{T_G{}^{1/2}}\right] \quad (3.7)$$

Evaporation works as a heat transfer mechanism until the heat given off by evaporation is in equilibrium with the heat absorbed from the environment. If we assume that the nitinol wire is very long as compared to its cross sectional area, we can assume that the conductive heat transfer is nil and only convective heat transfer will occur between the air and the wire. We also have radiant heat transfer from the environment and from the sun. Radiant heat transfer from the environment is given by

$$q_{rad} = \varepsilon\sigma\left(T_N{}^4 - T_0{}^4\right)A_s \quad (3.8)$$

where q is the rate of heat transfer, ε is the emissivity of the nitinol, σ is the Stefan-Boltzmann constant, T_N is the temperature of the nitinol, T_0 is the temperature of the environment, and A_s is the surface area of the nitinol.

The amount of sunlight that reaches the surface of the earth is approximately equal to 1100 W/m^2. This number varies based on cloud cover, latitude, and time of day. So, the amount of energy absorbed by the nitinol element from solar radiation during daylight hours can be found as

$$q_{sol} = \varepsilon\gamma Q A_x cos\theta \quad (3.9)$$

where γ is the atmospheric transmission coefficient, Q is the maximum solar radiation, A_x is the cross sectional area of the nitinol and θ is the angle that the sun makes with the axis of the nitinol element.

Newton's Law of Cooling tells us that the heat transfer between the nitinol element and the air is

$$q_{convect} = h_c A_s (T_N - T_0) \quad (3.10)$$

where h_c is the convective heat transfer coefficient. Our system is in equilibrium with the environment when

$$Eh_v = \sum_i q_i \tag{3.11}$$

where h_v is the enthalpy of vaporization of the liquid coolant. Now, if we assume that the layer of water on the nitinol is thin, we can approximate $T_L = T_N$. So, thermodynamic equilibrium is reached when

$$rh_v(2km)^{1/2}\left[T_N{}^{1/2} - \frac{p/R}{T_0{}^{1/2}}\right] = \varepsilon\sigma\left(T_N{}^4 - T_0{}^4\right)A_s + \varepsilon\gamma Q A_x cos\theta + h_c A_s(T_N - T_0) \tag{3.12}$$

Now, we know that $A_x = dL$ and $A_s = \pi dL$, so if we consider one unit length of wire in our scenario and ignore boundary effects, Equation 3.12 becomes

$$rh_v(2km)^{1/2}\left[T_N{}^{1/2} - \frac{p/R}{T_0{}^{1/2}}\right] = \varepsilon\sigma\pi d\left(T_N{}^4 - T_0{}^4\right) + \varepsilon\gamma Q d cos\theta + h_c\pi d(T_N - T_0) \tag{3.13}$$

While T_N and T_0 are easy to determine, h_c varies substantially and is difficult to determine analytically. So, it is important to experimentally determine the equilibrium point.

3.2 Experimental Set-up: We used a standard box fan to provide unidirectional airflow at low, medium, and high speeds in our test chamber. Air velocity was measured with an Extech Model 451126 Vane Thermo-Anemometer Datalogger. The sample that we used was a 5 mm diameter by 150 mm long aluminum rod with the center bored out and a thermocouple attached inside. Over the aluminum sample was a woven nylon sleeve which was soaked in the desired coolant and then allowed to evaporate in the air stream. An Omega OM-EL-USB-TC data logger was used to collect temperature data on one second intervals.

The first sample coolant we ran was Naphtha. Naphtha is a commercially available solvent comprised of a mixture of liquid hydrocarbons with a high vapor pressure—and a boiling point as low as 30°C. It is cheap and readily available at paint shops and home improvement centers. The second sample that we ran was Isopropyl Alcohol (91%vol). It is commercially available in the form of rubbing alcohol in nearly every drug store and grocery store, so accessibility is very high for the average person. With a melting point of -89°C, isopropyl alcohol can be used as a coolant at extremely low temperatures, making it a viable coolant for Arctic and Antarctic installations.

The third coolant that we used was regular tap water. The advantage of tap water is that it is available anywhere civilization is present for an extremely low cost. In fact, water is so cheap, we can consider it to be free when compared to the other coolants. Other advantages over the other coolants include the fact that water is very non-flammable and that it has an extremely high heat of vaporization, meaning that less water is required to evaporate to extract the required amount of heat. Drawbacks to using water include the high freezing point (0°C) and low vapor pressure.

All three coolants were allowed to stand at room temperature for 48 hours to acclimate to the temperature of the laboratory. Because we were using volatile liquids, the coolants were kept in closed containers so that evaporation would not cool the liquids prematurely.

3.3 Data Collection: The first step in the data collection process was to run side by side cooling experiments just to qualify the cooling qualities of these various liquids. To do this, we soaked the nylon sleeve with as much liquid as it could hold and placed it in the airstream at all four velocities. The data logger then recorded the temperature profiles of each of the three liquids. Only one sample was run at a time.

The first experiment we ran was in still air. To make the air as still as possible while maintaining the same humidity over the course of the experiment, we set up this test in an office situation.

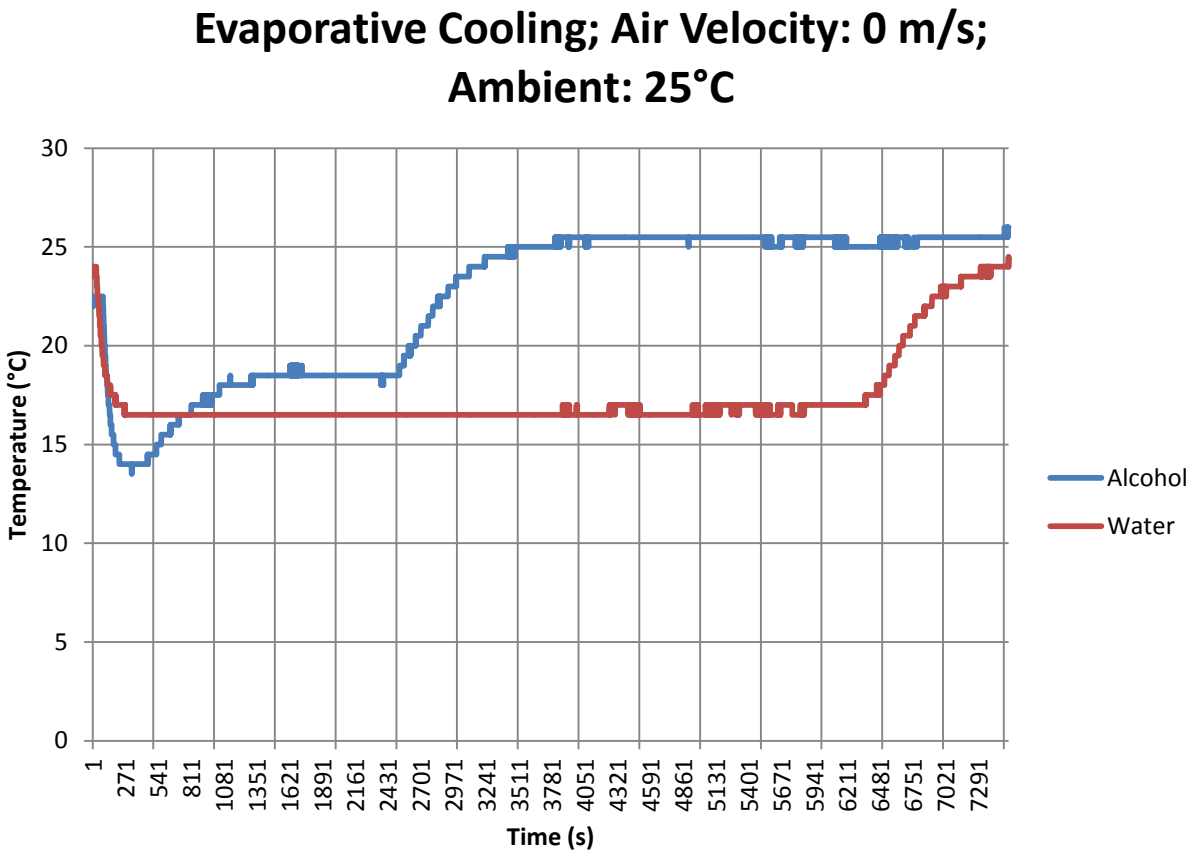

Figure 3.2: Evaporative cooling of isopropyl alcohol and water in still air. Data was collected on two different occasions, each being an overnight run to minimize circulation from people walking around the office.

We used a corner cubicle, which had two floor to ceiling walls and only one small door, to minimize circulation. The results of this experiment can be seen in Figure 3.2. On the day that we ran the experiment for water, the ambient temperature was 24°C and on the day we ran the experiment for isopropyl alcohol, the ambient temperature was 26°C. This is the reason for the discrepancy in the temperature data after both loggers had reached equilibrium. Naphtha was not used for this experiment because the building supervisor required that we maintain 100% visual accountability during naphtha evaporation experiments.

Next, we set all three coolants in a low speed airstream and allowed to evaporate. Results can be seen in Figure 3.3.

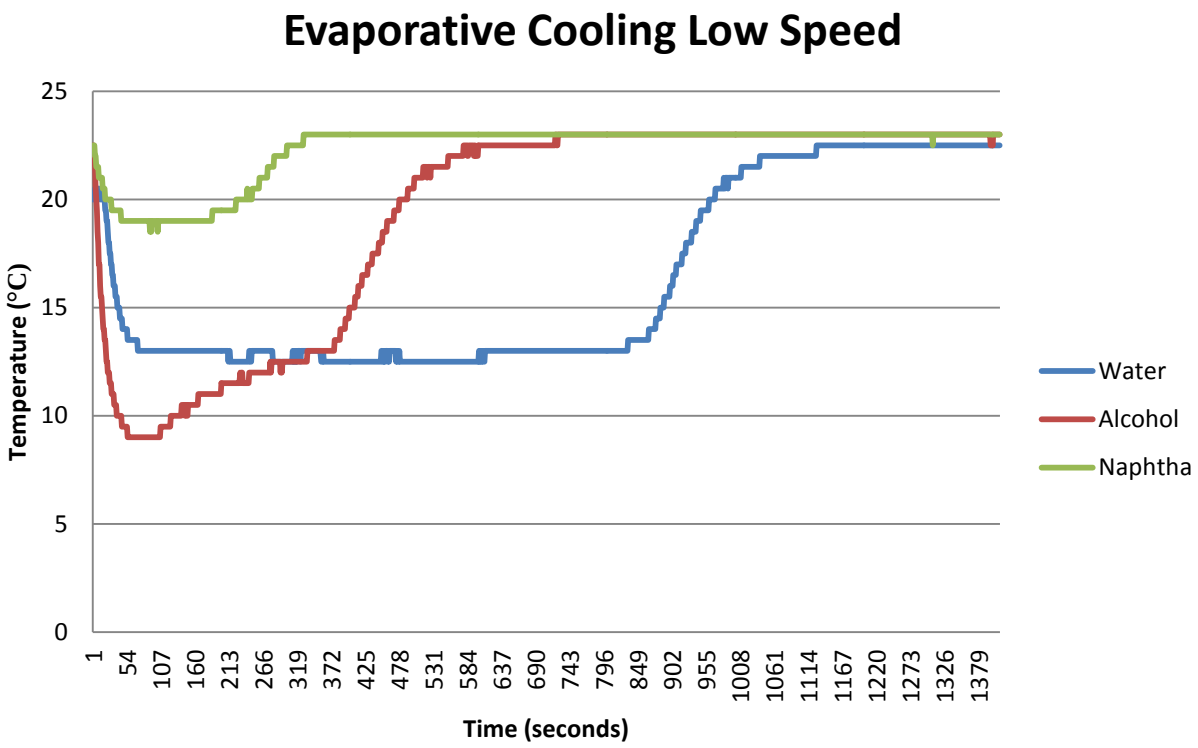

Figure 3.3: Experimental determination of the equilibrium cooling achievable through evaporative cooling using water, isopropyl alcohol (91%vol) and naphtha

For this experiment, all three experiments were run in one day. We were able to do this due to the expectation of an accelerated cooling curve as well as the fact that people walking through the lab resulted in negligible disturbances to the experimental set-up. The ambient temperature was 23°C and the average air velocity was approximately 5 mph with a standard deviation of 0.2 mph. We can see that the naphtha reached equilibrium after 4.5°C cooling, making it a very poor coolant. Since naphtha is such a poor coolant and because of the high levels of toxicity, we decided not to use it in any other experiments.

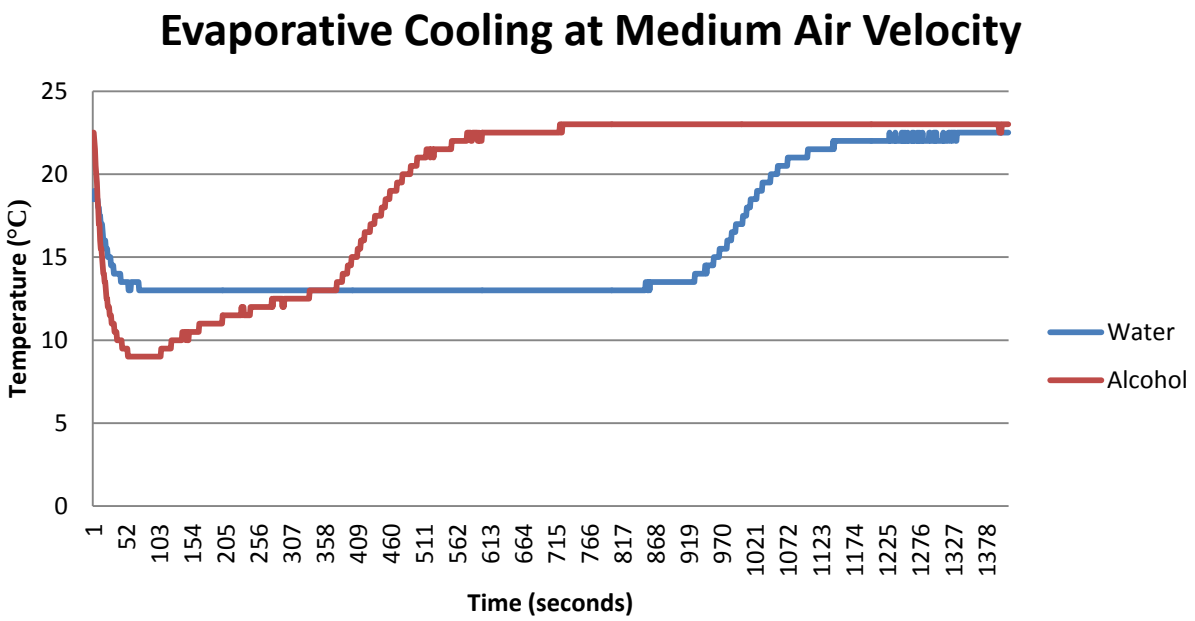

Figure 3.4: Evaporative cooling of water and isopropyl alcohol in a medium velocity airstream. Ambient temperature was 22°C. The cooling experiments were run consecutively.

Next, we ran an experiment with water and isopropyl alcohol in a medium speed airstream. The average air velocity was 7.05 mph with a standard deviation of 0.2 mph. The data from this experiment can be viewed in Figure 3.4.

For our final comparison of coolants, we placed isopropyl alcohol and water in a high speed airstream. The average air velocity was 9.15 mph with a standard deviation of 0.1 mph. The cooling experiments were run consecutively in the same day. The results of this experiment can be viewed in Figure 3.5.

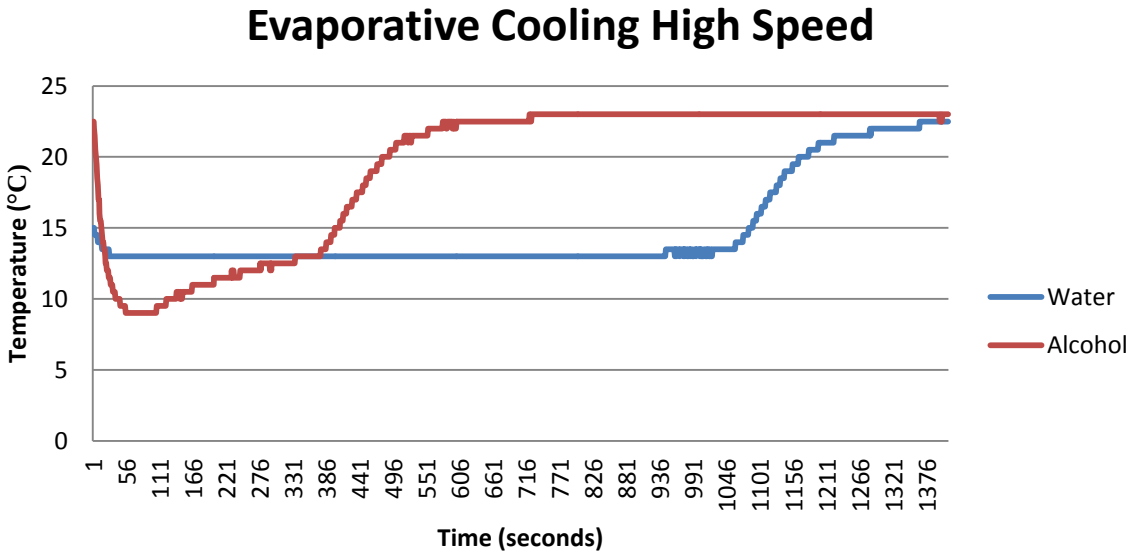

Figure 3.5: Evaporative cooling of water and isopropyl alcohol in a high speed airstream. Ambient temperature was 23°C

Now, we need to address water's biggest drawback—its high freezing point. Water freezes at 0°C meaning that it can't be used as an evaporative coolant below 10°C. Propylene glycol is a commercially available antifreeze which is used in automotive coolant systems to provide boil over and freeze protection. A 50% aqueous solution of propylene glycol yields freeze protection to -37°C, which the author has only experienced once. This should provide the capacity to use evaporation to cool to very low temperatures.[4]

To determine the equilibrium temperatures for evaporative cooing at these low temperatures, we built the following experiment. We used two thermocouples, each having a stainless steel probe approximately 10cm long. One probe was covered with a woven nylon sleeve while the other was left bare. The bare thermocouple collected data on the ambient temperature. The nylon sleeve was soaked in a 50% aqueous solution of propylene glycol and allowed to evaporate. Most iterations of this experiment were carried out outdoors to 1. Maximize the range of ambient temperatures and 2. We did not have a freezer in the lab which was big enough to conduct this experiment. We are very thankful to the Raymond Corporation for allowing us to use their freezer to collect data at an ambient temperature of -25°C.

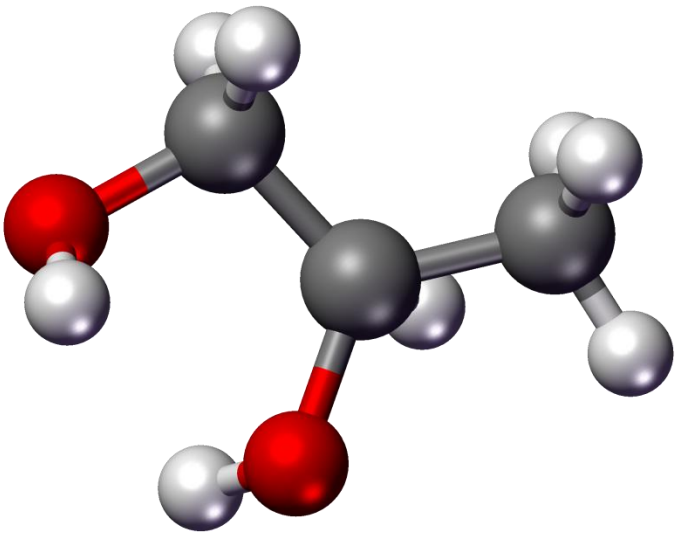

Figure 3.6: The molecular structure of propylene glycol.[5]

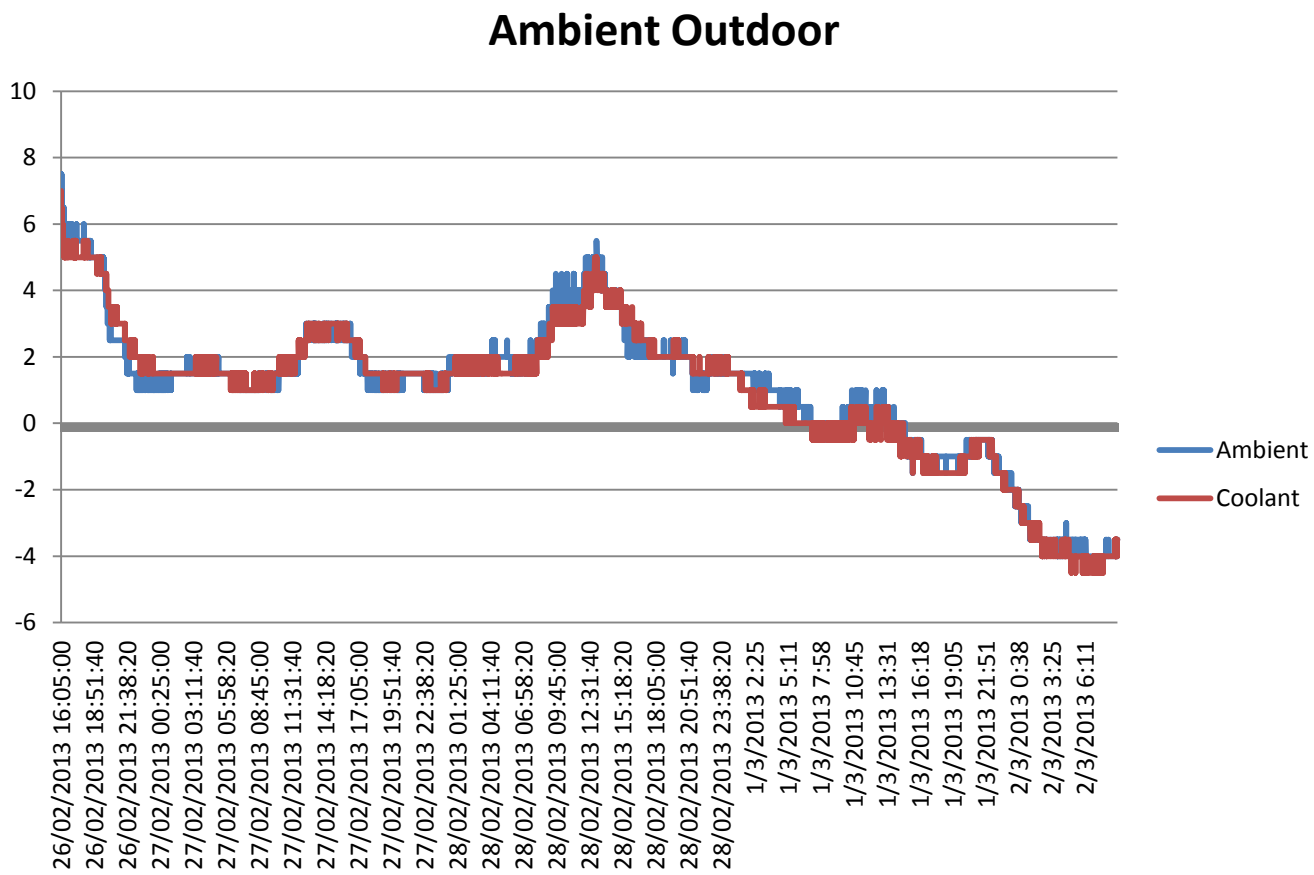

Figure 3.7: A comparison between ambient air temperature and a sample cooled with a water/propylene glycol solution.

From Figure 3.4, we can see that at low temperatures, the vapor pressure of water is too low to have a substantial effect on the temperature of the sample.

3.4 Conclusions: At first glance, the choice is clear as to which coolant is ideal. Alcohol has the steepest cooling curve—meaning greater chance of generating an additional cycle—and it cools the lowest below ambient temperature, which also increases the chance of generating an additional power cycle. However, there are two substantial trade-offs. The heat of vaporization of isopropyl alcohol is 732 kJ/kg whereas the heat of vaporization of water is 2260 kJ/kg, meaning that you would have to carry 3 times as much alcohol as water. This is a perfect segue into the second drawback of alcohol—cost. Retail alcohol costs approximately $4/gallon whereas, distilled water is available for substantially less than $1/gallon and tap water costs somewhere around ten cents per gallon.

From the perspective of our project, these drawbacks outweigh the benefits of the additional cooling achieved by the alcohol. Therefore, we will be using water as our coolant. In the optimization phase of this project (outside the realm of this paper), it would be important to optimize the use of water—for portable systems—because the enthalpy of vaporization of water is less than 1% of the chemical energy in gasoline. Of course, for stationary applications, the system could be tied directly into a full time water supply, so water storage is not important.

For temperatures more than 10°C, water is a great coolant to extract heat from the nitinol element. Even though isopropyl alcohol has a much higher vapor pressure—resulting in faster

cooling and lower equilibrium temperatures—the cost and low heat of vaporization make alcohol unsuitable for most applications. Therefore, we will be pursuing water as the coolant of choice for this project. For temperatures below 10°C, where evaporative cooling causes the temperature of water to drop below its freezing point, the vapor pressure of water is so low that the heat flow from the atmosphere into the sample was almost always equal to the heat extracted by evaporation. Therefore, if a coolant is needed below 10°C, alcohol or some other highly volatile coolant must be used.

Chapter 4: Materials Characterization

4.1 Optimizing Nitinol Wires

4.1.1 Choosing the Wire Size: There are several trade-offs between having thin wires that heat and cool quickly and having too many wires. One good example of why having too many wires is bad is it adds additional weight to the structure of our nitinol heat engine. Some researchers have also stated that having uneven heating in nitinol can cause plastic deformation on the micro scale when going through the martensitic transformation (or reverse). Heating time, as is commonly found in heat transfer textbooks can be calculated as

$$t = \frac{r^2}{\alpha} \qquad where \quad \alpha = \frac{k}{\rho c} \tag{4.1}$$

Here, r is the radius of the wire in centimeters, k is the thermal conductivity, ρ is the density of nitinol and c is the specific heat capacity.[1] Figure 4.1 shows the heating time of nitinol wires with radius 0.12-1.00 cm.

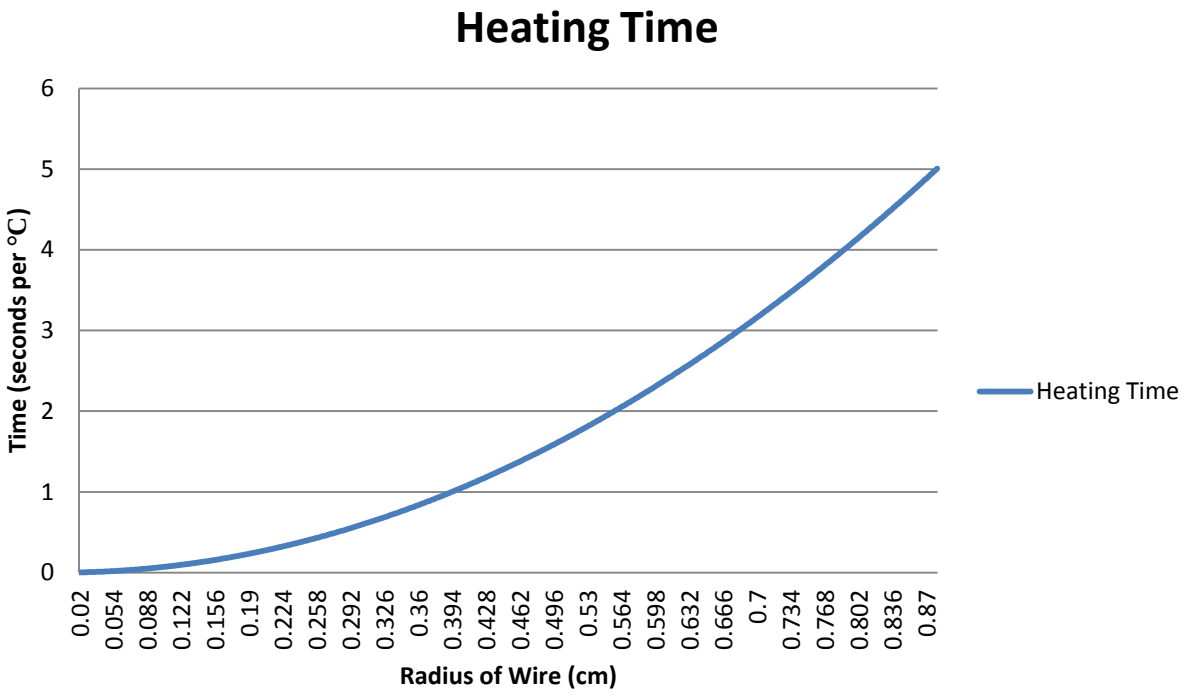

Figure 4.1: The relationship between heating time and radius of nitinol wires.

It must be noted that the specific heat capacity of nitinol is very much not a constant. When nitinol is not going through a phase change, the specific heat capacity remains very close to 0.84 J/g. However, when a phase change is occurring, the specific heat changes dramatically. Additionally, the latent heat of transformation varies substantially, depending on alloy and heat treatment.

In chapter 2, we found that in our test location—which is not prone to extreme temperature fluctuations—frequently observed temperature change rates of 3 seconds per °C.

Therefore, this instantly eliminates wires with a radius greater than 0.681 cm. Now, if we want the wire to heat as fast as the air through the phase transition, we must use even smaller wires. Differential scanning calorimetry reveals that during the phase transformations, the specific heat can spike by as much as three times.[2] Therefore, we need to keep heating time under 1 second per °C. So, from a heating angle, we need to keep the radius of the wires under 0.393 cm.

Now, let us determine how many wires would be required number of wires for a given project. We need to make some basic assumptions to rough out the number of wires that we will need. If we assume that we will need to generate a maximum of 4.53 kN of force (explained in Chapter 5) and that the recovery force is approximately 250 MPa, we get Figure 4.2, showing us how many wires would be required.

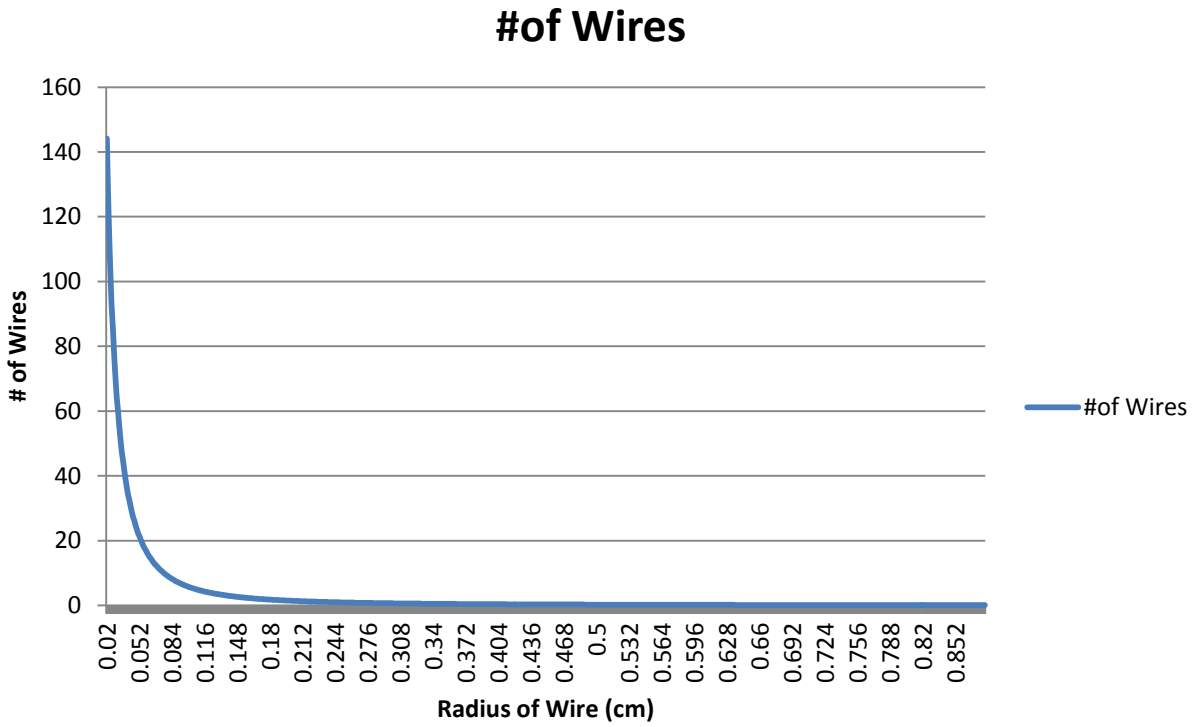

Figure 4.2: The number of wires required to generate 4.53 kN of force.

From this, we find that, when r = 0.16 cm, only one wire is required. Therefore, we have no need to use anything larger than this for this project. Now, unfortunately, this project is not funded by research funding, so the cost of running optimization experiments on 3 mm nitinol wire can easily run up into the thousands of dollars. Because of this, we decided to go with 0.5mm wires. Yes, 41 wires are required to generate the required force, but the nitinol cost of an optimization experiment is approximately $1-2 and the time in the oven is generally around 2-3 hours, allowing quick and cheap sample preparation.

4.1.2 Optimizing Heat Treatments: A full study of this matter requires optimizing both the alloy composition and the heat treatments. Since our lab does not have access to the equipment required to precisely determine the composition of an alloy (such as an X-Ray Diffractometer), we used one alloy and focused on optimizing the heat treatments.

4.1.2.1 Sample Preparation:

Samples were prepared using 0.5 mm diameter nitinol wire all cut from the same spool of wire. The precise make-up of this wire was not determined and it is assumed that the composition remains constant throughout the spool.

Samples were prepared using a jig plate, consisting of a 5/8" thick steel plate with approximately 300 holes drilled and tapped for a 6-32 machine screw on ½" centers. Each row was offset by ¼" for other manufacturing processes which have nothing to do with this project. Screws were screwed in from the back side, all the way down, to ensure that the plate sat flat inside the oven. On the front side, nuts were spun down to the plate and tightened. This provides a spacer to keep the nitinol wires up off of the steel. This allows the wires to only be heated by air and not have the heat source/sink of the steel affecting the heat treatment in a large way. It also prevents the diffusion of iron atoms into the nitinol matrix. This is important because interstitial iron suppresses M_s.[3] Wires were also trimmed 5mm shorter than where contact was made with the steel nut. The jig plate can be seen in Figure 4.3.

Figure 4.3: The jig plate used to hold nitinol wires during heat treatment. One of the benefits of this set-up is that the nitinol wire his held tight enough to go through several heat-quench cycles without loosening the wire. Wires can also be stacked on top of each other by using longer screws and spacing between them with nuts. Point A shows a nitinol wire prepared for heat treatment.

Figure 4.4: Experimental set-up for stretching wires. Machinist rule and nitinol wire are visible at the top.

Samples were first annealed at 550°C and quenched in water. Then they were aged at 375°C. Wires were annealed for 30, 60, or 90 minutes and aged for 0, 30, 60, 90 minutes. Measuring all six transition temperatures of the wire samples was very difficult because we did not have access to a differential scanning

calorimeter (DSC).[4] Instead, a rudimentary version of the bend and free recovery test was constructed.[5]

Samples were chilled below M_f and wrapped around a 20mm diameter mandrel giving the wires a 2.5% strain. They were then immersed in chilled water and gradually raised in temperature until the wire straightened. The temperature was monitored using a thermocouple thermometer. While this is rather basic, it gives us A_f with an accuracy of approximately 1-2°C, which is plenty for what we are doing.

Next, it was time to determine how much work could be done by each sample. Wires were attached to the top of an aluminum frame using a 6-32 machine screw and washer. A bucket was hung from the bottom of the wire with a gross weight of 5,000 g. This system can be seen in Figure 4.4. The wire was allowed to cool below M_f in ambient air. A hair dryer was then used to heat the nitinol wire above A_f. Data was photographically captured using a Canon T3i DSLR with a resolution of 18MP on a Targus tripod which had 4 degrees of freedom (3 rotational and one translational). The tripod also included a bubble level to ensure that shots were being taken perfectly horizontally to minimize error from parallax.

Image processing was accomplished using the public domain software package ImageJ. ImageJ was developed by the National Institutes of Health and has an open architecture which provides extensibility via Java plugins and recordable macros. The package is free to anyone who wishes to download it and it is very powerful. We only needed one function: to measure one-dimensional distances.

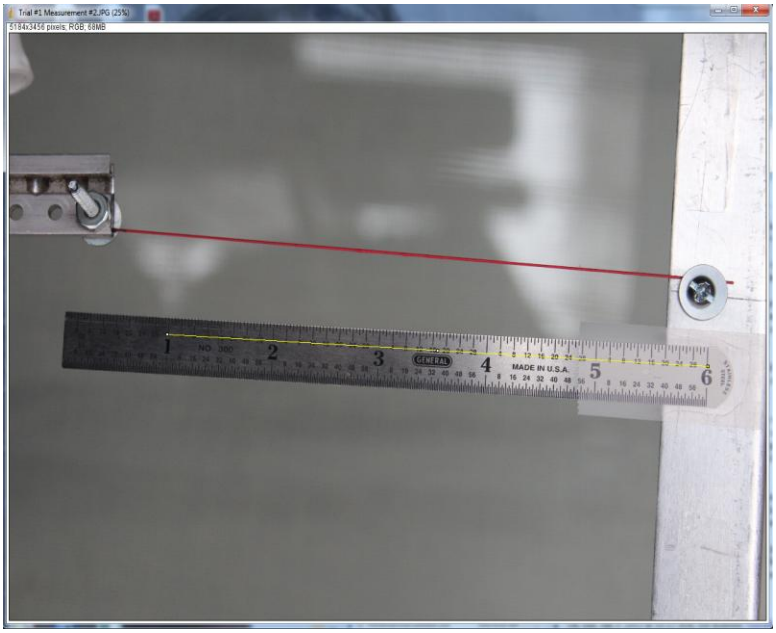

Figure 4.5: Using ImageJ to measure nitinol wires. The yellow line is the measurement line—currently being used to calibrate ImageJ to the distances measured in the picture. For the purpose of demonstration, the nitinol wire has been painted red to improve visibility.

For each image, ImageJ must be calibrated so that it knows how long of a distance is covered by each pixel. So, something with a known length must be used when capturing data. We used a machinist rule. It is marked to 1/64 of an inch and has an accuracy of 0.001" (25 μm). Here, we're calibrating a measurement of 5" (127 mm). This makes for a more accurate calibration because any error is spread across a larger distance.

For each sample, four wires were cut and tested. Each wire was photographed three times in its martensitic state and three times in its austenitic state. Measurements were averaged out and work per unit weight was calculated. One wire from each sample was tested for transition temperature.

Table 4.1

Anneal Temp (°C)	Anneal Time (min)	Aging Temp (°C)	Aging Time (min)	A_f (°C)
550	30	N/A	N/A	18
550	60	N/A	N/A	23
550	90	N/A	N/A	27
550	30	375	30	22
550	30	375	60	27
550	30	375	90	33

From Table 4.1, it is plain to see that, while the length of anneal time has a minimal effect on the transition temperature, aging at 375°C very rapidly raises with aging time. This confirms research published by Memry that annealing at 500-550°C sets the memory shape while aging at 350-400°C raises the transition temperature.

While there was some variation in the amount of work recovered from each sample of wire, the variation was small enough that it could have been caused by inaccuracies in our experimental set-up. So, for the purpose of this thesis, we will assume that varying the anneal time has little effect on the work output of the wire. For the remainder of this paper, we will assume that we can harvest 1.5 J/g per cycle. This experiment requires further examination, given additional time and funding. Before this experimental set-up can be fully trusted, it must be determined how to fully calibrate the set-up and determine the accuracy of the testing. Additionally, I'm not quite certain if this experimental set-up accurately models a nitinol wire producing work while acting against a bias spring.

Chapter 5: Proof of Concept Prototype

5.1 Design Process

In the early stages of this project, when we were brainstorming basic designs for this, we rapidly went through several possible designs. We started by considering a cart with a nitinol spring attached to a mass. When the nitinol spring warmed up, it would shoot the mass across the surface of the cart, propelling the cart in the opposite direction. The weakness of this design is obvious, that the cart can't travel much more than half its length per thermal cycle.

Next, we considered a mass on the end of a nitinol beam. The limitation here was two-fold: first that the cart couldn't change elevation any more than its own height in each thermal cycle and secondly that I read in The Proceedings on the Nitinol Heat Engine Conference that the recovery forces in nitinol are strongest in tension and in heat engines that used bending motion, mechanical failure occurred much sooner than in tensile engines. Additionally, if we could store the energy mechanically, then this frees us up in two ways: first that we can use the energy on demand rather than just when it is generated and secondly, that we can save up enough energy to accomplish significantly larger tasks. The advantage of storing energy mechanically rather than electrically or chemically is that the efficiency is near 100%. Each time energy is converted from one form to another, the efficiency goes down. So, to generate mechanical energy using nitinol and convert it to electrical energy (generate electricity), then convert it to chemical energy (charging batteries), then convert it back into electrical energy requires three conversions. If each conversion is optimistically rated at a 90% efficiency, we're looking at an efficiency of only 73%.

Figure 5.1: [illegible]way of a hydraulic-bladder accumulator. [illegible] parts of the hydraulic accumulator are: A) the steel casing, B) the nitrogen filled bladder and C) the oil storage area.

5.2 Energy Storage System

Building the energy storage system was relatively simple to do. There are really only a few ways to store mechanical potential energy: gravity, springs, and fluid pressure. As we discussed in Chapter 5.1, gravity has some rather severe limitations. Springs have the limitation that they can only sustain a certain strain elastically, and therefore have a relatively low upper limit of energy storage per unit weight. That leaves fluid pressure as the one effective method of storing mechanical energy. Air compressors can easily be purchased that run up to 120,000 psi, so scalability is not an issue. However, the

compressibility of air makes it an unsuitable medium for nitinol which has a relatively short stroke length. On the other hand, hydraulic oil is incompressible and hydraulic accumulators are readily available with working pressures up to 10,000 psi.

Hydraulic accumulators come in two styles: gravity and bladder. In a gravity-hydraulic accumulator, the pressurized oil lifts a weight. Clearly, this is not a good fit for our application. In a bladder accumulator, a rubber balloon filled with nitrogen initially fills the cavity of the accumulator. As oil fills the accumulator, the nitrogen is compressed. The one drawback to using a bladder accumulator is that the oil pressure in the accumulator drops as the volume of oil in the accumulator drops. But this weakness is small compared to the other options. For the purpose of this research, we used a 0.62 L accumulator with a maximum operating pressure of 1,500 psi (10MPa).

The amount of energy stored in a hydraulic accumulator can be found rather simply by

$$E = PV \qquad (6.1)$$

Since our accumulator holds 0.62 L (0.00062 m^3) of pressurized oil at a pressure of 10 MPa, it can store approximately 6,200 J.

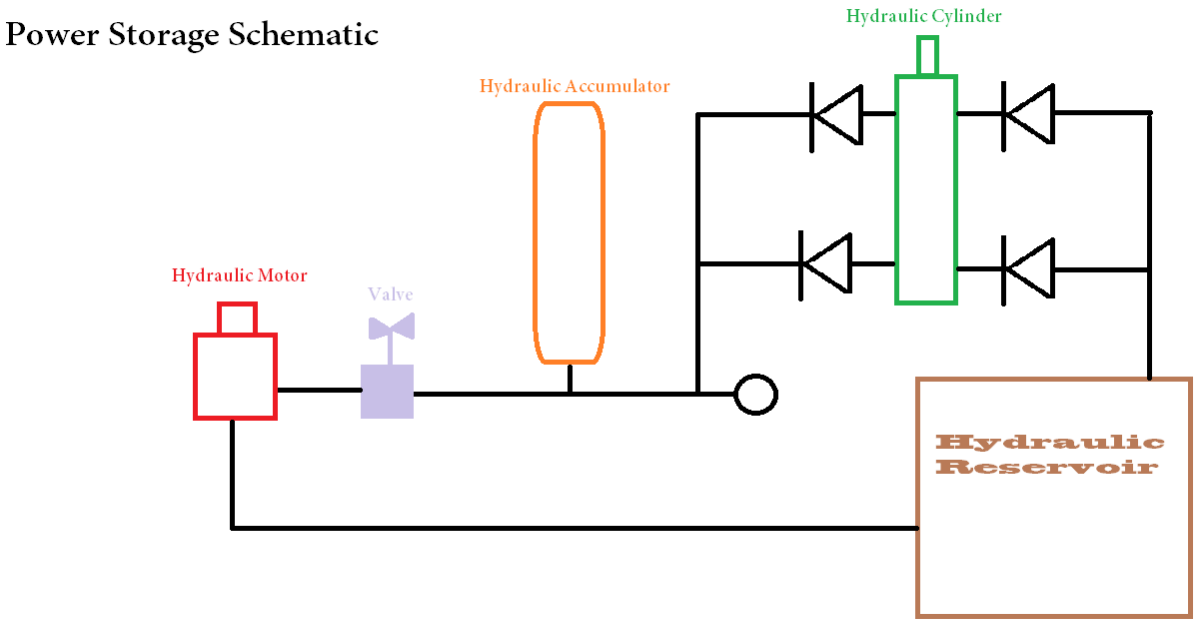

Figure 5.2: Schematic showing the power storage system used with this project.

5.3 Generator Construction

As we discussed in Chapter 5.1, it is important that the nitinol wires be acting in tension for optimal power generation. This presents a problem because hydraulic pumps use a rotary motion to pump oil. A simple solution to this problem was to use a hydraulic cylinder as a pump. Using a double acting hydraulic cylinder allows us to pressurize oil in both the recovery and the extension directions. Hydraulic check valves ensure that the oil can only travel in the desired direction. A schematic of this system can be seen in Figure 5.2. Since this is a double acting cylinder, the active area is different in each direction. According to the manufacturer's data, the area on the retraction cycle is 5.53 cm^2 and the area on the extension cycle is 4.53 cm^2. With a max pressure of 10 MPa, the force required to actuate this cylinder on its highest pressure stroke is 5.53 kN and 4.53 kN respectively.

For the nitinol mechanism, we decided to go with two layers of nitinol wires, one layer of shape memory wires to provide the actuation that we're looking for and one layer of superelastic nitinol wires to act as a bias spring. The advantage of using superelastic nitinol as the bias spring is tremendous: the deformations experienced by nitinol are so large that most metals cannot sustain them elastically. This means that if the bias spring were not made from nitinol, it would be required to be much larger than the nitinol element, adding weight and size to the generator. The two layers of nitinol wires are connected by a steel cable which wraps around a pulley. CAD drawings of the associated components of this generator can be found in Appendix C.

To keep track of the amount of energy stored in the hydraulic accumulator, we have a pressure gauge monitoring the pressure. Due to the small size of our oven, we were limited to making nitinol wires 160mm long—which results in a movement of just 3-5mm (depending on the strain level used). Therefore, it will take many thermal cycles to pressurize our hydraulic accumulator. So, we used a hair dryer to heat the nitinol wires above their transformation temperature. This way, we could make one thermal cycle every few minutes to quickly pressurize the accumulator. Then, to demonstrate that we stored usable energy, we used the oil to run a hydraulic motor to pick up a weight.

Chapter 6. Future Work

6.1 Scale Up

The obvious next step is to scale this model up to something useful. In our case, we will be scaling this large enough to power a golf cart. This will require a higher pressure hydraulic system, thicker nitinol wires, and an efficiently designed propulsion system. Additionally, the size of the hydraulic accumulators will need to be optimized for weight/performance ratio. ANSI Standard Z130.1 defines golf carts as being a small vehicle weighing 410-450 kg. If we add two 100 kg people plus 50 kg of cargo, this brings the total to 700 kg. If we assume that the coefficient of rolling friction is 0.1, then the energy to drive 1 km is

Figure 6.1: An example of a high end golf cart. Golf carts come in all shapes and sizes ranging from 2 passenger to 7 passenger vehicles.

$$E = \mu m d = 0.1 * 700 * 1000 = 70kJ \quad (6.1)$$

Following this model, given a 60 MPa system, we would need 117 L of storage to drive the one kilometer distance. Of course, designing for a lower coefficient of friction will extend the range of these vehicles.

On the scaled up model, it will be important to match the length of the hydraulic cylinder to the length of the wires. On the prototype, the cylinder had a stroke length of 100mm but the nitinol only had a stroke of 5mm—leaving most of the cylinder unused. Also, large diameter hydraulic cylinders have a higher power/weight ratio, so it will be important to use more wires per generator module to maximize this ratio.

This generator has a modular design so that the generator several generators can be slaved together to make a larger system. Additionally, if this generator is being used in a space constrained application (i.e.: powering a small cart), the generator modules can be easily swapped out when the weather dictates the need for a different transition temperature.

6.2 Wire Design

It is a bad assumption that wires need to have a circular cross-section. In fact, most nitinol suppliers also supply rectangular wire. A brief study of heat transfer reveals that the amount of time required for a nitinol wire to reach steady-state with its environment is related to the surface area of the wire (perimeter of the cross-section) and the radius of the thickest part of

the wire. Optimizing the heat transfer characteristics of the nitinol wires will allow us to use the thickest possible wire, reducing the number of wires required for a given generator. Fewer wires make for a more robust design with fewer points of failure.

By far, the most expensive part of the generator is the nitinol element. At 1.5 J/g, the cost of the nitinol required to build a generator that generates 1 Wh/cycle is somewhere in the area of $1,000. Improving the heat treatment profile of the wire to maximize the amount of work recovered per cycle will make the generator more efficient and cost effective. This requires an in depth look into the experiment detailed in Chapter 4.

In order to make an effective investigation into the heat treatment profile of the wires, acquiring access to a differential scanning calorimeter is an absolute must. With this instrumentation, we can look into the relationship between the indicator temperatures and the work harvested. I haven't been able to find any documentation on this topic.

Another good area of continued research would be to identify an optimum NiTiCu alloy. As the concentration of copper is reduced, the hysteresis grows. But, on the other hand, lower copper concentrations allow for greater strains which may result in greater work production per unit weight of nitinol—resulting in a lower cost of manufacture.

6.3 Coolant Integration

For the purpose of this research project, we did not use coolant in the proof of concept model. This was largely due to the need to simplify design, but as we discovered in Chapter 3, water makes a great evaporative coolant at temperatures greater than 10°C. Rubbing alcohol was another solution to evaporative cooling that wasn't horrendously expensive. Depending on the application, we may want to investigate the usefulness of using evaporative cooling to obtain additional thermal cycles per day. This would certainly bring the cost of the generator down substantially.

Bibliography

Chapter 1 References:

1. World Crude Oil and Natural Gas Reserves. US Department of Energy, Energy Information Administration, 2009.
2. Di Blasi, Colmba. Modeling Chemical and Physical Processes of Wood and Biomass Pyrolysis. Progress in energy and Combustion Science, 2008.
3. Araujo, C. D., et al. A Diffusion Model for Spin-Spin Relaxation of Compartmentalized Water in Wood. Journal of Magnetic Resonance, 1993.
4. Kocaefe, Duygu. Comparison of Different Models for the High-Temperature Heat-Treatment of Wood. International Journal of Thermal Sciences, 2007.
5. Sand, U. Numerical Predition of the Transport and Pyrolysis in the Interior and Surrounding of Dry and Wet Wood Log. Applied Energy, 2008.
6. Mader, Sylvia. Biology, 10th Edition. McGraw-Hill, 2009.
7. Hart, Peter W. Fundamental Advances and Innovations in the Pulp and Paper Industry. American Institute of Chemical Engineers, 1999.
8. Otsuka, K. and Wayman, C. M. Shape Memory Materials. Cambridge University Press, 1999.
9. Lagoudas, Dimitris C. Shape Memory Alloys: Modeling and Engineering Applications. Springer, 2008.
10. Li, Kam W. Power Plant System Design. John Wiley & Sons Inc., 1985.
11. Jackson, C. M. et al. Nitinol-55—The Alloy With a Memory: Its Physical Metallurgy, Properties and Applications. NASA-SP 5110, National Aeronautics and Space Administration, Washington, DC, 1972.
12. Mehta, A., et al. On the Electronic and Mechanical Instabilities in $Ni_{50.9}Ti_{49.1}$. Materials Science & Engineering A, 2004.
13. Shaw, J. A. Tips and Tricks for Characterizing Shape Memory Alloy Wire: Part 1—Differential Scanning Calorimetry and Basic Phenomena. Experimental Techniques, 2008.
14. Sergueeva, A. V. Structure and Properties of Amorphous and Nanocrystalline NiTi Prepared by Severe Plastic Deformation and Annealing. Materials Science & Engineering A, 2003.
15. Uchil, J. Effect of Thermal Cycling on R-Phase Stability in a NiTi Shape Memory Alloy. Materials Science & Engineering A, 2002.
16. Kauffman, George B. and Mayo, Isaac. The Story of Nitinol: The Serendipitous Discovery of the Memory Metal and its Applications. The Chemical Educator, Springer, 1996.
17. Ford, D. S. and White, S. R. Thermomechanical Behavior of 55Ni45Ti Nitinol. Acta Materialla, 1996.
18. Hall, E. O. Twinning and Diffusionless Transformations in Metals. Butterworth Publishing, 1954.
19. Bhattacharya, Kaushik. Microstructure of Martensite: Why It Forms and How It Gives Rise to the Shape Memory Effect. Oxford University Press, 2004.

20. Lei, Xu. The Optimization of Annealing and Cold Drawing in the Manufacture of the Ni-Ti Shape Memory Alloy Ultra-Thin Wire. International Journal of Advanced Manufacturing Technology, 2011.
21. Kim, J. I. and Miyazaki, S. "Effect of Low Temperature Aging on the R-Phase Transformation of a Ti-50.9at% Ni Alloy." Shape Memory Alloys and Its Applications: Proceedings of the International Conference on Shape Memory and Superelastic Technologies and Shape Memory Materials (SMST-SMM 2001). Trans Tech Publications, Ltd., 2002.
22. Nam, T. H. et al. "The B2-B19-B19' Transformation in a Ti-44.7Ni-5Cu-0.3Mo Alloy." Shape Memory Alloys and Its Applications: Proceedings of the International Conference on Shape Memory and Superelastic Technologies and Shape Memory Materials (SMST-SMM 2001). Trans Tech Publications, Ltd., 2002.
23. Bidaux, J. E. "Vibration Frequency Control of Composites Using the R-Phase Transformation of NiTi Alloys." Proceedings of the Second International Conference on Shape Memory and Superelastic Technologies. The International Organization on Shape Memory and Superelastic Technologies, 1997.
24. Sengupta, Arkaprabha and Papadopoulos, Panayiotis. Constitutive Modeling and Finite Element Approximation of B2-R-B19' Phase Transformations in Nitinol Poloycrystals. Computer Methods in Applied Mechanics and Engineering, 2009.
25. Lendlein, A. and Langer, R. Biodegradable Elastic Shape Memory Polymers for Potential Biomedical Applications. Science, May 2002.
26. Gall, K., et al. Internal Stress Storage in Shape Memory Polymer Nanocomposites. Applied Physics Letters, 2004.
27. Hayashi, Shunichi, et al. Room Temperature Functional Shape Memory Polymers. Plastics Engineering, Society of Plastics Engineers, 1995.
28. Leng, Jinsong, et al. Electroactive Thermoset Shape Memory Polymer Nanocomposite Filled with Nanocarbon Powders. Smart Materials and Structures, IOP Publishing, 2009.
29. Volk, Brent, Whitley, Karen. Characterization of Shape Memory Polymers. NASA Research and Technology Directorate, Mechanics of Structures and Materials Branch, 2007.
30. Leng, Jinsong and Du, Shanyi. Shape-Memory Polymers and Multifunctional Composities. CRC Press, 2010.
31. Bernal, Laura Isabel Barbero. Cyclic Behavior of Superelastic Nickel-Titanium and Nickel-Titanium-Chromium Shape Memory Alloys: A Thesis. Georgia Institute of Technology, 2004.
32. DesRoches, Reginald, et al. Cyclic Properties of Superelastic Shape Memory Alloy Wires and Bars. Georgia Institute of Technology, 2005.
33. McNaney, J. M., et al. An Experimental Study of the Superelastic Effect in a Shape-Memory Nitinol Alloy Under Biaxial Loading. Mechanics of Materials, 2003.
34. ASTM Standard F2005-05: Standard Terminology for Nickel-Titanium Shape Memory Alloys. ASTM International, 2010.
35. ASTM Standard F2633-07 Standard Specification for Wrought Seamless Nickel-Titanium Shape Memory Alloy Tube for Medical Devices and Surgical Implants. ASTM International, 2007.
36. ASTM Standard F2516-07E2: Standard Test Method for Tension Testing of Nickel-Titanium Superelastic Materials. ASTM International, 2007.

37. Sanders et al. Nitinol Spinal Instrumentation and Method for Surgically Treating Scoliosis. US Patent & Trademark Office, Patent # 5,290,289, 1994.
38. Wu, M. H., et al. "What is the Big Deal About the A_f Temperature?" SMST-2006: Proceedings of the International Conference on Shape Memory and Superelastic Technologies. ASM International, 2006.
39. ASTM Standard F2082-06: Standard Test Method for Determination of Transformation Temperature of Nickel-Titanium Shape Memory Alloys by Bend and Free Recovery. ASTM International, 2006.
40. ASTM Standard F2004-05: Standard Test Method for Transformation Temperature of Nickel-Titanium Alloys by Thermal Analysis. ASTM International, 2010.
41. Rice, C. and Sczerzenie, F. "Design and Performance of a Functional A_f Tester." SMST-97 Proceedings of the Second International Conference on Shape Memory and Superelastic Technologies. SMST, 1997.
42. Chanduszko, Andrzej. "Determination of Nitinol Transition Temperatures Using a Dynamical Mechanical Analyzer." SMST-2000: Proceedings on the International Conference on Shape Memory and Superelastic Technology. The International Organization on Shape Memory and Superelastic Technology.
43. Duerig, Thomas, et al. Nitinol. ASM International, 2012.
44. Saigal, Anil and Fonte, Matthew. Solid, Shape Recovered "Bulk" Nitinol: Part I—Tension-Compression Asymmetry. Materials Science & Engineering A, 2011.
45. Saigal, Anil and Fonte, Matthew. Solid, Shape Recovered "Bulk" Nitinol: Part II—Mechanical Properties. Materials Science & Engineering, 2011.
46. Adharapurapu, Raghavendra R. et al. Influence of Cold Work and Texture on the High-Strain-Rate Response of Nitinol. Materials Science & Engineering A, 2010.
47. Melton, K. Engineering Aspects of Shape Memory Alloys. Butterworth-Heinemann, LTD., 1990.
48. Neurohr, Anselm J. and Dunand, David C. Mechanical Anisotropy of Shape-Memory NiTi with Two-Dimensional Networks of Micro-Channels. Acta Materialia 59, 2011.
49. Duerig, T. W. and Pelton, A. R. "An Overview of Superelastic Stent Design." SMST-2001: Shape Memory Materials and Its Appications. Trans Tech Pubications, Inc., 2002.
50. Song, C. et al. "Thermal Modelling of a Shape-Memory Alloy Fixator for Minimal-Access Surgery." SMST-2001: Shape Memory Materials and Its Appications. Trans Tech Pubications, Inc., 2002.
51. Takaoka, S. et al. "Applications and Development of Shape-Memory and Superelastic Alloys in Japan." SMST-2001: Shape Memory Materials and Its Appications. Trans Tech Pubications, Inc., 2002.
52. Morgan, N. B. Medical Shape Memory Alloy Applications—The Market and Its Products. Materials Science & Engineering A, 2004.
53. Ryhanen, Jorma. "Biocompatability of Nitinol." SMST-2000: Proceedings on the International Conference on Shape Memory and Superelastic Technologies. SMST, The International Organization on Shape Memory and Superelastic Technology, 2001.
54. Wu, Ming H. and Schetky, L. McD. "Industrial Applications for Shape Memory Alloys." SMST-2000: Proceedings on the International Conference on Shape Memory and Superelastic Technologies. SMST, The International Organization on Shape Memory and Superelastic Technology, 2001.

55. Yoshida, Eiichi, et al. Micro Self-Reconfigurable Modular Robot Using Shape Memory Alloy. Mechanical Engineering Laboratory, AIST, MITI, Japan.
56. Ahn, Kyoung Kwan and Nguyen, Bao Kha. Position Control of Shape Memory Alloy Actuators Using Self Tuning Fuzzy PID Controller. International Journal of Control, Automation, and Systems, 2006.
57. Wu, Tony and Wu, Ming H. "NiTi-Nb Plugs for Sealing High Pressure Fuel Passages in Fuel Injector Applications." SMST-2000: Proceedings on the International Conference on Shape Memory and Superelastic Technologies. SMST, The International Organization on Shape Memory and Superelastic Technology, 2001.
58. Orlando, Carl. Trigger Circuit: US Patent 4,002,954. United States Patent and Trademark Office, 1977.
59. Bidaux, J. E., et al. "Active Modification of the Vibration Frequencies of a Polymer Beam Using Shape Memory Alloy Fibers." Third International Conference on Intelligent Materials: Third European Conference on Smart Structures and Materials. The International Society for Optical Engineering, 1997.
60. Song, G., et al. Applications of Shape Memory Alloys in Civil Structures. Engineering Structures, 2006.
61. Li, Yao T. Nitinol Engine for Low Grade Heat: US Patent 4,302,938. United States Patent and Trademark Office, 1981.
62. Banks, Ridgway M. Linear Output Nitinol Engine: US Patent 4,563,876. United States Patent and Trademark Office, 1986.
63. Banks, Ridgway M. Single Wire Nitinol Engine: US Patent 4,450,686. United States Patent and Trademark Office, 1984.
64. Banks, Ridgway M. "The Banks Engine: Past, Present and Future." Proceedings on the Nitinol Heat Engine Conference. Naval Surface Weapons Center, 1978.
65. Ginell, W. S., et al. "One Horsepower Thermoturbine Nitinol Engine." Proceedings on the Nitinol Heat Engine Conference. Naval Surface Weapons Center, 1978.

Chapter 3 References:

1. Li, Kam W. Power Plant System Design, John Wiley & Sons, Inc. 1985
2. Ashbez, K. H. G. "Representation of Martensitic Transformation in Shape Change Space, the Nature of Internal Stress Retained During SM Transformation, and the Operational Performance of a Simple Nitinol Engine." Proceedings on the Nitinol Heat Engine Conference. Naval Surface Weapons Center, 1978.
3. Wikipedia. "Vapor Pressure." 20 December 2012.
4. Material Safety Data Sheet for Propylene Glycol. Prestone. 2012
5. Wikipedia. "Propylene Glycol." 29 December 2007.

Chapter 4 References:

1. Ashbez, K. H. G. "Representation of Martensitic Transformation in Shape Change Space, the Nature of Internal Stress Retained During SM Transformation, and the Operational Performance of a Simple Nitinol Engine." Proceedings on the Nitinol Heat Engine Conference. Naval Surface Weapons Center, 1978.
2. Shaw, J. A. Tips and Tricks for Characterizing Shape Memory Alloy Wire: Part 1—Differential Scanning Calorimetry and Basic Phenomena. Experimental Techniques, 2008.

3. Duerig, Thomas, et al. Nitinol. ASM International, 2012.
4. ASTM Standard F2082-06: Standard Test Method for Determination of Transformation Temperature of Nickel-Titanium Shape Memory Alloys by Bend and Free Recovery. ASTM International, 2006.
5. ASTM Standard F2004-05: Standard Test Method for Transformation Temperature of Nickel-Titanium Alloys by Thermal Analysis. ASTM International, 2010.

Appendix A: Material Safety Data Sheets for Chemicals Used

Product Safety Assessment (PSA): Propylene Glycol

Names

- CAS No. 57-55-6
- Propylene glycol
  - PG
- 1,2-Dihydroxypropane
  - Propane-1,2-diol
  - 1,2-Propanediol
- Monopropylene glycol
  - MPG

Product Overview

- Propylene glycol (PG or MPG) is a colorless, odorless liquid[1] which is generally recognized as safe (GRAS) by the U.S. Food and Drug Administration (FDA) in 21 CFR § 184.1666, for use as a direct food additive under the conditions prescribed. It is approved by the U.S. FDA for certain indirect food additive uses.[2] PG is used in cosmetics and as an excipient (inert solvent or carrier) in pharmaceuticals. PG has a wide range of practical applications such as antifreezes, coolants and aircraft deicing fluids; heat transfer and hydraulic fluids; solvents; food; flavors and fragrances; cosmetics and personal care products; pharmaceuticals; chemical intermediates; plasticizers; and thermoset plastic formulations.[3] See Product Uses.
- PG is not acutely toxic (single dose, high exposure). It is essentially non-irritating to the skin and mildly irritating to the eyes. Numerous studies support that PG is not a skin sensitizer or a carcinogen.[4] See Health Information.
- Occupational and consumer exposure is possible because PG is used in a variety of consumer items. See Exposure Potential.
- PG is not volatile and is miscible with water. It is not expected to bio-accumulate and it is not acutely toxic to water organisms except at very high concentrations.[5] See Environmental Information.

Manufacture of Product

- **Capacity –** Dow is the world's largest producer of propylene glycols, with about 35% of the world's capacity. Dow has plants in the U.S. Germany, Brazil and Australia. Total world consumption of PG in 2003 was estimated at 2.6 billion pounds (1.2 million metric tons).[6]
- **Process**[7]**–** Practically all commercial production of PG is by non-catalytic hydrolysis of propylene oxide using high temperatures and high pressures.

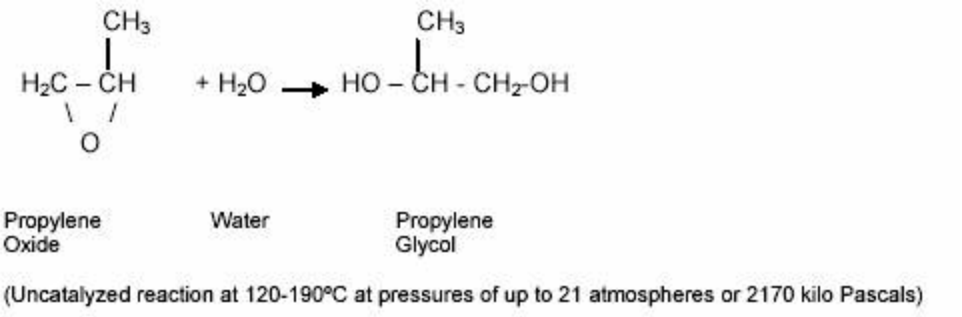

Product Description

PG is a colorless, odorless liquid. It is soluble to various extents in a wide range of organic materials, and is completely soluble in water.[8]

Product Uses

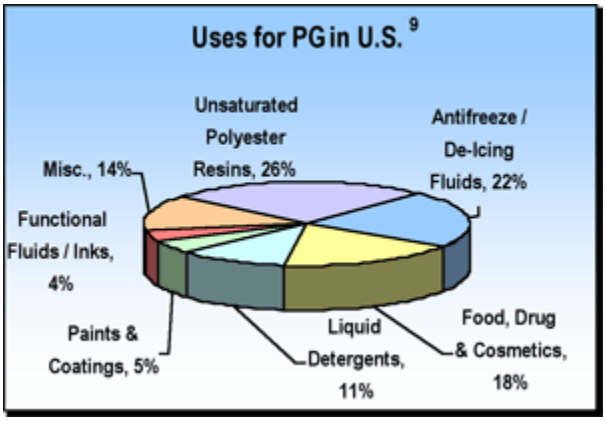

Dow markets two grades of PG to meet the requirements of the various applications. PG is used in a wide range of applications, including:[9,10,11]

- USP/EP grade:
  - Solvent in the flavor concentrate and fragrance industry, an excipient in elixirs and pharmaceuticals, and a coupling agent in sunscreens, shampoos, shaving creams and other personal care products
  - Wetting agent for natural gums to simplify compounding
  - Humectant, preservative and stabilizer in diverse applications.
- Industrial grade:
  - Raw material to produce high-performance unsaturated polyester resins (UPR) used for marine construction, gel coats, sheet molding compounds and synthetic marble castings
  - Chemical intermediate in the production of resins for paints and varnishes
  - Solutions with water to make antifreeze, heat-transfer fluids and aircraft and runway deicing fluids
  - Solvent in printing inks
  - Solvent and enzyme stabilizer in laundry detergents
  - Stabilizer in hydraulic fluids
  - Plasticizer to improve the processability of plastics

Exposure Potential

PG is used in the production of consumer and industrial products. Based on the uses for PG, the public could be exposed through:

- **Workplace exposure** – Exposure can occur either in a PG manufacturing facility or in the various industrial, commercial service or consumer settings that use PG. Because PG is not acutely toxic and is not a sensitizer, low incidental exposures do not pose high health risks. However, each manufacturing, commercial service and consumer facility should have appropriate work processes and safety equipment policies in place to limit unnecessary PG exposure. Skin exposure is the most likely site for PG exposure in the work place; however in commercial service and consumer settings, use as a functional fluid or in deicing solutions presents a potential for inhalation exposure in addition to skin contact.[12] For more information on inhalation, see Health Information.
- **Consumer exposure to products containing PG** – Dow does not sell PG for direct consumer use, but it is used as a component in cosmetics, food additives, antifreeze, deicers, liquid detergents, etc. Consumers will likely have contact with PG. In general, exposure by ingestion is a result of the approved use of PG USP/EP grade in food, personal care and pharmaceutical products. Skin exposure, and to a lesser degree, inhalation exposure, are expected from the use of cosmetic products containing PG. Please review product labels and follow all instructions and guidelines for proper use to help prevent unnecessary exposure.[13] See Health Information.
- **Environmental releases** – In the event of a spill, the focus is on containing the spill to prevent contamination of soil, surface or ground water. If PG does reach soil and water nearby, it is considered practically non-toxic to aquatic organisms and it biodegrades rapidly. If PG is present in a fire situation, it can produce toxic fumes. Proper protective equipment should be worn.[14] See Environmental, Health and Physical Hazard Information.
- **Large release** – Industrial spills or releases are infrequent and are generally contained. If a large spill does occur, the material should be captured, collected and re-processed, or disposed of according to applicable governmental requirements. If PG is exposed to a fire situation, it can decompose and release toxic fumes. Emergency personnel should wear proper protective equipment and follow emergency procedures carefully. When relevant in scale or risk, the community should be notified of the hazards associated with the specific release event. See Environmental, Health and Physical Hazard Information.

Health Information

The toxicology database for PG has been reviewed and agreed upon by the Organization for Economic Co-operation and Development (OECD) SIAM[15] process. The oral toxicity of PG is low. In one study, rats were provided with feed containing as much as 5% PG over a period of 104 weeks and they showed no apparent ill effects.[16] Because of its low chronic oral toxicity, PG is generally recognized as safe (GRAS) for use as a direct food additive. Since 1942, it has been included in New and Non-Official Remedies as a proper ingredient for pharmaceutical products and it is listed in the United States Pharmacopoeia. It is also widely used and accepted as an ingredient in dental preparations.[17] PG is not approved for use in cat food.

Prolonged PG contact is essentially non-irritating to the skin. Undiluted PG is minimally irritating to the eye, and can produce slight transient conjunctivitis (the eye recovers after the exposure is removed). Exposure to mists may cause eye irritation, as well as upper respiratory

tract irritation.[18] Inhalation of the PG vapors appears to present no significant hazard in ordinary applications. However, limited human experience indicates that inhalation of PG mists may be irritating to some individuals. Therefore inhalation exposure to mists of these materials should be avoided. In general, Dow does not support or recommend the use of PG in applications where inhalation exposure or human eye contact with the spray mists of these materials is likely, such as fogs for theatrical productions or antifreeze solutions for emergency eye wash stations.[19]

PG does not cause sensitization and shows no evidence of being a carcinogen or of being genotoxic.[20]

For more information on the health hazards of PG and recommended protective equipment, view the Safety Data Sheet.

Environmental Information

PG is not volatile, and is miscible with water. Concentrations of PG in the air are expected to be extremely low because of its low vapor pressure. It is readily biodegraded in water or soil (*via* aerobic and anaerobic mechanisms).

If a spill should occur, PG partitions almost equally in water and soil. Relatively little will go into the air because of its low vapor pressure. PG is not expected to bio-accumulate and is considered to be practically non-toxic to fish and aquatic invertebrates on an acute basis except at very high concentrations.

Physical Hazard Information

PG has a low vapor pressure and is not expected to volatilize. PG is stable unless elevated to high temperatures, at which point it can decompose. During a fire, smoke may contain the original material in addition to unidentified toxic and/or irritating compounds. Hazardous combustion products may include and are not limited to: aldehydes and carbon monoxide.

As with any liquid, spills can create slip hazards. Small spills should be cleaned up with absorbent material which should then be properly labeled and disposed of. Even though the toxicity of PG is low, PG should not be dumped into any sewer, on the ground or into any body of water. All disposal methods must be in compliance with all applicable governmental requirements.

PG should be stored in stainless steel, aluminum, Plasite 3066-lined containers, 316 stainless steel, or opaque plastic containers. Product should not be stored in direct sunlight or at elevated temperatures. Avoid contact with oxidizing materials. Additional physical property information for PG is available on the Safety Data Sheet.

Regulatory Information

Regulations may exist that govern the manufacture, sale, transportation, use and/or disposal of PG. These regulations may vary by city, state, country or geographic region. Information may be found by consulting the relevant Safety Data Sheet

1. Product and Company Identification
Product Code: QVM46
Product Name: Klean Strip VM&P Naphtha
Reference #: 1650
Manufacturer Information
Company Name: W. M. Barr
2105 Channel Avenue
Memphis, TN 38113
Phone Number: (901)775-0100
Emergency Contact: 3E 24 Hour Emergency Contact (800)451-8346
Information: W.M. Barr Customer Service (800)398-3892
Web site address: www.wmbarr.com
2. Composition/Information on Ingredients
Petroleum ether
Hazardous Components (Chemical Name)
CAS # 8032-32-4 **ACGIH TWA** 300 ppm
Percentage 95.0 -100.0 % **Other Limits** No data.
OSHA TWA 100 ppm
Hazardous Components (Chemical Name) Petroleum ether
RTECS # OI6180000 **ACGIH STEL** 150 ppm
OSHA STEL 500 ppm/(10min) **ACGIH CEIL** No data.
OSHA CEIL 300 ppm
3. Hazards Identification
Danger! Flammable. Keep away from heat, sparks, flame and all other sources of ignition. Vapors may cause flash fire or ignite explosively. Vapors may travel long distances to other areas and rooms away from work site.
Do not smoke. Extinguish all flames and pilot lights, and turn off stoves, heaters, electric motors and all other sources of ignition anywhere in the structure, dwelling or building during use and until all vapors are gone from the work site and all areas away from the work site. Keep away from electrical outlets and switches. Beware of static electricity that may be generated by synthetic clothing and other sources.
Emergency Overview
OSHA Regulatory Status: This material is classified as hazardous under OSHA regulations.
Inhalation Acute Exposure Effects: Vapor harmful. May cause dizziness, headache, irritation of respiratory tract, weakness, drowsiness, depression of central nervous system, and watering of eyes. Severe overexposure may cause unconsciousness, anesthesia, irregular heartbeat, and death. Intentional misuse of this product by deliberately concentrating and inhaling can be harmful or fatal.
Skin Contact Acute Exposure Effects: This product is a skin irritant. It may be absorbed through the skin. It may cause irritation, dermatitis, drying of skin, and numbness in fingers and arms. May increase severity of symptoms listed under inhalation.
Eye Contact Acute Exposure Effects: This material is an eye irritant. It may cause irritation, redness, stinging, tearing, excessive swelling of the conjunctiva; and or excessive blinking.
Ingestion Acute Exposure Effects: Harmful or fatal if swallowed. May cause nausea, vomiting, gastrointestinal irritation, or diarrhea.
Health Hazards (Acute and Chronic)

Chronic Exposure Effects: Reports have associated repeated and prolonged overexposure to solvents with neurological and other physiological damage. Prolonged or repeated contact may cause dermatitis. May cause skin irritation, permanent central nervous system changes, kidney damage, and liver damage.
Primary Routes of Exposure: Inhalation; ingestion; and dermal.

Signs and Symptoms Of Exposure

Diseases of the skin, liver, and kidneys.

Medical Conditions Generally Aggravated By Exposure

HEALTH HAZARDS : N/E
PHYSICAL HAZARDS : N/E
TARGET ORGANS & EFFECTS: N/E

OSHA Hazard Classes:

4. First Aid Measures

Inhalation: If user experiences breathing difficulty, move to air free of vapors. Administer oxygen or artificial respiration until medical assistance can be rendered.
Skin Contact: Irritation may result. Immediately wash with soap and water.
Eye Contact: Immediately flush with water, remove any contact lenses, continue flushing with water for at least 15 minutes, then get medical attention.
Ingestion: Do not induce vomiting. Call you local poison control center, hospital emergency room, or physician immediately for instructions.

Emergency and First Aid Procedures

Call your local poison control center for further information.

Note to Physician

5. Fire Fighting Measures

Flammability Classification: OSHA Class IB
Flash Pt: 50.00 F Method Used: SCC
Explosive Limits: LEL: 0.9 UEL: No data.
Autoignition Pt: No data.

Special Fire Fighting Procedures

Self-contained respiratory protection should be provided for fire fighters fighting fires in buildings or confined areas. Storage containers exposed to fire should be kept cool with water spay to prevent pressure build-up. Stay away from heads of containers that have been exposed to intense heat or flame.

Unusual Fire and Explosion Hazards

No data available.

Extinguishing Media

Use carbon dioxide, dry powder, or foam.

Unsuitable Extinguishing Media

No data available.

6. Accidental Release Measures

Cleanup: Keep unnecessary people away; isolate hazard area and deny entry. Stay upwind, out of low areas, and ventilate closed spaces before entering. Shut off ignition sources; keep flares, smoking or flames out of hazard area.
Small Spills: Take up liquid with sand, earth or other noncombustible absorbent material and place in a plastic container where applicable.
Large Spills: Dike far ahead of spill for later disposal.

Steps To Be Taken In Case Material Is Released Or Spilled

7. Handling and Storage

Read carefully all cautions and directions on product label before use. Since empty container retains residue, follow all label warnings even after container is empty. Dispose of empty container according to all regulations. Do not reuse this container.

Precautions To Be Taken in Handling

Keep container tightly closed when not in use. Store in a cool, dry place. Do not store near flames or at elevated temperatures.

Precautions To Be Taken in Storing

8. Exposure Controls/Personal Protection

For OSHA controlled work place and other regular users --Use only with adequate ventilation under engineered air control systems designed to prevent exceeding appropriate TLV. For occasional use, where engineered air
control is not feasible, use properly maintained and properly fitted NIOSH approved respirator for organic solvent vapors. A dust mask does not provided protection against vapors.

Respiratory Equipment (Specify Type)

Safety glasses, chemical goggles or face shields are recommended to safeguard against potential eye contact, irritation, or injury. Contact lenses should not be worn while working with chemicals.

Eye Protection

Wear impermeable gloves. Gloves contaminated with product should be discarded. Promptly remove clothing that becomes soiled with product.

Protective Gloves

Various application methods can dictate the use of additional protective safety equipment, such as impermeable aprons, etc., to minimize exposure. A source of clean water should be available in the work area for flushing eyes and skin. Do not eat, drink, or smoke in the work area. Wash hands thoroughly after use. Before reuse, thoroughly clean any clothing or protective equipment that has been contaminated by prior use. Discard any clothing or other protective equipment that cannot be decontaminated, such as gloves or shoes.

Other Protective Clothing

Use only with adequate ventilation to prevent buildup of vapors. Do not use in areas where vapors can accumulate and concentrate such as basements, bathrooms, or small enclosed areas. Whenever possible, use outdoors in an open area. If using indoors, open all windows and doors and maintain a cross ventilation of moving fresh air across the work area. If strong odor is noticed or you experience slight dizziness, headache, nausea or eye-watering -- Stop -- ventilation is inadequate. Leave area immediately. If the work area is not well ventilated, then do not use this product. A dust mask does not provide protection against vapors.

Ventilation

9. Physical and Chemical Properties

Physical States: [ ] Gas [X] Liquid [ ] Solid
Melting Point: No data.
Boiling Point: > 242.00 F
Autoignition Pt: No data.
Flash Pt: 50.00 F Method: SCC
Explosive Limits: LEL: 0.9 UEL: No data.
Specfic Gravity: 0.000000

Bulk Density: 6.250 LB/GA
Vapor Presure: No data.
Vapor Density: No data.
Evaporation Rate: No data.
Solubility in Water: No data.
Percent Volatile: 99.999 % by weight.
VOC / Volume: 749.0000 G/L
Corrosion Rate: No data.
pH: No data.
Appearance and Odor No data available.

10. Stability and Reactivity

Stability: Unstable [ ] Stable [X]
Conditions To Avoid – Instability No data available.
Incompatibility - Materials To Avoid Incompatible with strong oxidizing agents.
Hazardous Decomposition Or Byproducts Decomposition may produce carbon monoxide and carbon dioxide.
Hazardous Polymerization: Will occur [ ] Will not occur [X]
Conditions To Avoid - Hazardous Polymerization No data available.

11. Toxicological Information

Toxicological Information
No data available.
Carcinogenicity/Other Information
No data available.
Carcinogenicity: NTP? No IARC Monographs? No OSHA Regulated? No

12. Ecological Information

Ecological Information
No data available.

13. Disposal Considerations

Waste Disposal Method
Dispose in accordance with local, state, and federal regulations.

14. Transport Information

LAND TRANSPORT (US DOT)
DOT Proper Shipping Name
No data available.

15. Regulatory Information

US EPA SARA Title III
Hazardous Components (Chemical Name) Petroleum ether

CAS #8032-32-4	**Sec.304 RQ** No	**Sec.110** No
Sec.302 (EHS) No	**Sec.313 (TRI)** No	

US EPA CAA, CWA, TSCA
Hazardous Components (Chemical Name) Petroleum ether

CAS #8032-32-4	**EPA CWA NPDES** No	**CA PROP 65** No
EPA CAA No	**EPA TSCA** No	

SARA (Superfund Amendments and Reauthorization Act of 1986) Lists:

Sec.302: EPA SARA Title III Section 302 Extremely Hazardous Chemical with TPQ. * indicates 10000 LB TPQ if not volatile.
Sec.304: EPA SARA Title III Section 304: CERCLA Reportable + Sec.302 with Reportable Quantity. **indicates statutory RQ.
Sec.313: EPA SARA Title III Section 313 Toxic Release Inventory. Note: -Cat indicates a member of a chemical category.
Sec.110: EPA SARA 110 Superfund Site Priority Contaminant List
TSCA (Toxic Substances Control Act) Lists:
5A(2): Chemical Subject to Significant New Rules (SNURS)
6A: Commercial Chemical Control Rules
8A: Toxic Substances Subject To Information Rules on Production
8A CAIR: Comprehensive Assessment Information Rules - (CAIR)
8A PAIR: Preliminary Assessment Information Rules - (PAIR)
8C: Records of Allegations of Significant Adverse Reactions
8D: Health and Safety Data Reporting Rules
8D TERM: Health and Safety Data Reporting Rule Terminations
Other Important Lists:
CWA NPDES: EPA Clean Water Act NPDES Permit Chemical
CAA HAP: EPA Clean Air Act Hazardous Air Pollutant
CAA ODC: EPA Clean Air Act Ozone Depleting Chemical (1=CFC, 2=HCFC)
CA PROP 65: California Proposition 65
This material meets the EPA 'Hazard Categories' defined for SARA Title III Sections 311/312 as indicated:
EPA Hazard Categories:
[ ] Yes [X] No Acute (immediate) Health Hazard
[ ] Yes [X] No Chronic (delayed) Health Hazard
[ ] Yes [X] No Fire Hazard
[ ] Yes [X] No Reactive Hazard
[ ] Yes [X] No Sudden Release of Pressure Hazard

16. Other Information

The information contained herein is presented in good faith and believed to be accurate as of the effective date shown above. This information is furnished without warranty of any kind. Employers should use this information only as a supplement to other information gathered by them and must make independent determination of suitability and completeness of information from all sources to assure proper use of these materials and the safety and health of employees. Any use of this data and information must be determined by the user to be in accordance with applicable federal, state and local laws and regulations.

Material Safety Data Sheet
Isopropyl alcohol 70% in water

ACC# 89530

Section 1 - Chemical Product and Company Identification

MSDS Name: Isopropyl alcohol 70% in water
Catalog Numbers: AC613190040, AC613245000, A459-1, A459-20, A459-4, A459-500, NC9290641, NC9405257, NC9524653, NC9761180
Synonyms: Isopropanol; Dimethylcarbinol; sec-Propyl alcohol; Rubbing alcohol; Petrohol; 1-Methylethanol; 1-Methylethyl alcohol; 2-Hydroxypropane; 2-Propyl alcohol; Isopropyl alcohol; Propan-2-ol; IPA; 2-Propanol.
Company Identification:
Fisher Scientific
1 Reagent Lane
Fair Lawn, NJ 07410
For information, call: 201-796-7100
Emergency Number: 201-796-7100
For CHEMTREC assistance, call: 800-424-9300
For International CHEMTREC assistance, call: 703-527-3887

Section 2 - Composition, Information on Ingredients

CAS#	Chemical Name	Percent	EINECS/ELINCS
67-63-0	Isopropyl alcohol	70	200-661-7
7732-18-5	Water	30	231-791-2

Section 3 - Hazards Identification

EMERGENCY OVERVIEW

Appearance: colorless liquid. Flash Point: 18 deg C.
Warning! Flammable liquid and vapor. Breathing vapors may cause drowsiness and dizziness. Causes eye and respiratory tract irritation. Aspiration hazard if swallowed. Can enter lungs and cause damage. Prolonged or repeated contact causes defatting of the skin with irritation, dryness, and cracking. May cause central nervous system depression.
Target Organs: Central nervous system, respiratory system, eyes, skin.

Potential Health Effects
Eye: Produces irritation, characterized by a burning sensation, redness, tearing, inflammation, and possible corneal injury. May cause transient corneal injury. In the eyes of a rabbit, 0.1 ml of 70% isopropyl alcohol caused conjunctivitis, iritis, and corneal opacity.
Skin: May cause irritation with pain and stinging, especially if the skin is abraded. Isopropanol has a low potential to cause allergic skin reactions; however, rare cases of allergic contact dermatitis have been reported. May be absorbed through intact skin. Dermal absorption has been considered toxicologically insignificant. The cases of deep coma associated with skin contact are thought to be a consequence of gross isopropanol vapor inhalation in rooms with inadequate ventilation, rather than being attributable to percutaneous absorption of isopropanol per se.
Ingestion: Causes gastrointestinal irritation with nausea, vomiting and diarrhea. May cause kidney damage. May cause central nervous system depression, characterized by excitement, followed by headache, dizziness, drowsiness, and nausea. Advanced stages may cause collapse, unconsciousness, coma and possible death due to respiratory failure. Aspiration of material into the lungs may cause chemical pneumonitis, which may be fatal. The probable oral lethal dose in humans is 240 ml (2696 mg/kg), but ingestion of only 20 ml (224 mg/kg) has caused poisoning.
Inhalation: Inhalation of high concentrations may cause central nervous system effects characterized by nausea, headache, dizziness, unconsciousness and coma. May cause narcotic effects in high concentration. Causes upper respiratory tract irritation. Inhalation of vapors may cause drowsiness and dizziness.
Chronic: Prolonged or repeated skin contact may cause defatting and dermatitis.

Section 4 - First Aid Measures

Eyes: In case of contact, immediately flush eyes with plenty of water for a t least 15 minutes. Get medical aid.
Skin: In case of contact, flush skin with plenty of water. Remove contaminated clothing and shoes. Get medical aid if irritation develops and persists. Wash clothing before reuse.
Ingestion: Potential for aspiration if swallowed. Get medical aid immediately. Do not induce vomiting unless directed to do so by medical personnel. Never give anything by mouth to an unconscious person. If vomiting occurs naturally, have victim lean forward.
Inhalation: If inhaled, remove to fresh air. If not breathing, give artificial respiration. If breathing is difficult, give oxygen. Get medical aid.
Notes to Physician: Urine acetone test may be helpful in diagnosis. Hemodialysis should be considered in severe intoxication. Treat symptomatically and supportively.

Section 5 - Fire Fighting Measures

General Information: As in any fire, wear a self-contained breathing apparatus in pressure-demand, MSHA/NIOSH (approved or equivalent), and full protective gear. Vapors may form an

explosive mixture with air. Use water spray to keep fire-exposed containers cool. Flammable liquid and vapor. Vapors are heavier than air and may travel to a source of ignition and flash back. Vapors can spread along the ground and collect in low or confined areas.
Extinguishing Media: Water may be ineffective. Do NOT use straight streams of water. For large fires, use dry chemical, carbon dioxide, alcohol-resistant foam, or water spray. For small fires, use carbon dioxide, dry chemical, dry sand, or alcohol-resistant foam. Cool containers with flooding quantities of water until well after fire is out.
Flash Point: 18 deg C (64.40 deg F)
Autoignition Temperature: 399 deg C (750.20 deg F)
Explosion Limits, Lower:2.0 vol %
Upper: 12.7 @ 93.3°C
NFPA Rating: (estimated) Health: 1; Flammability: 3; Instability: 0

Section 6 - Accidental Release Measures

General Information: Use proper personal protective equipment as indicated in Section 8.
Spills/Leaks: Absorb spill with inert material (e.g. vermiculite, sand or earth), then place in suitable container. Use water spray to dilute spill to a non-flammable mixture. Clean up spills immediately, observing precautions in the Protective Equipment section. Remove all sources of ignition. Use a spark-proof tool. Provide ventilation. A vapor suppressing foam may be used to reduce vapors.

Section 7 - Handling and Storage

Handling: Wash thoroughly after handling. Remove contaminated clothing and wash before reuse. Ground and bond containers when transferring material. Use spark-proof tools and explosion proof equipment. Avoid contact with eyes, skin, and clothing. Empty containers retain product residue, (liquid and/or vapor), and can be dangerous. Take precautionary measures against static discharges. Keep container tightly closed. Do not pressurize, cut, weld, braze, solder, drill, grind, or expose empty containers to heat, sparks or open flames. Use only with adequate ventilation. Avoid breathing vapor or mist.
Storage: Keep away from sources of ignition. Store in a tightly closed container. Keep from contact with oxidizing materials. Store in a cool, dry, well-ventilated area away from incompatible substances.

Section 8 - Exposure Controls, Personal Protection

Engineering Controls: Use explosion-proof ventilation equipment. Facilities storing or utilizing this material should be equipped with an eyewash facility and a safety shower. Use adequate general or local exhaust ventilation to keep airborne concentrations below the permissible

exposure limits.
Exposure Limits

Chemical Name	ACGIH	NIOSH	OSHA - Final PELs
Isopropyl alcohol	200 ppm TWA; 400 ppm STEL	400 ppm TWA; 980 mg/m3 TWA 2000 ppm IDLH (10% LEL)	400 ppm TWA; 980 mg/m3 TWA
Water	none listed	none listed	none listed

OSHA Vacated PELs: Isopropyl alcohol: 400 ppm TWA; 980 mg/m3 TWA Water: No OSHA Vacated PELs are listed for this chemical.
Personal Protective Equipment
Eyes: Wear chemical splash goggles.
Skin: Wear appropriate protective gloves to prevent skin exposure.
Clothing: Wear appropriate protective clothing to prevent skin exposure.
Respirators: A respiratory protection program that meets OSHA's 29 CFR 1910.134 and ANSI Z88.2 requirements or European Standard EN 149 must be followed whenever workplace conditions warrant respirator use.

Section 9 - Physical and Chemical Properties

Physical State: Liquid
Appearance: colorless
Odor: alcohol-like
pH: Not available.
Vapor Pressure: 33 mm Hg @ 20 deg C
Vapor Density: 2.1 (Air=1)
Evaporation Rate:1.7 (n-butyl acetate=1)
Viscosity: 2.27 mPas @ 20 deg C

Boiling Point: 82 deg C @ 760 mm Hg
Freezing/Melting Point:-88 deg C
Decomposition Temperature: Not available.
Solubility: Miscible.
Specific Gravity/Density:0.7850 (water=1)
Molecular Formula:C3H8O
Molecular Weight:60.09

Section 10 - Stability and Reactivity

Chemical Stability: Stable.
Conditions to Avoid: Ignition sources, excess heat.
Incompatibilities with Other Materials: Strong oxidizing agents, strong acids, strong bases, amines, ammonia, ethylene oxide, isocyanates, acetaldehyde, chlorine, phosgene, Attacks some forms of plastics, rubbers, and coatings., aluminum at high temperatures.
Hazardous Decomposition Products: Carbon monoxide, carbon dioxide.
Hazardous Polymerization: Will not occur.

Section 11 - Toxicological Information

RTECS#:
CAS# 67-63-0: NT8050000
CAS# 7732-18-5: ZC0110000
LD50/LC50:
CAS# 67-63-0:
Draize test, rabbit, eye: 100 mg Severe;
Draize test, rabbit, eye: 10 mg Moderate;
Draize test, rabbit, eye: 100 mg/24H Moderate;
Draize test, rabbit, skin: 500 mg Mild;
Inhalation, mouse: LC50 = 53000 mg/m3;
Inhalation, rat: LC50 = 16000 ppm/8H;
Inhalation, rat: LC50 = 72600 mg/m3;
Oral, mouse: LD50 = 3600 mg/kg;
Oral, mouse: LD50 = 3600 mg/kg;
Oral, rabbit: LD50 = 6410 mg/kg;
Oral, rat: LD50 = 5045 mg/kg;
Oral, rat: LD50 = 5000 mg/kg;
Skin, rabbit: LD50 = 12800
CAS# 7732-18-5:
Oral, rat: LD50 = >90 mL/kg;
.

Carcinogenicity:
CAS# 67-63-0: Not listed by ACGIH, IARC, NTP, or CA Prop 65.
CAS# 7732-18-5: Not listed by ACGIH, IARC, NTP, or CA Prop 65.

Epidemiology: No information found
Teratogenicity: A rat & rabbit developmental toxicity study showed no teratogenic effects at doses that were clearly maternally toxic. In a separate rat study, no evidence of developmental neurotoxicity was associated with gestational exposures to IPA up to 1200 mg/kg/d.
Reproductive Effects: See actual entry in RTECS for complete information.
Mutagenicity: See actual entry in RTECS for complete information.
Neurotoxicity: In rats exposed to isopropanol by inhalation, acute neurotoxicity was noted at 1 and 6 hours at 5000 ppm, but only minimal effects were seen at 1500 ppm and the animals recovered within 5 hours. No toxicity was noted at 500 ppm.
Other Studies:

Section 12 - Ecological Information

Ecotoxicity: Fish: Fathead Minnow: >1000 ppm; 96h; LC50Daphnia: >1000 ppm; 96h; LC50Fish: Gold orfe: 8970-9280 ppm; 48h; LC50 IPA has a high biochemical oxygen demand and a potential to cause oxygen depletion in aqueous systems, a low potential to affect aquatic organisms, a low potential to affect secondary waste treatment microbial metabolism, a low potential to affect the germination of some plants, a high potential to biodegrade (low persistence) with unacclimated microorganisms from activated sludge.
Environmental: No information available.

Physical: THOD: 2.40 g oxygen/gCOD: 2.23 g oxygen/gBOD-5: 1.19-1.72 g oxygen/g
Other: No information available.

Section 13 - Disposal Considerations

Chemical waste generators must determine whether a discarded chemical is classified as a hazardous waste. US EPA guidelines for the classification determination are listed in 40 CFR Parts 261.3. Additionally, waste generators must consult state and local hazardous waste regulations to ensure complete and accurate classification.
RCRA P-Series: None listed.
RCRA U-Series: None listed.

Section 14 - Transport Information

	US DOT	Canada TDG
Shipping Name:	ISOPROPANOL	ISOPROPANOL
Hazard Class:	3	3
UN Number:	UN1219	UN1219
Packing Group:	II	II

Section 15 - Regulatory Information

US FEDERAL

TSCA
CAS# 67-63-0 is listed on the TSCA inventory.
CAS# 7732-18-5 is listed on the TSCA inventory.
Health & Safety Reporting List
CAS# 67-63-0: Effective 12/15/86, Sunset 12/15/96
Chemical Test Rules
CAS# 67-63-0: 40 CFR 799.2325
Section 12b
None of the chemicals are listed under TSCA Section 12b.
TSCA Significant New Use Rule
None of the chemicals in this material have a SNUR under TSCA.

CERCLA Hazardous Substances and corresponding RQs
None of the chemicals in this material have an RQ.
SARA Section 302 Extremely Hazardous Substances
None of the chemicals in this product have a TPQ.
SARA Codes
CAS # 67-63-0: immediate, delayed, fire.
Section 313
This material contains Isopropyl alcohol (CAS# 67-63-0, 70%),which is subject to the reporting requirements of Section 313 of SARA Title III and 40 CFR Part 373.
Clean Air Act:
This material does not contain any hazardous air pollutants.
This material does not contain any Class 1 Ozone depletors.
This material does not contain any Class 2 Ozone depletors.
Clean Water Act:
None of the chemicals in this product are listed as Hazardous Substances under the CWA.
None of the chemicals in this product are listed as Priority Pollutants under the CWA.
None of the chemicals in this product are listed as Toxic Pollutants under the CWA.
OSHA:
None of the chemicals in this product are considered highly hazardous by OSHA.
STATE
CAS# 67-63-0 can be found on the following state right to know lists: California, New Jersey, Pennsylvania, Minnesota, Massachusetts.
CAS# 7732-18-5 is not present on state lists from CA, PA, MN, MA, FL, or NJ.

California Prop 65

California No Significant Risk Level: None of the chemicals in this product are listed.

European/International Regulations
European Labeling in Accordance with EC Directives
Hazard Symbols:
XI F
Risk Phrases:
R 11 Highly flammable.
R 36 Irritating to eyes.
R 67 Vapours may cause drowsiness and dizziness.

Safety Phrases:
S 16 Keep away from sources of ignition - No smoking.
S 24/25 Avoid contact with skin and eyes.
S 26 In case of contact with eyes, rinse immediately with plenty of water and seek medical advice.
S 7 Keep container tightly closed.

WGK (Water Danger/Protection)
CAS# 67-63-0: 1

CAS# 7732-18-5: No information available.

Canada - DSL/NDSL

CAS# 67-63-0 is listed on Canada's DSL List.

CAS# 7732-18-5 is listed on Canada's DSL List.

Canada - WHMIS

This product has a WHMIS classification of B2, D2A.

This product has been classified in accordance with the hazard criteria of the Controlled Products Regulations and the MSDS contains all of the information required by those regulations.

Canadian Ingredient Disclosure List

CAS# 67-63-0 is listed on the Canadian Ingredient Disclosure List.

Material Safety Data Sheet - Water©

I. PRODUCT IDENTIFICATION

Manufacturer's Name: MOTHER NATURE, Inc.
Address: Everywhere, The World
Business Tele. #: Not available
Emergency Tele. #: Not available
Trade name: Water, Aqua pura
Synonyms: Dihydrogen Monoxide; H_20

II. HAZARDOUS INGREDIENTS

NONE when compound is in the pure state.

III. PHYSICAL DATA

Boiling point (760 mm Hg): 100°C (212°F)
Melting point: 0°C (32°F)
Specific gravity (H2O = 1):1
Vapor pressure - 100°C (212°F) 760 mm Hg
- 0°C (32°F) 17.5 mm Hg

Solubility in water (% by wt.): 100%
% Volatiles by volume: 100%
Evap. rate (Butyl acetate = 1): Not available
Appearance and Odor: Clear liquid; No odor

IV. FIRE & EXPLOSION DATA

Flash Point: Not applicable
Autoignition Temperature: Not applicable
Flammable limits in air (% by Vol.): Not applicable
Extinguishing Media: Not applicable

Special firefighting procedures: Not applicable
Unusual Fire and Explosion Hazard: Rapid temperature rise of liquid can result in explosive vaporization, particularly if in a sealed container.

V. HEALTH HAZARD INFORMATION

Routes of Exposure and Effects of Overexposure

Inhalation
Acute over exposure: *Inhalation can result in asphyxiation and is often fatal.*
Chronic overexposure: *Chronic inhalation overexposure not encountered.*

Skin Contact
Acute overexposure: *Prolonged but constant contact with liquid may cause a mild dermatitis.*
Chronic overexposure: *Mild to severe dermatitis.*

Skin Absorption
Acute overexposure: *No effects noted.*
Chronic overexposure: *No effects noted.*

Eye Contact
Acute overexposure: *No effects noted.*
Chronic overexposure: *No effects noted.*

Ingestion
Acute overexposure: *Excessive ingestion of liquid form can cause gastric distress and mild diarrhea.*
Chronic overexposure: *No effects noted.*

Emergency and First Aid Procedures
Eyes: *None*
Skin: *None*
Inhalation: *Remove to fresh air; Provide artificial respiration; Provide oxygen.*
Ingestion: *None*

Notes to Physician: *None*

VI. REACTIVITY DATA

Conditions contributing to instability: Exposure to direct current electricity.

Incompatibility: Strong acids and bases can cause rapid heating. Reaction with sodium metal can result in explosion.

Hazardous decomposition products: Hydrogen - Explosive gas Oxygen - Supports rapid combustion

Conditions contributing to hazardous polymerization: None

VII. SPILL or LEAK PROCEDURES

Steps to be taken if material is released or spilled:

Small quantities can be mopped or wiped up with rags.
Large quantities should be directed to collecting basin or drain with dikes or swabs.

Neutralizing chemicals

None required.

Waste disposal method:

Process contaminated material through treatment plant prior to discharge into environment. Discharge permit may be required.

VIII. SPECIAL PROTECTION INFORMATION

Ventilation requirements:

Remove hot vapor from environment using local exhaust systems.

Specific personal protective equipment:

Respiratory: *None required.*
Eyes: *Goggles or full face splash shield when dealing with hot liquid.*
Hands: *Use insulating gloves when extensive exposure to solid state or high temperature liquid state is contemplated.*
Other clothing and equipment: *Use heat protective garment when exposed to large quantities of heated vapor.*

IX. SPECIAL PRECAUTIONS

Precautionary statements:

Compound readily exists in all three phases at atmospheric pressure. Phase changes occur over a narrow ($100^{o}C/212^{o}F$) temperature range.
Compound is known as "the universal solvent" and does dissolve, at least to some extent, most common materials.
Compound will conduct electricity when dissolved ionic solutes are present.

Other handling and storage requirements:

A high pressure containment vessel should be used for the vapor at high temperatures.
Do not allow filled, closed containers to solidify as compound expands upon freezing.

Appendix B: Instrumentation Used

Omega OM-EL-USB-TC Datalogger
The OM-EL-USB-TC data logger measures and stores over 32,000 temperature readings from either a Type J, Type K or Type T thermocouple which plugs into a miniature female thermocouple receptacle at the base of the unit. The user can easily set up the initial data logging parameters including thermocouple type, logging rate, start-time, high/low alarm settings, logging mode and desired temperature units (°C or °F) and also download the stored data by plugging the module straight into a PC's USB port and running the easy-to-use Windows software.

Downloaded data can then be graphed, printed and exported to other applications such as Excel. The data logger is supplied complete with a long-life lithium battery. Data logger status is indicated by flashing red, green and orange LEDs.

Specifications
Temperature Measurement Range:
Type J: -130 to 900°C (-202 to 1652°F)
Type K: -200 to 1300°C (-328 to 2372°F)
Type T: -200 to 350°C (-328 to 662°F)
Resolution**:** 0.5°C (1°F)
Accuracy: ±1.0°C (±2.0°F)
Thermocouple Connection: Female subminiature thermocouple connector
Temperature Units: °C or °F selectable in software
Memory: 32,000 readings
Logging Interval: 1 sec, 10 sec, 1 min, 5 min, 30 min, 1 hr, 6 hr, 12 hr (selectable in software)
High/Low Alarms: Selectable in software
Start Date/Time: Selectable in software
Operating Temperature Range: -10 to 40°C (-14 to 104°F)
Visual Indicators (LEDs): 2 LEDs; the first LED flashes orange to indicate a problem condition with the data logger such as low battery; the second LED indicates alarm status and flashes green (temperature within limits) or red (temperature out of limits)
Software: Windows® 2000/XP/VISTA
Power: 1/2 AA 3.6 V lithium battery (included)
Battery Life: 6 months (at 25°C and 1 minute logging interval)
Weight: 43 g (1.5 oz)

Omega OM-EL-USB-3 Data logger

The OM-EL-USB Series of data loggers includes models for temperature, temperature/relative humidity, voltage, and current measurement. The user can easily set up the data logger and download the stored data by plugging the module into a PC's USB port and running the easy-to-use Windows software. Software-selectable setup parameters include logging rate, start-time, high/low alarm settings, and temperature units (°C or °F). Data can then be graphed, printed, and exported to other applications such as Excel. Each data logger is supplied complete with a long-life lithium battery. Built-in LED indicators show data logger status. OM-EL-USB Series data loggers are protected against moisture to IP67 standards when the protective cap is fitted.

Specifications
VOLTAGE DATA LOGGER
Range: 0 to 30 Vdc
Resolution: 100 mV
Accuracy: ±1%

GENERAL
Memory: 32,000 voltage readings
Logging Interval: 1 seconds to 12 hours
Operating Temperature Range: -25 to 80°C (-13 to 176°F)
Alarm Thresholds: High/low alarm thresholds selectable in software
Start Date/Time: Selectable in software
Status Indicators (LEDs): Red and green
Power: ½ AA 3.6 V lithium battery (included)
Battery Life: 1 year typical (depends on sample rate, ambient temperature and use of alarm LEDs)
Weight: 57 g (2 oz)
Dimensions: See dimensional drawing

Dimensions: mm (in)

Omega FMA-904-V Air Velocity Transducer

The unique FMA-900 air velocity transducer utilizes both a velocity sensor and a temperature sensor to accurately measure air velocity (in SFPM, standard feet per minute). The built-in temperature sensor automatically corrects the flow rate for temperature variations. Both sensors are rugged glass-coated platinum resistance detectors (RTDs). The circuit heats the velocity sensor to a constant temperature differential above ambient temperature and measures the cooling effect of the air flow. This design provides excellent low velocity sensitivity and high accuracy. The FMA-900 also features negligible pressure drop. To obtain mass flow rate in SCFM (standard cubic feet/minute), the SFPM velocity indicated by the FMA-900 is multiplied by the cross-sectional area of the pipe or duct in square feet. A traverse across the pipe or duct can be performed to determine the mounting location for average velocity indication. The FMA-900 can be mounted in pipes (down to 1.5" size) with the use of OMEGA ® SSLK compression fittings (SSLK-14-14). PTFE ferrules are required. (model T-FER- 14). Each unit is individually calibrated in OMEGA's NIST-traceable wind tunnel. Suggested power supply; FPW-15, ($75)

The **New Remote Electronics Option (-R)** comes with a 12 foot cable from the sensor to a quick disconnect connector and then to the mating connector with two feet of wire which connects directly into the electronics box. The electronics box has another connector on the opposite side with a 15 foot cable with strip leads. A total of 30 feet of cable. Designed for tight spaces.

SPECIFICATIONS

Accuracy: 1.5% FS @ room temp. Add ±0.5% of reading from 0 to 50°C (32° to 122°F); add 1% FS below 1000 SFPM
Repeatability**:** ±0.2% FS
Initial Stabilization Time in Flow: 40 sec
Response Time/After Stabilization: 400 msec to within 63% of final value at room temperature
Probe**:** Aluminum oxide ceramic glass coating, epoxy; probe body 304 SS
Probe **Temperature:** -40 to 121°C (-40 to 250°F)
Probe Pressure: 150 PSIG Max
Electronics Temperature: 0 to 50°C (32 to 122°F), operating; 0 to 70°C (32 to 158°F), storage
Operating Relative Humidity: less than 80% RH, without condensation Ambient Temp Compensation: about 5 min for 11°C (20°F) temp change
Outputs: 0 to 5 Vdc or 4 to 20 mA

Voltage Load Resistance**:** 250 ohms minimum
Current Loop Resistance**:** 0 ohms min. to 400 ohms max.; 4 wire
Power: 15 to 24 Vdc,300 mA (0 to 100 and 0 to 200 SFPM only); 15 to 18 Vdc, 300 mA (all other ranges)300 mA (0 to 100 and 0 to 200 SFPM only); 15 to 18 Vdc, 300 mA (all other ranges) 300 mA (0 to 100 and 0 to 200 SFPM only); 15 to 18 Vdc, 300 mA (all other ranges)
Accessories: Mating connector pre-wired to 15' shielded cable (with built-in ferrite core) included
Dimensions:
Case: 89 H x 51 W x 31.8 mm D (3.5 H x 2 W x 1.25" D)
Probe: 6.35 mm (0.250") O.D., 330 mm (13") length, optional 3.75" available (-S)
Weight: 160 g (5.6 oz)

Extech Instruments Model 451126 Thermo-Anemometer Data Logger

Extech 451126-NIST Vane Thermo-Anemometer Datalogger, Dual 4 digit (9999 count) Multifunction LCD with Data Hold, Dual Display provides Air velocity + Temperature" or "Air flow + Area, User selectable ºC/ºF units, Accurate (3%) air velocity measurements in ft/min m/sec, knoots, km/hr, and MPH units, Accurate (±1.5ºF and ±0.8ºC) temperature measurements, Measures air volume in CFM (ft3/min) and CMM (m3/min), Internal 1000 point datalogger plus built-in RS-232 PC interface, Remote vane sensor with built-in temperature sensor

General Information	
Manufacturer	Extech
Manufacturer Part Number	451126-NIST
Product Name	Vane Thermo-Anemometer Datalogger with NIST Certificate

Features

- Dual 4 digit (9999 count) Multifunction LCD with Data Hold
- Dual Display provides "Air velocity + Temperature" or "Air flow + Area"
- Accurate (3%) air velocity measurements in ft/min m/sec, knoots, km/hr, and MPH units
- Accurate (±1.5ºF and ±0.8ºC) temperature measurements
- User selectable ºC/ºF units
- Measures air volume in CFM (ft3/min) and CMM (m3/min)
- Internal 1000 point datalogger plus built-in RS-232 PC interface
- Remote vane sensor with built-in temperature sensor
- MAX/MIN/Average record and recall functions
- Complete with RS-232 interface, PC Windows software, cable, 9V battery and carrying case

Appendix C: Generator CAD Drawings

Figure C1: 3 dimensional rendering of the full generator

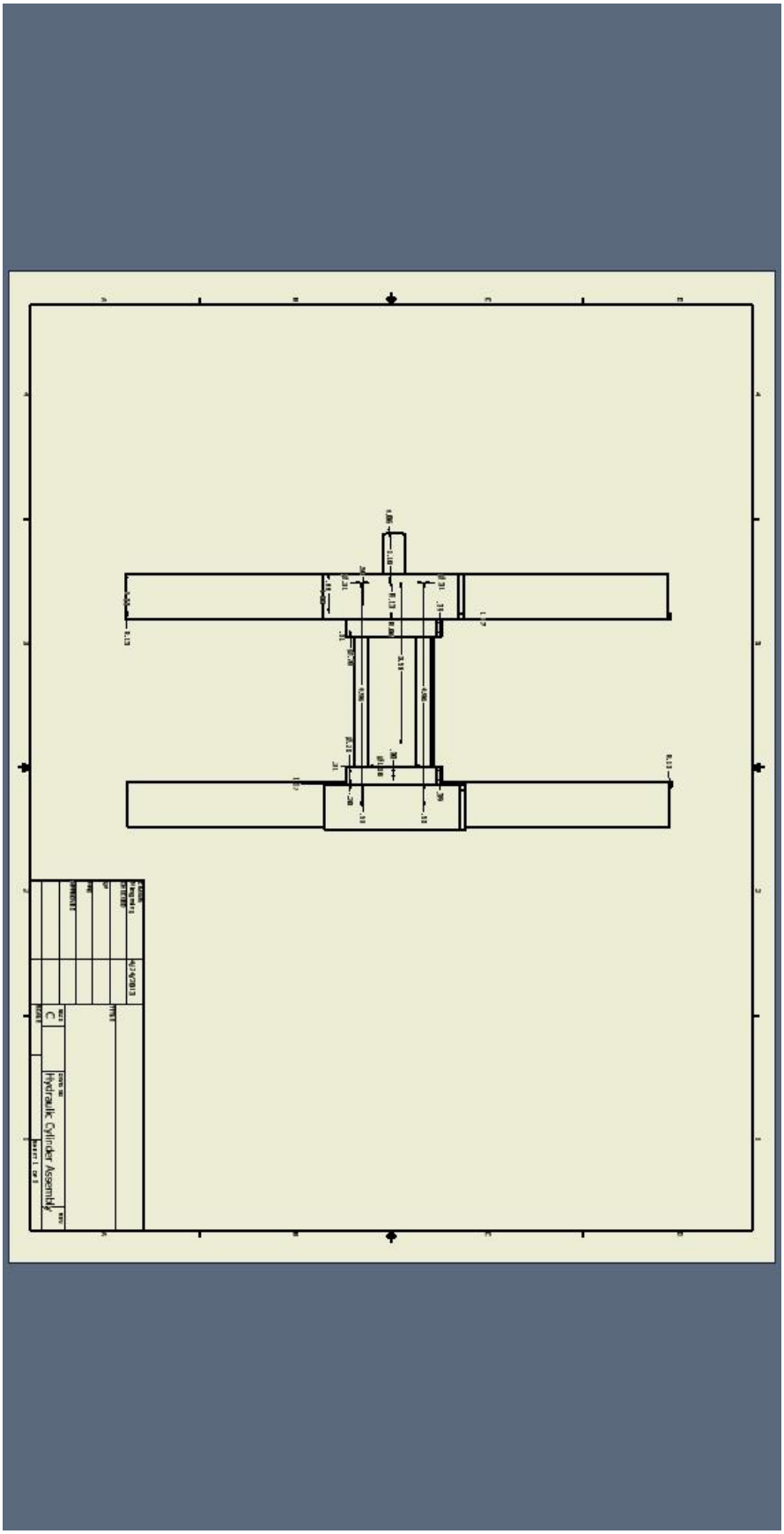
Hydraulic Cylinder Assembly

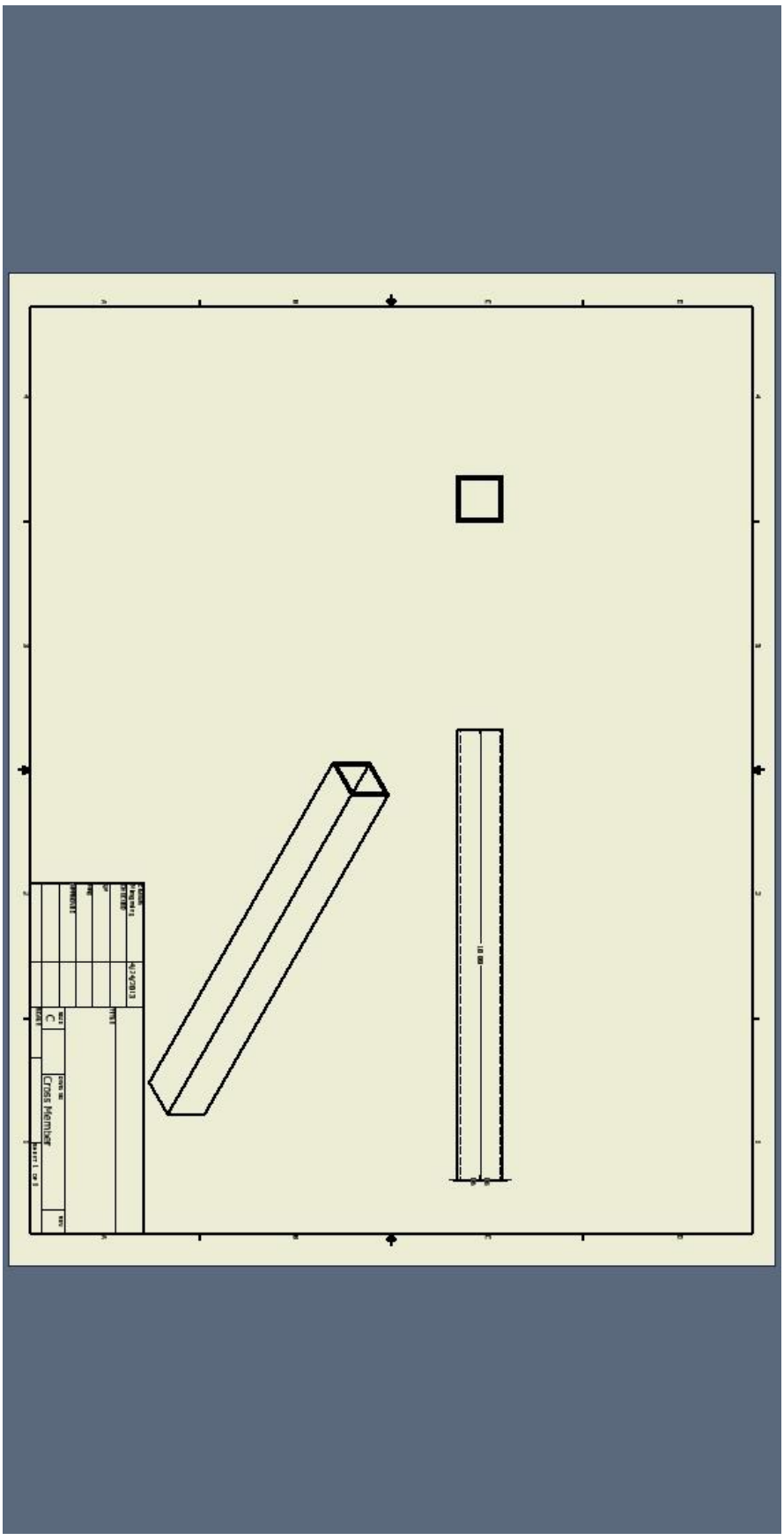
Cross Member

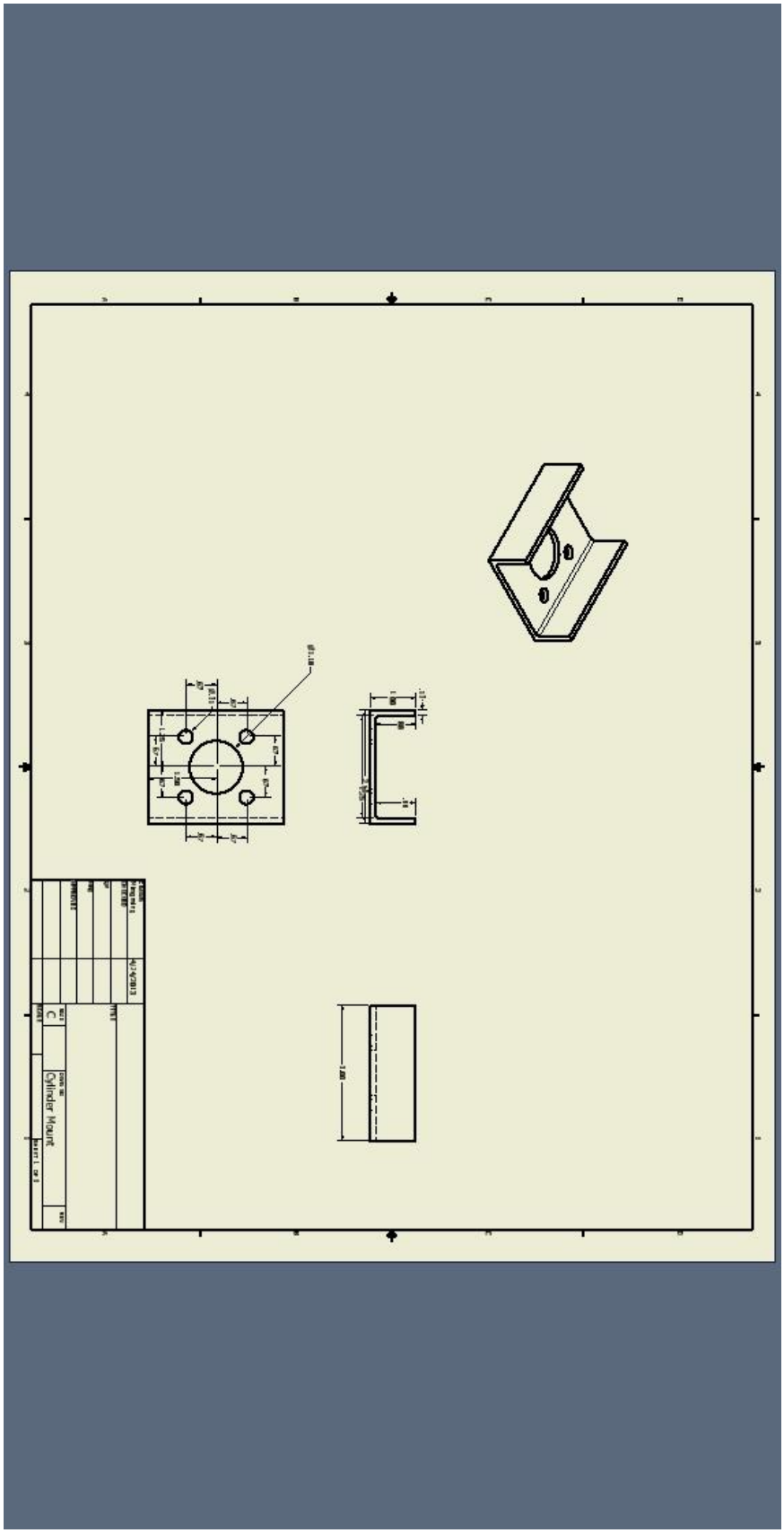
Cylinder Mount

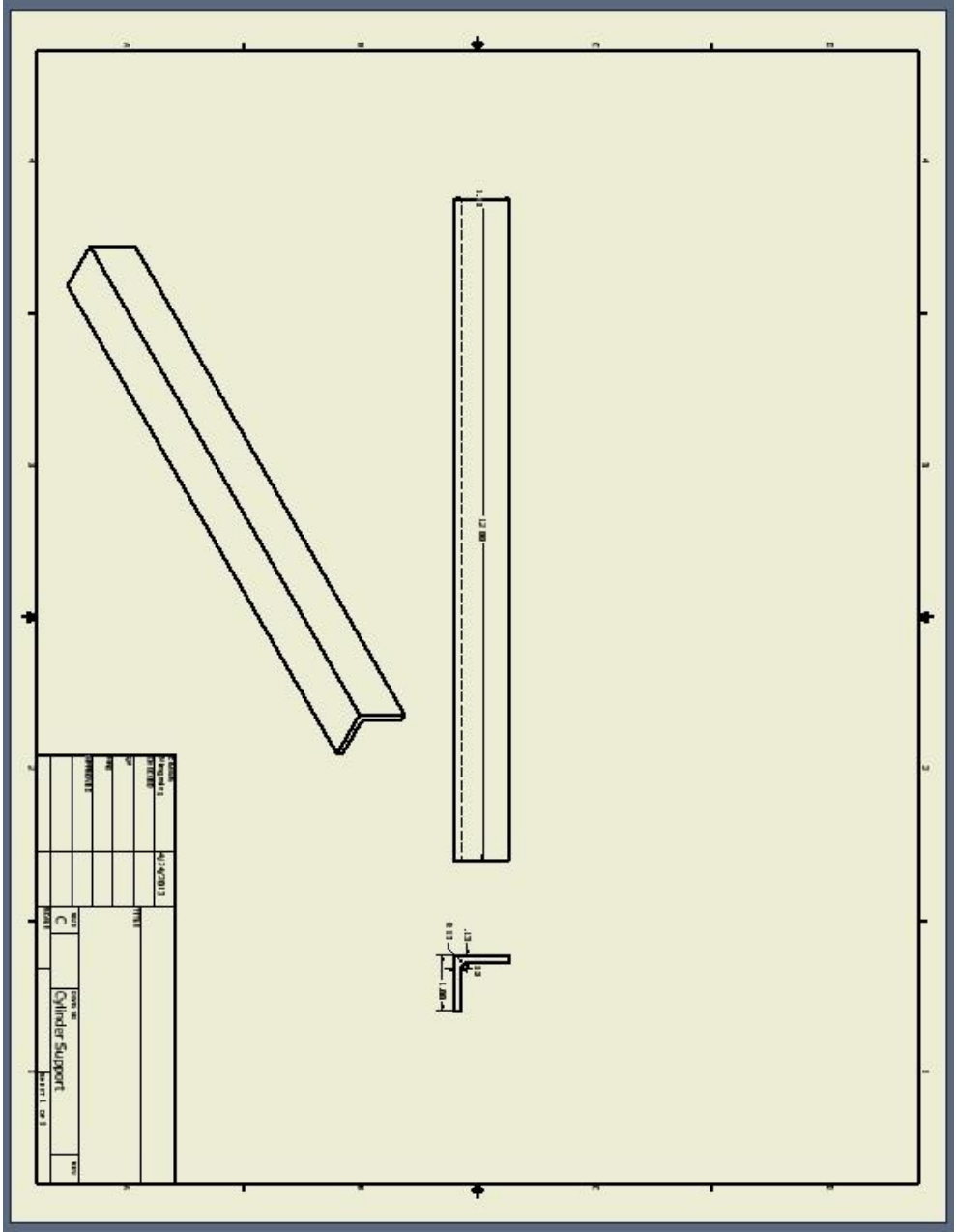
Cylinder Support

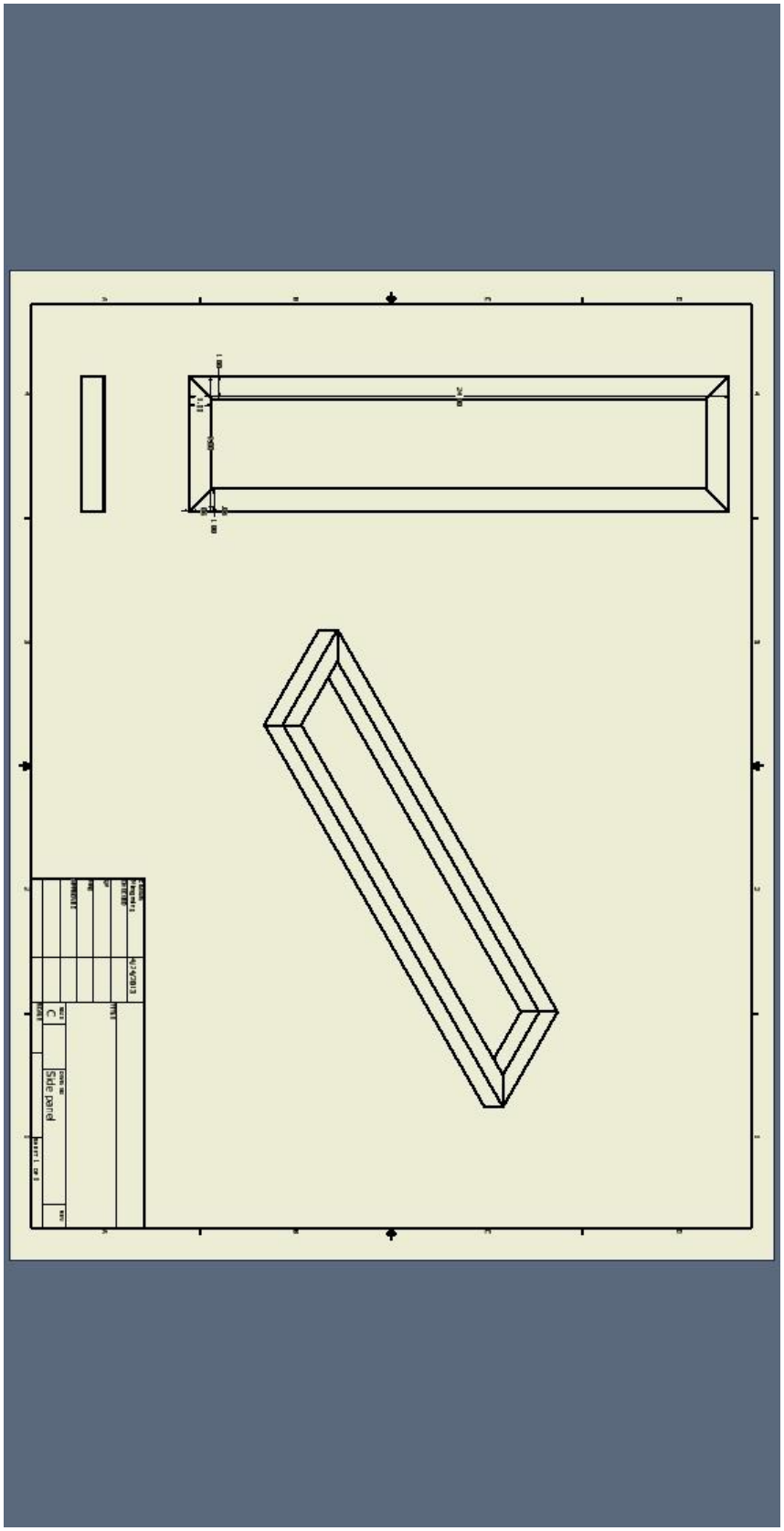
Side panel

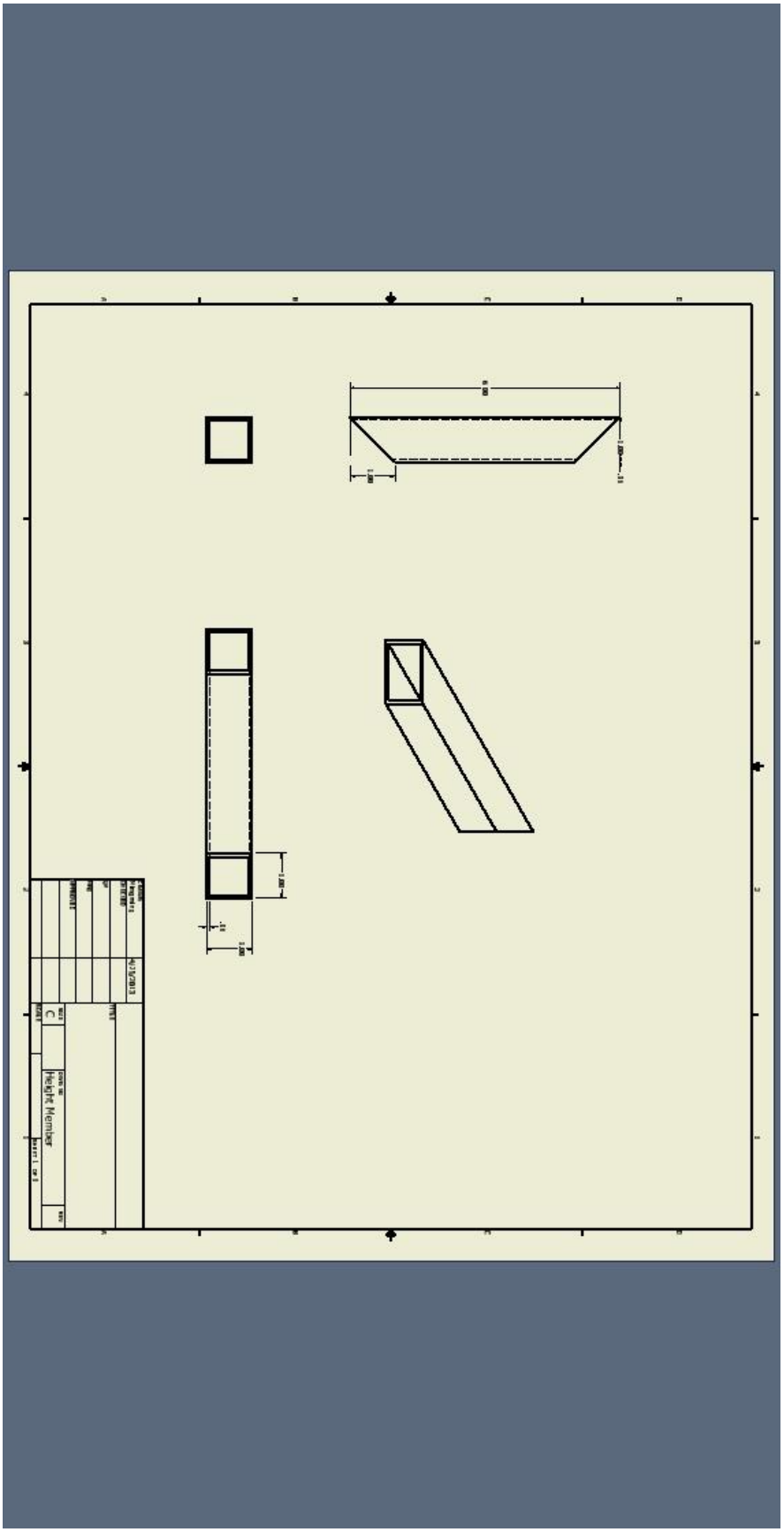
Height Member

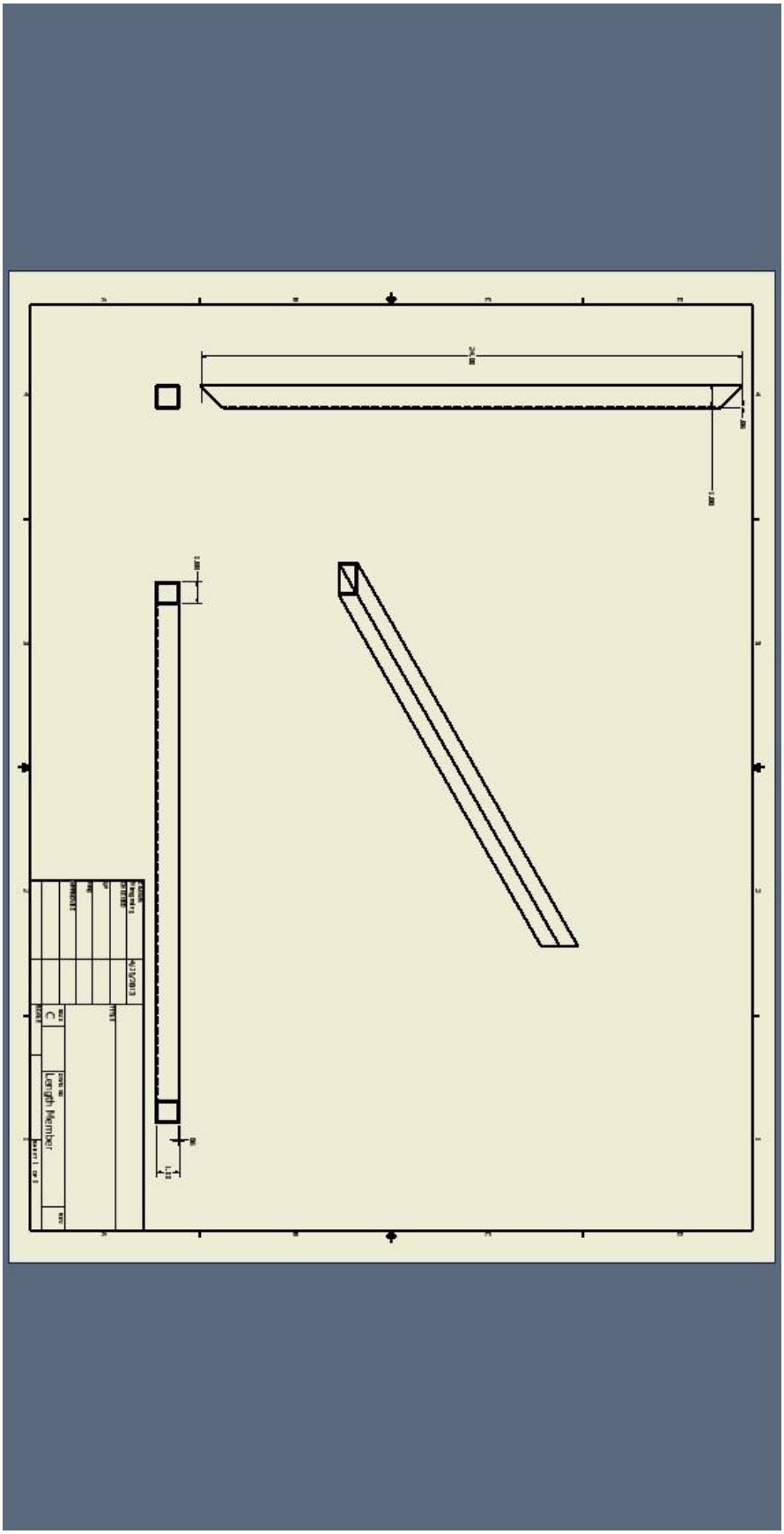
Length Member
C

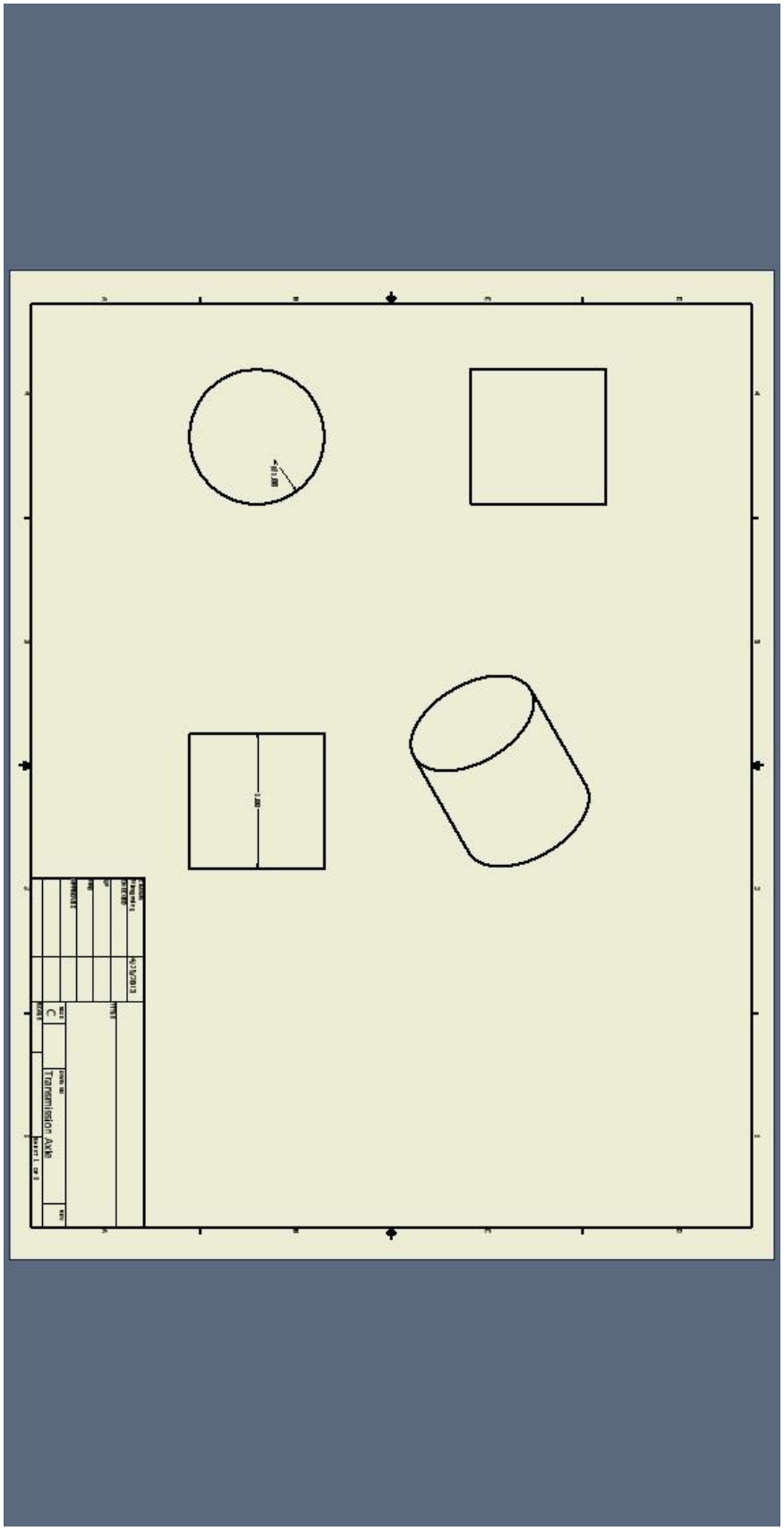
Transmission Axle
C
4/15/2013

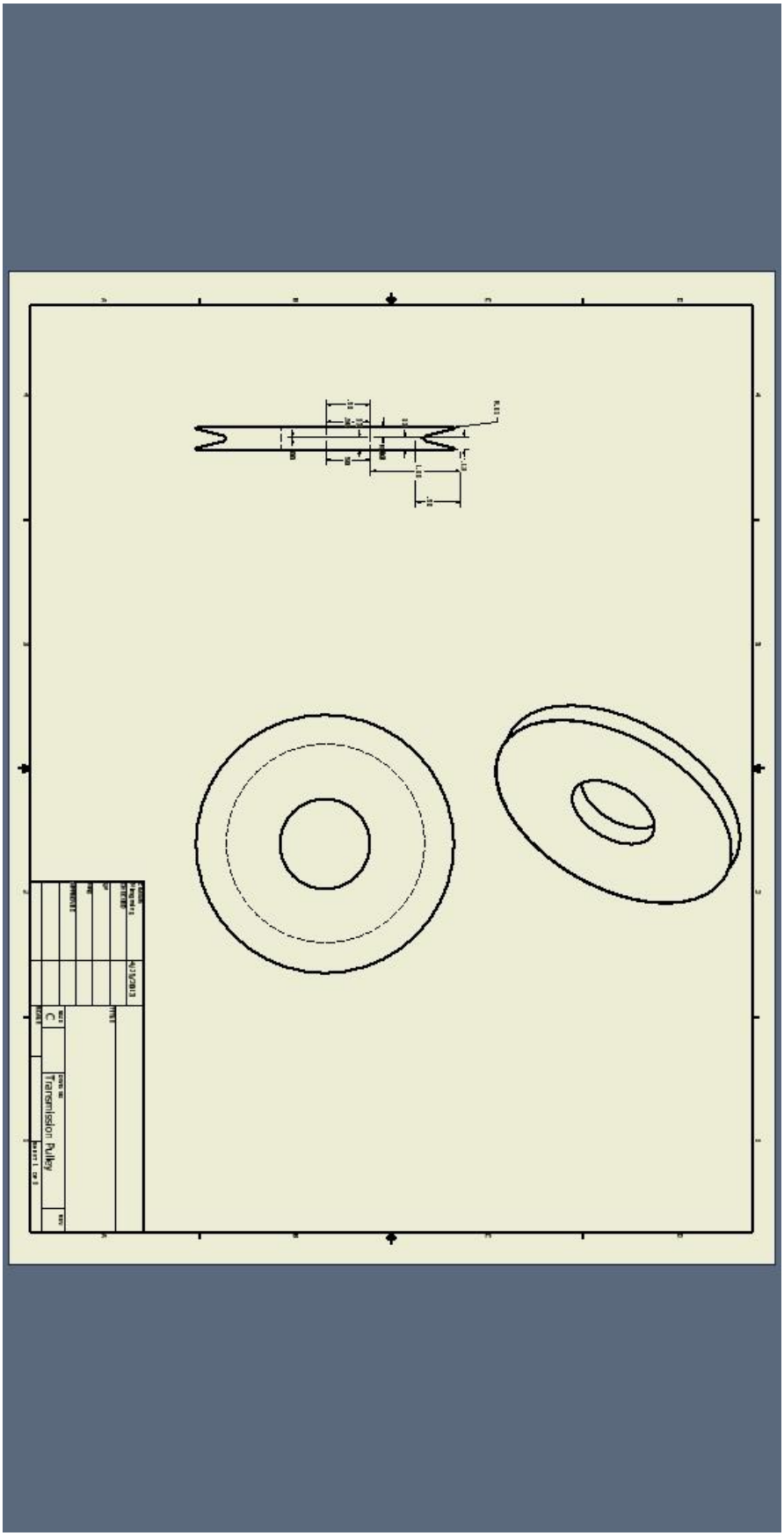
Transmission Pulley
C
4/15/2013

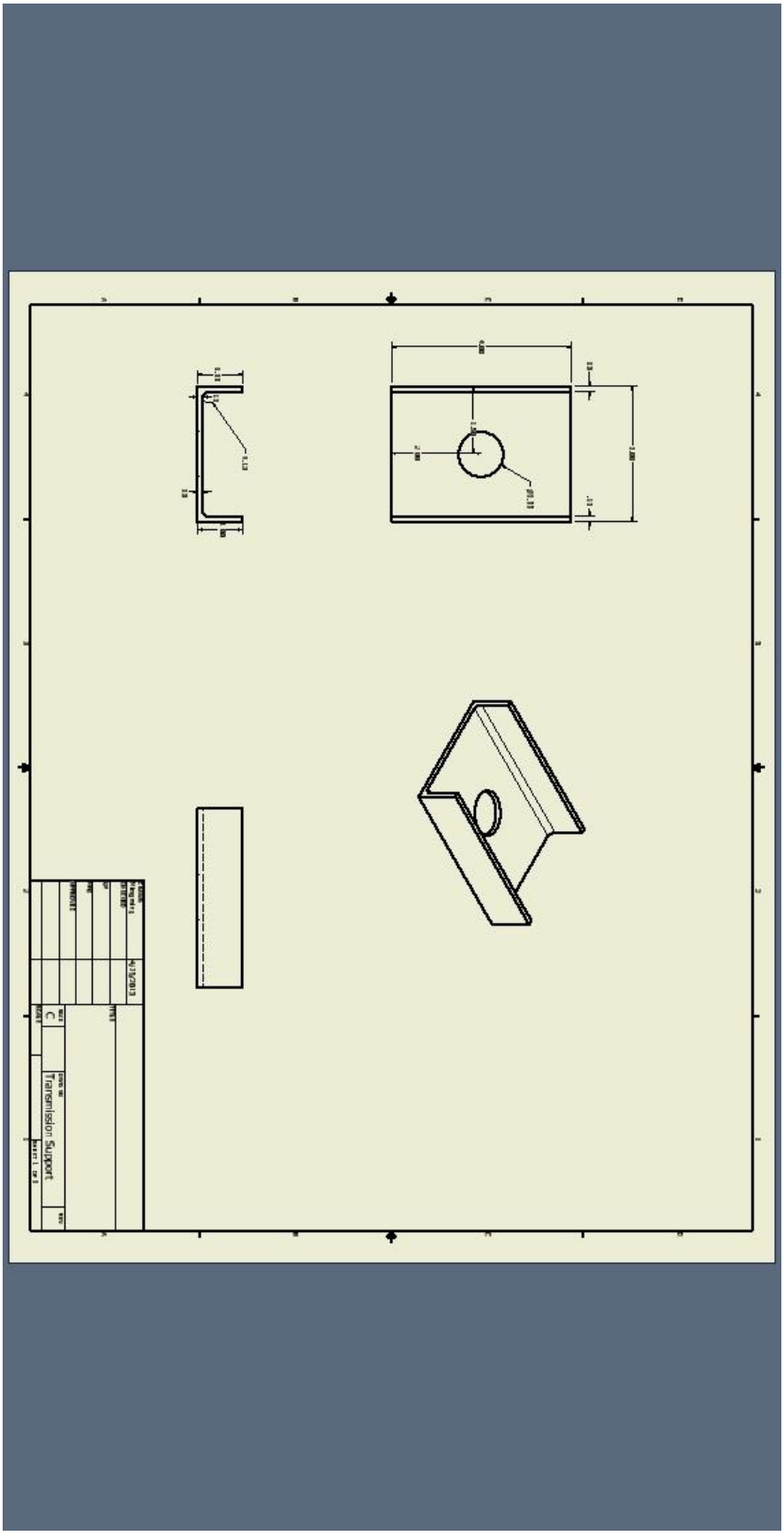
Transmission Support
C

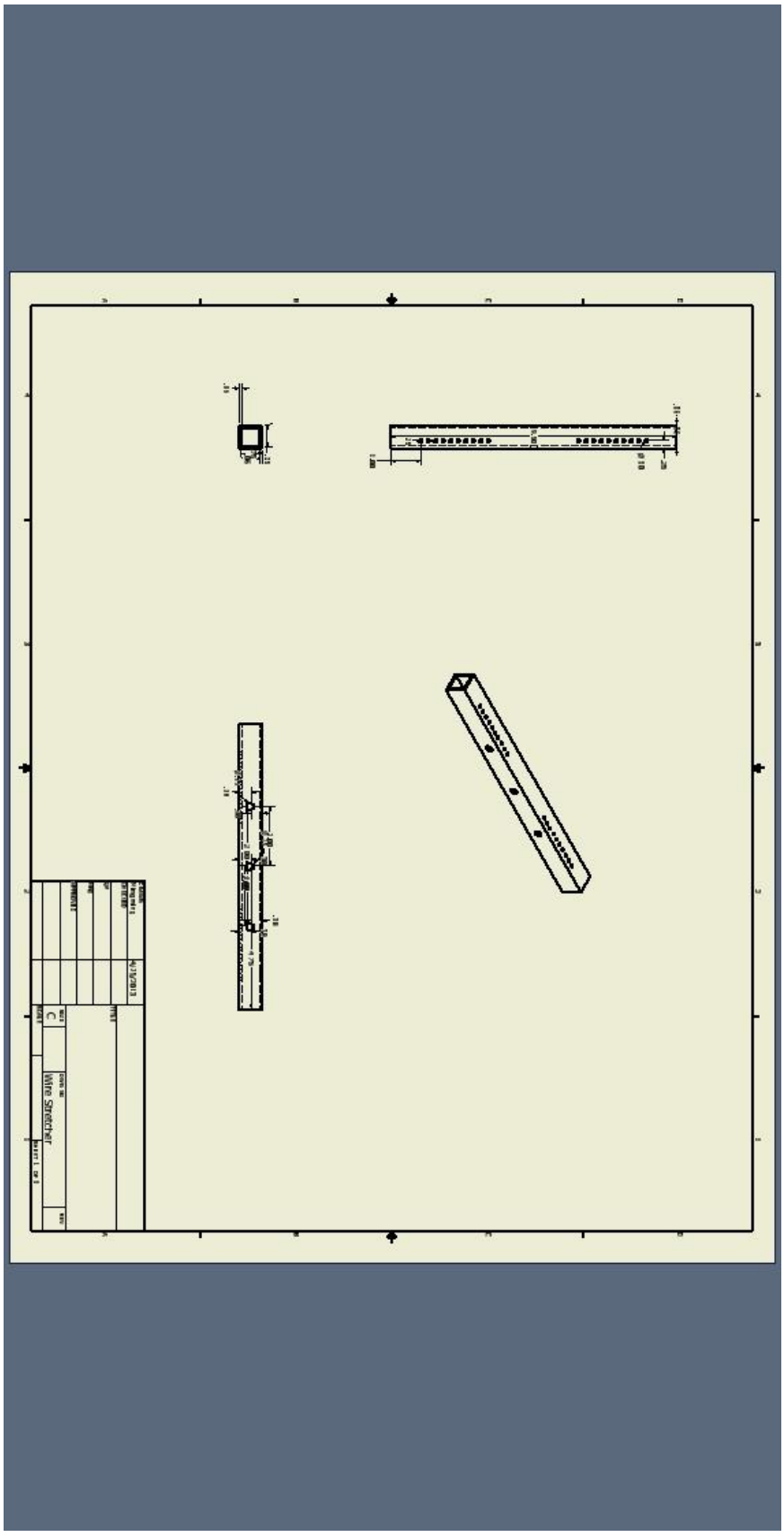
Wire Stretcher

Appendix D: Assembly Instructions

Structural Framework:

Materials required:
1. Length Member (4 each)
2. Height Member (4 each)
3. Cross Member (4 each)

Assembly Instructions
1. Butt weld Height Member to Length Member at 90° angles to form two rectangular Side Panels.
2. Grind all welds smooth.
3. On each Side Panel, in opposite corners, butt weld Cross Member at 90° to the plane of Side Panel. Keep the sides of Cross Member aligned with the sides of Side Panel.
4. Clamp the two Side Panel assemblies together to form a rectangular box. Butt weld the remaining edges of Cross Member to complete the structural framework.

Hydraulic Cylinder Mount

Materials required:
1. Cylinder Support (2 each)
2. Cylinder Mount (2 each)
3. Hydraulic cylinder (1 each)

Assembly Instructions
1. Butt weld the 1" side of Cylinder Mount to the center of the 10" long side of Cylinder Support.
2. Bolt the assemblies from #1 to the hydraulic cylinder with the recessed sides facing OUT.
3. Bolt the assembly from #2 to one of the 10x24" sides of the structural framework with the cylinder facing IN. The assembly must be bolted near one end of the assembly with the piston facing the other end of the assembly.

Transmission

Materials needed:
1. Transmission Support (2 each)
2. Transmission Pulley (1 each)
3. Transmission Axle (1 each)

Assembly Instructions
1. Insert Transmission Axle through Transmission Pulley. Transmission Axle may be replaced by a bolt of appropriate size to allow for regular servicing.
2. Insert Transmission Axle into the hole in Transmission Support with the recessed side of Transmission Support facing OUT. Weld flush and grind smooth. If a bolt is used in place of the Transmission Axle, welding and grinding is not required.

3. Weld to the structural framework on the end opposite the Hydraulic Cylinder. The Transmission Assembly should be welded such that the pulley is centered on the outside of the Structural Framework.

Wire Stretching Assembly

Materials required

1. Wire Stretchers	(4 each)
2. Steel cable assembly	(1 each)
3. Eye bolts	(2 each)
4. Tensioning bolts	(4 each)

Assembly Instructions

1. Lay out two wire stretchers so that they are parallel to each other. Ensure that the mounting holes on the wire stretchers are coplanar with each other.
2. From the outside, in, in a symmetrical fashion, attach the shape memory wires to the wire stretchers.
3. Repeat steps 1 & 2 for the bottom side of the wire stretchers.
4. Repeat steps 1-3 for the super elastic wires.
5. Run the steel cable assembly around the transmission pulley, attaching both ends to the eye bolts.
6. Mount the eye bolts into the wire stretchers with the shape memory wire assembly on top and super elastic wire assembly on the bottom.
7. Use tensioning bolts to draw the system snug. Once the wires are generally straight, continue tensioning the super elastic wires until the shape memory wires have undergone approximately a 2-3% stretch.

Notes

Notes

Notes